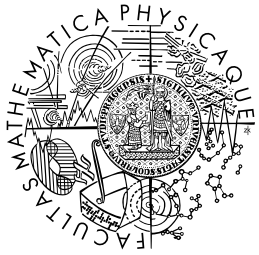

FACULTY
OF MATHEMATICS
AND PHYSICS
Charles University

DOCTORAL THESIS

Robert Navrátil

On Market Efficiency, Optimal Distributional Trading Gain, and Utility Maximization

Department of Probability and Mathematical Statistics, MFF UK

Supervisor of the doctoral thesis: doc. RNDr. Jan Večeř, Ph.D.

Study programme: Mathematics

Study branch: Probability and mathematical statistics

Prague 2022

I declare that I carried out this doctoral thesis independently, and only with the cited sources, literature and other professional sources. It has not been used to obtain another or the same degree.

I understand that my work relates to the rights and obligations under the Act No. 121/2000 Sb., the Copyright Act, as amended, in particular the fact that the Charles University has the right to conclude a license agreement on the use of this work as a school work pursuant to Section 60 subsection 1 of the Copyright Act.

In ..... date ....

Author's signature

I am grateful to my supervisor, doc. RNDr. Jan Večeř, Ph.D., for his guidance over the past four years. I would also like to thank him for proposing many exciting research topics and challenging problems; some of them are solved in this thesis. Similarly, I also owe thanks to my co-author Stephen M. Taylor, who made many valuable suggestions and improvements to our research, improving our now published papers, and therefore also this thesis.

Similarly, I would like to express thanks to my family. My special thanks go to my mother Sylva for continuously encouraging me to pursue higher education as well as raising me in an environment that led to my desire to learn new things and solve complex problems. In alphabetical order to my brothers Michal and Miroslav, who were always available when I needed help. Last but not least, to my wife Kristýna, this thesis would not exist without her continuous support and to my one-year-old son Oliver, who once tried to eat this thesis.

Title: On Market Efficiency, Optimal Distributional Trading Gain, and Utility Maximization

Author: Robert Navrátil

Department: Department of Probability and Mathematical Statistics, MFF UK

Supervisor: doc. RNDr. Jan Večeř, Ph.D., Department of Probability and Mathematical Statistics, MFF UK

Abstract: The aim of this thesis is multifold. First, using results from the optimal distributional trading gain problem, we determine a utility-maximizing portfolio that optimizes the benefit an agent may receive by trading the difference between his perceived future distribution of a security price and the risk-neutral density provided by the corresponding option market. Moreover, we show how one can fit the risk-neutral density directly from option market data using the SVI parameterization. We use integer programming with kernel search heuristics to statically replicate the optimal payoff. Second, we show that the United States equity market was inefficient during the weeks following the initiation of the COVID-19 pandemic. This is demonstrated by showing that utility-maximizing agents over the period ranging from mid-February to late March 2020 could generate statistically significant profits by utilizing historical price and virus-related data to forecast future equity ETF returns. Finally, we focus on the passport option. We present a version of insurance of a traded account that symmetrically treats both of its underlying assets. In our approach, we impose a natural symmetric limit in which the agent can fully invest in any underlying asset up to his current wealth and without shorting any asset. The optimal solution leads to a well-known stop-loss strategy when all wealth is invested in only one asset.

Keywords: Utility maximization, Optimal distributional trading gain, Efficient market hypothesis, Passport option

Contents

Introduction

The main goal of this dissertation is to present contributions to the efficient market hypothesis and the optimal distributional trading gain problem as described in the following articles:

1. Večeř, J., J. Kampen, and R. Navrátil (2020). Options on a traded account: symmetric treatment of the underlying assets. *Quantitative Finance 20* (1), 37–47, `https://doi.org/10.1080/14697688.2019.1634278`

2. Navrátil, R., S. Taylor, and J. Večeř (2021). On equity market inefficiency during the COVID-19 pandemic. *International Review of Financial Analysis 77*, 101820, `https://doi.org/10.1016/j.irfa.2021.101820`

3. Navrátil, R., S. Taylor, and J. Večeř (2022). On the Utility Maximization of the Discrepancy between a Perceived and Market Implied Risk Neutral Distribution, *European Journal of Operational research*, `https://doi.org/10.1016/j.ejor.2022.01.048`

We start by briefly introducing the main contributions of the articles. We study the symmetric version of a passport option in Večeř et al. (2020), where we find the optimal strategy for the holder of the option. In Navrátil et al. (2021), we study the market efficiency during the COVID-19 pandemic, and we conclude that the market was inefficient. Finally, in Navrátil et al. (2022), we focus on the optimal distributional trading gain problem from a practitioner's perspective, and we show how one can approximate the replication of the optimal payoff using a portfolio with integer positions in vanilla options.

All the articles are based upon the premise of the efficient market hypothesis, which plays a fundamental role in modern finance and economics. Introduced by Nobel price winner Eugene Francis Fama in his seminal work Fama (1965), the efficient market hypothesis has had a tremendous influence on our understanding of capital markets. In its most potent form, the efficient market hypothesis states that prices fully reflect available information, both public and private, and thus it is impossible to outperform the market systematically. Even though the efficient market theory has been widely studied in the scientific literature, there is still no consensus on whether this theory should be rejected or accepted. To this day, the efficient market hypothesis is still veryactively studied in the scientific literature to better understand financial markets.

Closely related to the efficient market hypothesis is the notion of a market equilibrium, which can be viewed as an aggregated opinion of all agents in the market. The market's distributional opinion $\mathbb{Q}$ represents the risk-neutral density, and a utility-maximizing agent with distributional opinion $\mathbb{P}$ can only trade contracts with zero expected value from the market's perspective. This leads to the optimal distributional trading gain problem formally introduced by Večeř (2020), which provides a flexible framework for utility-maximizing agents that seek to find the optimal payoff given a distributional discrepancy between their opinion and that of the market.

This thesis is divided into six chapters. The first chapter contains preliminaries from stochastic calculus and dynamic programming needed throughout the

text. The second chapter focuses on stochastic finance. In this chapter, we discuss the efficient market hypothesis. Moreover, we discuss the optimal distributional trading gain problem introduced above. Unfortunately, there does not typically exist a traded instrument with a payoff that corresponds to the optimal payoff from the trading gain problem. Thus for practitioners, it is crucial to replicate this optimal payoff. In chapter three, we show how one can theoretically replicate the desired payoff using a static portfolio by trading in bonds, forwards, and vanilla put and call options.

Chapter 4 is based on the article Navrátil et al. (2021). In this part, we study the efficiency of the United States equity market during the COVID-19 pandemic contributing to the ongoing research on the effect of COVID-19 on financial data, see, for example, Baker et al. (2020); Azimli (2020); Cepoi (2020); Baek et al. (2020); Just and Echaust (2020); Mazur et al. (2021); Ahmar and Boj del Val (2020); Al-Awadhi et al. (2020); Topcu and Gulal (2020); Mirza et al. (2020). Using utility-maximizing agents, we demonstrate that the market was semi-strong inefficient from mid-February to late March 2020. An agent using Merton's portfolio would generate statistically significant profits across all studied ETFs during this period. Another important observation concerns the individual constituents of the S&P 500. We show that the larger the market beta of the constituent, the greater the inefficiency of the stock and thus the greater the opportunity for the utility-maximizing agent. On the other hand, the stock's leverage and cash assets were shown to negatively impact the final wealth of the utility-maximizing agent, corresponding to the result of Ramelli and Wagner (2020).

In Chapter 5, we extend the optimal trading gain problem using the results that appeared in Navrátil et al. (2022). In the current literature, the downside of the optimal trading gain problem is that there is generally no tradeable asset with the optimal payoff. Since the market's distributional opinion can be extracted from European option premia (Breeden and Litzenberger (1978)), one can use the SVI model to estimate the implied volatility surface, and then we can theoretically replicate the optimal payoff using a static portfolio. Theoretical replication is achieved using fractional positions in infinitely many vanilla options. However, it is impossible to have fractional positions in the option contracts, and only a limited set of options is traded. Restricting set used for replication was studied by Leung and Lorig (2016) and Bossu et al. (2021). We go a step further in the application for practitioners and study the problem as an integer programming problem conditioned on the number of options used for replication. Even for a small number of options used, we encounter extensive computational issues, and so we use kernel search heuristics introduced by Angelelli et al. (2010, 2012) to obtain an approximate solution to the problem. To our knowledge, we present the first constructive method to create an options portfolio that maximized the expected utility of an agent based upon the difference between his view on the future price distribution of an underlying asset price and that of the associated options market.

Chapter 6 is devoted to passport options and the role of volatility in the option contract. Passport option contracts introduced by Hyer et al. (1997) in its most common form allows the client to continuously move wealth between two assets S resp. M, typically representing the stock market and the money market. The

contract has a contractual constraint on the position in the first asset S, typically $[-1, 1]$, and the rest of the client's wealth is invested in the second asset M. The client can keep the trading profits at the option contract's expiration while his loss is forgiven. Even though this contract was traded, it was not very popular, probably due to the fact that it was expensive. In Večeř et al. (2020) we present a version of the passport option that works like insurance on actively traded accounts. To make the contract attractive for investors with longer horizons, we need to modify the passport option contract in two ways. Firstly, we treat both assets symmetrically, and we set the payoff of the contract to be in the index asset with equal weights $I = \frac{S+M}{2}$. Secondly, we remove the leverage by allowing only long positions, making the option contract less expensive. We show that the optimal strategy is fully investing in the cheaper asset, and we discuss a possible extension of the model to multiple assets.

1. Preliminaries

This chapter covers topics from stochastic calculus theory and dynamic programming principle. First, in the stochastic calculus section, we introduce the definition of a martingale. In finance, martingales are often used to model market prices, as they do not allow arbitrage opportunities. Next, we formulate Itô's formula and Girsanov's Theorem. Girsanov's Theorem describes the dynamics of a stochastic process when we change the associated probability measure to an equivalent probability measure. Girsanov's Theorem is often used in pricing theory when changing the associated measure to the risk-neutral measure. In the second section, we introduce the Hamilton-Jacobi-Bellman (HJB) equation. The HJB equation is used to find the optimal control of a given stochastic control problem. Finally, we illustrate the usage of the dynamic programming principle on a classic Merton's problem in one dimension. In this case, the agent can continuously transfer wealth between a risky asset and a riskless bond. The agent's goal is to find the optimal strategy that maximizes his expected terminal utility.

1.1 Stochastic calculus

Definition 1.1.1. *Let $(\Omega, \mathcal{F}, \mathbb{P})$ be a probability space. By filtration we mean the family $\{\mathcal{F}_t, t \geq 0\}$ of σ–algebras such that for all $0 \leq s \leq t < \infty$ it holds*

$$\mathcal{F}_s \subset \mathcal{F}_t \subset \mathcal{F}.$$

Definition 1.1.2. *Let $(\Omega, \mathcal{F}, \mathbb{P})$ be a probability space. We say that the filtration $\{\mathcal{F}_t, t \geq 0\}$ satisfies the usual conditions if the filtration*

- *is right continuous, i.e., $\mathcal{F}_t = \bigcap_{s>t} \mathcal{F}_s$ for all $t \geq 0$.*
- *contains all null sets in $\mathcal{F}$, i.e. $\mathcal{F}_0 \supset \{N \in \mathcal{F} : P(N) = 0\}$.*

We will always assume that the filtration satisfies the usual conditions throughout this text. Even though this condition is sometimes not necessary, it simplifies mathematical technicalities. For example, instead of assuming that $\mathbb{P}$–almost all trajectories of a stochastic process are continuous, we can, without loss of generality, instead assume that all trajectories are continuous. For more information, see, for example, Karatzas and Shreve (1991).

Definition 1.1.3. *(Martingale) We say that process $M = \{M(t), t \geq 0\}$ is $\mathcal{F}_t$–martingale, if*

(i) M is $\mathcal{F}_t$–adapted;

(ii) $\mathbb{E}[|M(t)|] < \infty$ for all $t \geq 0$;

(iii) $\mathbb{E}[M(t) \mid \mathcal{F}_s] = M(s)$ $P-a.s.$ for all $0 \leq s \leq t < \infty$.

Definition 1.1.4. *(Local martingale) Let $X = \{X(t), t \geq 0\}$ be a continuous $\mathcal{F}_t$–adapted process. We say that X is a continuous $\mathcal{F}_t$–local martingale, if there exist $\mathcal{F}_t$–stopping times T_n, $n \in \mathbb{N}$ such that*

- *the sequence* $\{T_n\}_{n=1}^{\infty}$ *is increasing and* $T_n \underset{n\to\infty}{\longrightarrow} +\infty \quad P-a.s.;$
- *processes* $X^{(n)} = \{X(\min\{t, T_n\}) - X(0), \quad t \geq 0\}$ *are continuous* $\mathcal{F}_t$*–martingales.*

The following definition is a generalization of a local martingale.

Definition 1.1.5. *(Semimartingale) We say that* $\mathcal{F}_t$*–adapted process* $X = \{X(t), t \geq 0\}$ *is a continuous* $\mathcal{F}_t$*–semimartingale if there exists a representation*

$$X(t) = X(0) + M(t) + V(t), \quad \text{for every } t \geq 0 \quad P-a.s.,$$

where $M = \{M(t), t \geq 0\}$ *is a continuous* $\mathcal{F}_t$*–local martingale and* $V = \{V(t), t \geq 0\}$ *is a continuous* $\mathcal{F}_t$*–adapted process with trajectories in* $BV_{loc}(\mathbb{R}_+) = \{f : \mathbb{R}_+ \to \mathbb{R} : \forall t \ f$ *has locally bounded variation on [0,t]}* P*-a.s. and* $M(0) = V(0) = 0$*.*

Theorem 1.1.6. *(Doob–Meyer decomposition) For any two continuous* $\mathcal{F}_t$*–local martingales* M*,* N *there is a unique* $\mathcal{F}_t$*–adapted continuous process of bounded variation* $\langle M, N\rangle = \{\langle M, N\rangle_t, t \geq 0\}$ *satisfying* $\langle M, N\rangle_0 = 0, \ \mathbb{P}$*–a.s., such that process* $MN - \langle M, N\rangle$ *is a continuous* $\mathcal{F}_t$*–local martingale. If* $M = N$*, we write* $\langle M\rangle = \langle M, N\rangle$ *and this process is non-decreasing.*

Proof. See Karatzas and Shreve (1991) Problem 1.5.17. □

The uniqueness in the Theorem 1.1.6 is meant in the sense of indistinguishability; see Karatzas and Shreve (1991).

Definition 1.1.7. *We call the process* $\langle M, N\rangle$ *in the Theorem* 1.1.6 *the cross-variation of* M *and* N*. If* $M = N$*, we call the process* $\langle M\rangle$ *the quadratic variation of* M*.*

We shall introduce a new notation for the following Theorem. For a function f, by $f_{x_i x_j}$ we mean $\frac{\partial^2 f}{\partial x_i \partial x_j}$, similarly for f_t and f_{x_i}. Furthermore, by $\mathcal{C}^{1,2}(\mathbb{R}^n)$ we mean a set of functions $f(t,x) : [0,\infty) \times \mathbb{R}^n \mapsto \mathbb{R}$ such that the partial derivatives $f_t, f_{x_i}, f_{x_i,x_j}$ exist and are continuous for $1 \leq i \leq j \leq n$. Similarly, we will use $\mathcal{C}_p^{1,2}(\mathbb{R}^n)$ for functions f that also satisfies polynomial growth condition on $\mathbb{R}^n$, i.e. for some constants C, k we have $f(t,x) \leq C(1 + (x^T x)^k)$.

Theorem 1.1.8. *(Itô's formula) Let* $M = (M^{(1)}, \ldots, M^{(n)})^T$ *be a vector of continuous* $\mathcal{F}_t$*–local martingales,* $V = (V^{(1)}, \ldots, V^{(n)})^T$ *be a vector of* $\mathcal{F}_t$*–adapted processes of bounded variation with* $V(0) = 0$ *and finally, let* $W = (W^{(1)}, \ldots, W^{(n)})^T$ *be n-dimensional* $\mathcal{F}_t$*–Wiener proces. Set*

$$X(t) = X(0) + M(t) + V(t), \qquad 0 \leq t < \infty.$$

Then for any $f(t,x) : [0,\infty) \times \mathbb{R}^n \mapsto \mathbb{R}$ *such that* $f \in \mathcal{C}^{1,2}(\mathbb{R}^n)$ *holds*

$$\begin{aligned} f(t, X(t)) = f(0, X(0)) &+ \int_0^t f_t(s, X(s))ds + \sum_{i=1}^n \int_0^t f_{x_i}(s, X(s))dV^{(i)}(s) \\ &+ \sum_{i=1}^n \int_0^t f_{x_i}(s, X(s))dM^{(i)}(s) \\ &+ \frac{1}{2}\sum_{i=1}^n \sum_{j=1}^n \int_0^t f_{x_i x_j}(s, X(s))d\langle M^{(i)}, M^{(j)}\rangle_s, \ \text{for any } t \geq 0 \ \mathbb{P}-a.s. \end{aligned}$$

This can be rewritten in a differential form as

$$df(t,X(t)) = f_t(t,X(t))dt + \sum_{i=1}^{n} f_{x_i}(t,X(t))dV^{(i)}(t) + \sum_{i=1}^{n} f_{x_i}(t,X(t))dM^{(i)}(t) + \frac{1}{2}\sum_{i=1}^{n}\sum_{j=1}^{n} f_{x_i x_j}(t,X(t))d\langle M^i, M^j\rangle_t, \quad 0 \le t < \infty.$$

Moreover, process $\{f(t,X(t)), t \ge 0\}$ *is* $\mathcal{F}_t$*–semimartingale.*

Proof. The proof of the one-dimensional case is in Karatzas and Shreve (1991), Theorem 3.3.3. □

The following Theorem is a useful generalization of Itô's formula. It allows us to extend the class of functions used in Itô's formula to convex functions, which are not necessarily differentiable at all points. Convex functions are widely used in finance and often represent the payoff of some option contract. Thus it is desirable to generalize the Itô's formula to this class of functions. To do that, let us denote by D^- the left-hand derivative.

Theorem 1.1.9. *(Generalized Itô's formula) Let* X *be a continuous local martingale, then there exists a martingale local time for* X*, i.e. a non-negative random field* $\Lambda = \{\Lambda_t(a,\omega), (t,a) \in [0,\infty) \times \mathbb{R}, \omega \in \Omega\}$ *such that the following hold:*

- *For every convex function* $f : \mathbb{R} \mapsto \mathbb{R}$*, we have the generalized change of variable formula:*

$$f(X(t)) = f(X(0)) + \int_0^t D^- f(X(s))dX(s) + \int_{-\infty}^{\infty} \Lambda_t(a)d\mu(a); \qquad 0 \le t < \infty,\ P-a.s,$$

  where μ *is the second derivative measure of the function* f*, that is*

$$\mu[a,b) = D^- f(b) - D^- f(a).$$

- *for every Borel measurable function* $k : \mathbb{R} \mapsto [0,\infty)$ *the identity*

$$\int_0^t k(X(s,\omega))d\langle X\rangle_s(\omega) = 2\int_{-\infty}^{\infty} k(a)\Lambda_t(a,\omega)da, \quad 0 \le t < \infty \tag{1.1}$$

  holds for almost all $\omega \in \Omega$*.*

- *For almost all* $\omega \in \Omega$ *it holds for each* $a \in \mathbb{R}$ *that*

$$\int_0^{\infty} \mathbb{1}_a(X(s))\langle X\rangle_s ds = 0. \tag{1.2}$$

Proof. This Theorem is a martingale version of more general semimartingale Theorem 3.7.1. and Exercise 3.7.10. in Karatzas and Shreve (1991). □

As mentioned earlier, martingales are an important term in stochastic finance. For example, martingales are widely used in asset pricing theory. However, the process $\{f(t, X(t)), t \geq 0\}$ from Itô's formula is $\mathcal{F}_t$–semimartingale and not a (local) $\mathcal{F}_t$–martingale. Thus, we need some way to change the process $\{f(t, X(t)), t \geq 0\}$ into $\mathcal{F}_t$–martingale. The next Theorem plays a fundamental role in the asset pricing literature, as it allows us to describe the evolution of the stochastic process under an equivalent probability measure.

Theorem 1.1.10. *(Girsanov's Theorem) Let $W = (W^{(1)}, \ldots, W^{(n)})^T$ be n-dimensional $\mathcal{F}_t$–Wiener process and let $X = (X^{(1)}, \ldots, X^{(n)})^T$ be a vector of $\mathcal{F}_t$–progressively measurable process such that $\mathbb{E}\left[\int_0^T X(t)^T X(t) dt\right] < \infty$ for some $T > 0$. Set*

$$G(t, X) = \exp\left(\sum_{i=1}^{n} \int_0^t X^{(i)}(s) dW^{(i)}(s) - \frac{1}{2} \int_0^t X(s)^T X(s) ds\right), \quad 0 \leq t \leq T.$$

Assume

$$\mathbb{E}[G(T, X)] = 1. \tag{1.3}$$

Define the probability measure $\tilde{\mathbb{P}}$ on $\mathcal{F}_T$ by $\frac{d\tilde{\mathbb{P}}}{d\mathbb{P}} = G(T, X)$ and set

$$\widetilde{W}^{(i)}(t) = W^{(i)}(t) - \int_0^t X^{(i)}(s) ds, \quad 0 \leq t \leq T, \quad i \in 1, \ldots, n.$$

Then $\widetilde{W} = (\widetilde{W}^{(1)}, \ldots, \widetilde{W}^{(n)})^T$ is an n-dimensional $\mathcal{F}_t$–Wiener process on probability space $(\Omega, \mathcal{F}_T, \tilde{\mathbb{P}})$.

Proof. See Theorem 3.5.1. in Karatzas and Shreve (1991) or Girsanov (1960). □

To use the Theorem, 1.1.10 we need some criterion to check (1.3). One of such criteria is the Novikov's condition.

Theorem 1.1.11. *(Novikov's condition) Let $W = (W^{(1)}, \ldots, W^{(n)})^T$ be n-dimensional $\mathcal{F}_t$–Wiener process and let $X = (X^{(1)}, \ldots, X^{(n)})^T$ be a vector of $\mathcal{F}_t$–adapted processes satisfying*

$$\mathbb{P}\left(\int_0^T (X^{(i)}(t))^2 dt < \infty\right) = 1, \quad 1 \leq i \leq n, \ 0 \leq T < \infty.$$

If

$$\mathbb{E}\left[\exp\left(\frac{1}{2} \int_0^T X(t)^T X(t) ds\right)\right] < \infty, \quad 0 \leq T < \infty,$$

then process $Z = \{Z(X, t), 0 \leq t < \infty\}$ defined by

$$Z(X, t) = \exp\left(\sum_{i=1}^{n} \int_0^t X^{(i)}(s) dW^{(i)}(s) - \frac{1}{2} \int_0^t X(t)^T X(t) ds\right)$$

is $\mathcal{F}_t$–martingale.

Proof. See Corollary 3.5.13 in Karatzas and Shreve (1991). □

1.2 Dynamic programming

This section introduces the Hamilton-Jacobi-Bellman equation, which gives necessary and sufficient conditions for the optimality of both control and value of a stochastic control problem. Given a smooth solution v of the dynamic programming equation, we present the sufficient conditions for v to be the value function V of the presented problem. With the value function known, we can find the optimal stochastic control by finding the maximizer in the HJB equation. Even though the results are far-reaching, the proof relies on Itô's formula. Finally, we illustrate the dynamic programming principle on a typical control problem example in mathematical finance, Merton's optimal portfolio problem.

Before we get to the verification Theorem, we need to introduce Markov processes first. These processes are commonly used in mathematical finance because at any time r, the state of the process $\xi(r)$ contains all relevant information for the evolution of the process ξ for times $t > r$. For example, this means that we can omit the whole history of the process ξ prior to time r when studying the optimal control. This is often used in the efficient market hypothesis, where it is assumed that asset prices reflect all available information on the market, and thus do not depend on history. In this section, we closely follow sections 5.5., 6.3 and 6.4 in Fleming and Rishel (2012).

To ease the notation, we introduce the transition function $\hat{P}$ by

$$\hat{P}(s, y, t, B) = \mathbb{P}(\xi(t) \in B | \xi(s) = y).$$

Furthermore, similarly, we introduce the conditional expectation $\mathbb{E}^{sy}$. Moreover, throughout this section, we assume that ξ is a stochastic process on a time interval $\mathcal{T}$ with state-space Σ, which is a complete separable metric space. Mathematically, the definition of the Markov process is

Definition 1.2.1. *(Markov process) A stochastic process ξ on a time parameter set $\mathcal{T}$ with state space Σ is a Markov process if*

- *For any $t_1 < t_2 < \cdots < t_n$ in $\mathcal{T}$ and $B \in \mathcal{B}(\Sigma)$ holds*

$$\mathbb{P}(\xi(t) \in B | \xi(t_1), \ldots, \xi(t_n)) = \mathbb{P}(\xi(t) \in B | \xi(t_n)).$$

- *$\hat{P}(s, \cdot, t, B)$ is $\mathcal{B}(\Sigma)$–measurable for fixed s, t, and B.*
- *$\hat{P}(s, y, t, \cdot)$ is a probability measure on $\mathcal{B}(\Sigma)$ for fixed s, y, and t.*
- *For $s < r < t, s, r, t \in \mathcal{T}$ holds the Chapman-Kolmogorov equation*

$$\hat{P}(s, y, t, B) = \int_{\Sigma} \hat{P}(r, x, t, B) \hat{P}(s, y, r, dx).$$

We will often work with a class of Markov processes called diffusion processes.

Definition 1.2.2. *(Diffusion process) A Markov process on an interval $\mathcal{T}$ is called an n-dimensional diffusion process if*

- *For every $\epsilon > 0, t \in \mathcal{T}, x \in E^n$*

$$\lim_{h \mapsto 0} \frac{1}{h} \int_{|x-z|>\epsilon} \hat{P}(t, x, t+h, dz) = 0$$

- *There exist functions* $a_{ij}(t,x), b_i(t,x), i,j = 1,\dots,n$ *such that for every* $\epsilon > 0$ *and* $t \in \mathcal{T}, x \in E^n$

$$\lim_{h\mapsto 0}\frac{1}{h}\int_{|x-z|\leq\epsilon}(z_i - x_i)\hat{P}(t,x,t+h,dz) = b_i(t,x)$$
$$\lim_{h\mapsto 0}\frac{1}{h}\int_{|x-z|\leq\epsilon}(z_i - x_i)(z_j - x_j)\hat{P}(t,x,t+h,dz) = a_{ij}(t,x).$$

Under sufficient conditions, diffusion processes are solutions to a stochastic differential equation

$$\xi^{t,x}(s) = x + \int_t^s b(u,\xi^{t,x}(u))du + \int_t^s \sigma(u,\xi^{t,x}(s))dW(u), \quad s \geq t, \tag{1.4}$$

with $a(t,x) = \sigma(t,x)\sigma^T(t,x)$ and starting point $\xi^{t,x}(t) = x$. The vector function b is called the local drift coefficient, and the matrix-valued function a is called the local covariance matrix. The meaning is apparent from (1.4).

Definition 1.2.3. *Let* $X^{t,x} = \{X^{t,x}(s), s \geq t\}$ *be the unique strong solution of*

$$X^{t,x}(s) = x + \int_t^s b(u,X^{t,x}(u))du + \int_t^s \sigma(u,X^{t,x}(s))dW_u, \quad s \geq t,$$

where μ *and* σ *satisfy the condition required for the existence and uniqueness of a strong solution.*

For a function $f : \mathbb{R}^n \mapsto \mathbb{R}$ *we define the function* $\mathcal{A}(t)f$ *by*

$$\mathcal{A}(t)f(x) = \lim_{h\mapsto 0}\frac{\mathbb{E}\left[f(X^{t,x}(t+h))\right] - f(x)}{h}$$

if the limit exists.

We can immediately see that the domain of the operator $\mathcal{A}(t)$, called the generator of X, contains all $\psi \in \mathcal{C}^2(\mathbb{R}^n)$ and

$$\mathcal{A}(t)\psi = \frac{1}{2}\sum_{i,j=1}^n a_{i,j}(t,x)\frac{\partial^2\psi}{\partial x_i \partial x_j} + \sum_{i=1}^n b_i(t,x)\frac{\partial\phi}{\partial x_i}.$$

There is a helpful link between diffusions and solutions to stochastic differential equations.

Theorem 1.2.4. *Assume that* Q *is an open set,* τ *is the exit time from* Q*, and* $(s,y) \in Q$*. Moreover, assume*

- b, σ *satisfy linear growth*
- ψ *is in* $\mathcal{C}_p^{1,2}(Q)$*,* ψ *is continuous on the closure of* Q
- $\psi_t + \mathcal{A}(t)\psi + M(t,x) \geq 0$ *for all* $(t,x) \in Q$ *where* $\mathbb{E}^{sy}\left[\int_s^\tau |M(t,\xi(t))|dt\right] < \infty$

Then

$$\psi(s,y) \leq \mathbb{E}\left[\int_s^\tau M(t,\xi(t))dt + \psi(\tau,\xi(\tau))\right].$$

Proof. See Theorem 5.5.1 in Fleming and Rishel (2012). □

Theorem 1.2.4 has important consequence.

Theorem 1.2.5. *Assume that Q is an open set, τ is the exit time from Q, and $(s,y) \in Q$. Moreover, assume*

- *b, σ satisfy linear growth*
- *ψ is in $\mathcal{C}_p^{1,2}(Q)$, ψ is continuous on the closure of Q*
- *$\mathbb{E}^{sy}\left[\int_s^\tau |\psi_t + \mathcal{A}(t)\phi| dt\right] < \infty$ for each $(s,y) \in Q$.*

Then

$$\psi(s,y) = -\mathbb{E}^{sy}\left[\int_s^\tau (\psi_t + \mathcal{A}(t)\psi)\, dt\right] + \mathbb{E}^{sy}\psi(t, \xi(\tau)).$$

Proof. Easily follows from Theorem 1.2.4. □

Theorem 1.2.5 shows the role of a generator $\mathcal{A}$ as the link between linear partial differential equations and the conditional expectation of a diffusion process. This link plays an important role in the theory of stochastic optimal control in the form of a verification theorem. Until the end of the section, consider a stochastic differential equation of the form

$$d\xi(t) = f(t, \xi(t), u(t))dt + \sigma(t, \xi(t), u(t))dw, \quad t \geq s \tag{1.5}$$

where u represents the control process of the agent. The goal of the agent is to find the optimal control $\boldsymbol{u}^\star$ that minimizes

$$J(s, y, \boldsymbol{u}) = \mathbb{E}^{sy}\left[\int_s^T L(t, \xi(t), u(t)) + \Psi(\xi(T))\right],$$

over all admissible $\boldsymbol{u}$ for some a priori given continuous functions L and Ψ with polynomial growth. First, we need to introduce the control process to present the verification theorem formally.

Definition 1.2.6. *An admissible feedback control law is a borel measurable function $\boldsymbol{u} : [T_0, T] \times \Sigma \mapsto U$ satisfying*

- *For each initial data (s,y), there exists a Brownian motion W such that the SDE (1.5) has a unique probability law solution ξ with $\xi(s) = y$*
- *For each $k > 0$ the expected value $\mathbb{E}^{sy}[|\xi(t)|^k]$ is bounded for $t \in [s,T]$*
- *For each $k > 0$ we have $\mathbb{E}\left[\int_s^T |\boldsymbol{u}(t)(t, \xi(t))|^k dt\right] < \infty$.*

At each time t, the control $u(t)$ is applied via a feedback control law $\boldsymbol{u}$

$$u(t) = \boldsymbol{u}(t, \xi(t)).$$

With this feedback control $\boldsymbol{u}$, there is an associated transition function $\hat{P}^{\boldsymbol{u}}$ and the generator $\mathcal{A}^{\boldsymbol{u}}$ defined in an obvious manner.

Finally, we make the following assumptions about f and σ. We suppose that $f, g \in \mathcal{C}^1([T_0, T] \times E^n \times U)$ and for some C

$$|f(t,0,0)| \leq C \qquad |\sigma(t,0,0)| \leq C$$
$$|f_x| + |f_u| \leq C \qquad |\sigma_x| + |\sigma_u| \leq C.$$

The above conditions ensure that the function J depends only on the control $\boldsymbol{u}$ and is finite for every admissible control.

Theorem 1.2.7. *(Verification Theorem) Let $W(s,y)$ be a solution of the dynamic programming equation*

$$0 = W_s + \min_{v \in U} \left[\mathcal{A}^v(s) + L(s,x,v) \right], \quad (s,y) \in Q, \tag{1.6}$$

with boundary data

$$W(s,y) = \Psi(s,y), \quad (s,y) \in \partial^\star Q,$$

such that W is in $\mathcal{C}_p^{1,2}(Q)$, continuous on the closure of Q and $\partial^\star Q$ is a closed subset of boundary of Q such that $(\tau, \xi(\tau)) \in \partial^\star Q$ with probability 1. Then:

- *$W(s,y) \leq J(s,y,\boldsymbol{u})$ for any admissible feedback control $\boldsymbol{u}$ and any initial data $(s,y) \in Q$.*
- *If $\boldsymbol{u}^\star$ is an admissible feedback control such that*

  $$\mathcal{A}^{\boldsymbol{u}^\star}(s)W + L^{\boldsymbol{u}^\star}(s,y) = \min_{v \in U} \left[\mathcal{A}^v(s)W + L(s,y,v) \right]$$

  for all $((s,y) \in Q)$ then $W(s,y) = J(s,y,\boldsymbol{u}^\star)$ for all $(s,y) \in Q$, i.e. $\boldsymbol{u}^\star$ is optimal.

Proof. See Theorem 6.4.1 in Fleming and Rishel (2012). □

Typically, the optimal control is thus found by showing the existence of a smooth solution W to the HJB equation (1.6) and then showing that this smooth solution is the value function of the stochastic control problem, which quickly yields the optimal control. Unfortunately, the smoothness assumption of the value function W can fail even for simple examples, and thus one has to consider the viscosity solutions introduced by Crandall and Lions (1983). We illustrate the dynamic programming theory with a classical example in mathematical finance called the Merton problem, which was first introduced in Merton (1969) and Merton (1975). Since then, the Merton problem has been actively researched. For an excellent review, see the book Rogers (2013) which is solely dedicated to the Merton problem.

Commonly, the Merton problem describes an agent who invests in one or more risky assets and wishes to maximize his final expected utility. The agent can invest in n-dimensional risky asset S described by a semimartingale process with dividend rate δ or accrue interest at risk-free rate r. The dynamics of the wealth of the agent with some initial wealth $w(0)$ can be described through equation of the form

$$dw(t) = r(t)w(t)dt + u(t)\left(dS(t) - r(t)S(t)dt + \delta(t)dt\right) + e(t)dt - c(t)dt,$$

where process u represents the control of the agent and processes e resp. c represents endowment resp. consumption.

For the simplest example, we assume that only one asset is available on the market, i.e. n=1. The price of the risk-free asset B follows

$$dB(t) = B(t)rdt$$

and the price of the risky asset S follows a geometric Brownian motion

$$dS(t) = \alpha S(t)dt + \sigma S(t)dW(t).$$

The parameter α is called the drift and the parameter $\sigma > 0$ is called the volatility of the asset S. The common assumption is that $r < \alpha$, which we also assume. The agent invests at any time t a fraction $u(t)$ of his wealth w in a stock S, while the remainder is invested in the bond B. We assume no consumption process c and we impose no constraint on the control, i.e. $u(t) \in \mathbb{R}$. The evolution of the agent's wealth w satisfies the following stochastic differential equation

$$\begin{aligned} dw(t) &= w(t)rdt + u(t)w(t)\left((\alpha - r)dt + \sigma dW(t)\right) \\ w(s) &= y. \end{aligned}$$

We suppose that the agent uses power utility function $U(x) = \frac{x^{1-a}-1}{1-a}$ with risk aversion parameter a, and wishes to maximize his expected terminal utility

$$J = \mathbb{E}^{sy}\left[U(W(\tau))\right],$$

where $\rho > 0$ and τ denotes the time the agent goes bankrupt or the final time T, whichever occurs first. Clearly, τ is a stopping time. The dynamic programming equation can be written in the form

$$0 = W_s + rxW_x + \max_u \left[u(\mu - r)xW_x + \frac{1}{2}x^2u^2\sigma^2W_{xx}\right], \tag{1.7}$$

with $y > 0$ and boundary conditions $W(\tau, x) = U(x)$. Guessing $W(t, y) = g(t)\frac{x^{1-a}}{1-a}$ and plugging into HJB equation (1.7) we have

$$0 = g'(t)\frac{x^{1-a}}{1-a} + rx^{1-a}g(t) + g(t)\max_u \left[u(\mu - r)x^{1-a} + \frac{1}{2}u^2\sigma^2(-ax^{1-a})\right].$$

Thus, g should satisfy ordinary differential equation

$$\begin{aligned} 0 &= g'(t) + (1-a)g(t)\left(r + \max_u \left[u(\mu - r) - \frac{1}{2}au^2\sigma^2\right]\right), \\ g(\tau) &= 1. \end{aligned}$$

To ease notation, denote

$$\rho = \left((1-a)r + (1-a)\max_u \left[u(\mu - r) - \frac{1}{2}au^2\sigma^2\right]\right).$$

Solving the linear differential equation, one can find that

$$g(s) = e^{\rho(T-s)},$$

and so

$$W(t, x) = e^{\rho(T-s)}\frac{x^{1-a}}{1-a}.$$

Finally, substituting to the HJB equation we arrive at the optimal position

$$u(t) = \frac{\mu - r}{a\sigma^2}, \tag{1.8}$$

which is often called Merton's fraction.

It is interesting to note that we have found both the optimal control and the optimal value in the Merton's portfolio example above. However, it can be challenging for some problems to find their optimal value, yet one can say enough about the optimal value process to find the optimal control using the verification theorem. A typical example is passport options, where one can easily show the convexity in the spatial variable of the value function, which is sufficient to guess the optimal solution cleverly, see Henderson and Hobson (2000). Another approach, first used by Shreve and Večeř (2000) in this setting, is to use Hajek's mean comparison theorem.

Theorem 1.2.8 (Hajek's mean comparison Theorem)**.** *Let $\{M_t, t \in [0,T]\}$ be a continuous martingale with representation $M_t = M_0 + \int_0^t \sigma_s dW_s$. Assume that for some function ρ on $\mathbb{R}$, we have $|\sigma_s| \leq \rho(M_s)$ and there exists a unique solution (in the sense of probability law) N_t to the stochastic differential equation*

$$N_t = M_0 + \int_0^t \rho(N_s) dW_s. \tag{1.9}$$

Then for any convex function Φ and any $t \geq 0$,

$$\mathbb{E}[\Phi(M_t)] \leq \mathbb{E}[\Phi(N_t)].$$

Proof. See Theorem 3 in Hajek (1985). However, it is required that the function ρ is Lipschitz continuous in order for the stochastic differential equation (1.9) to have a unique solution in the sense of probability law. □

Hajek's Theorem states that maximizing volatility also maximizes the expected convex payoff. Theorem 1.2.8 has been generalized to stochastic sums by Kampen (2016).

2. Stochastic finance

2.1 Efficient market hypothesis

In this section, we introduce the efficient market hypothesis (EMH). EMH had a substantial influence on modern mathematical finance and is widely used as an underlying assumption in many financial models as it allows us to price assets fairly. EHM states that it is impossible to make a risk-free profit on the market and that the available information is fully reflected in the asset price. To fully grasp the impact of EMH on finance, it is useful to review its history. We follow an excellent overview from the articles Sewell (2011), Degutis and Novickytė (2014), and the references therein.

Louis Bachelier published his Ph.D. thesis in 1900 Bachelier (1900), where he argues that the expected profit of the speculator is always equal to zero. Bachelier used the Brownian motion to model stock prices ahead of his time. Later Cowles (1933) analyzed the trade statistics of investment professionals and concluded that the professionals were not able to earn excess returns over the market. Cowles came to the same conclusion eleven years later in his follow-up work Cowles (1944). Twenty years later, Fama laid the foundation stone of the efficient market hypothesis in his influential article Fama (1965). In his empirical analysis, Fama concluded that prices followed a random walk process, and he was the first to use the term efficient market. In the same year, Samuelson (1965) focused on martingale processes instead of a random walk for price processes, and thus was the first to provide formal arguments for the efficient market hypothesis. The efficient market hypothesis was popularized outside of academia by Malkiel (1973).

Roberts (1967) and Fama (1970) divided the efficient market hypothesis into three levels depending on how strong its assumptions are. The levels differ by the information set Ω_t available to traders at time t. In the weakest form, Ω_t consists only of current and past asset prices. Sometimes, Ω_t also consists of dividends, trading volume, or other information. If Ω_t also consists of all publicly known information, then EHM is in its semi-strong form. Most of the scientific literature focuses on these two forms. The third form is that Ω_t is enlarged by private information. Because the third form is a powerful assumption, it has many opponents. For example, Grossman and Stiglitz (1980) argues that private information can be costly, and one should expect excess returns over the market. Otherwise, agents would not allocate resources to obtain and analyze the information as it would not offer them any competitive edge.

One of the strongest arguments for the efficient market hypothesis is mutual funds' inability to systematically outperform the index. In Jensen (1968), the author analyzed actively managed funds in the US in the period 1945 to 1964. Surprisingly, the author found that the funds underperformed the market by approximately their expenses. In the continuation study, Malkiel (1995) analyzed US equity mutual funds in the period 1971 to 1991 and came to the same conclusion.

Not everyone agreed with the efficient market hypothesis, and from the 1980s, a growing amount of literature challenged the hypothesis. For example,

De Bondt and Thaler (1985) found empirical evidence that stock prices overreact to unexpected and dramatic news, thus weak form market inefficiency. In addition, they found that most of the excess returns were earned in January. This article is contributed to starting an alternative theory to EHM called behavioral finance. Chopra et al. (1992) found that the overreaction of stock prices is more substantial for smaller firms. Haugen (1995) argues that the short-run overreaction may lead to price reversal in the future. Finally, another competing theory to the efficient market hypothesis is the stochastic portfolio theory introduced by Fernholz (2002). Stochastic portfolio theory is a framework for studying the market microstructure and behavior of controlled portfolios while allowing arbitrage opportunities on the market.

At the same time, there was also a growing literature that supports efficient market hypothesis. In Metcalf and Malkiel (1994) the authors studied the recommendations of four expert portfolio managers and found no evidence that the experts can systematically beat the market. In Malkiel (2003), the author closely studied scientific articles that are against the efficient market hypothesis and concludes that markets are far more efficient than those papers suggest. Schwert (2003) studied market anomalies inconsistent with the efficient market hypothesis. The author concludes that once the anomalies were published in the scientific literature, practitioners implemented the associated trading strategies and the opportunities weakened or vanished, thus making the market more efficient. In Malkiel (2005), the author shows that professionally managed investment funds do not outperform index benchmarks. Recently, Richard and Večeř (2021) studied the efficient market hypothesis in football prediction market data and found no substantial trading opportunities.

We now return to the concept of martingales to better understand their role in the efficient market hypothesis via the First Fundamental Theorem of Asset Pricing; see Theorem 2.1.3 below. Even though the proof of this Theorem is short and straightforward, it plays a central role in the asset pricing literature and highlights the importance of the no-arbitrage principle. Before we formulate the Theorem, we first define no-arbitrage assets, and we discuss the distinction between an asset and its price as given by Večeř (2011).

Definition 2.1.1. *Asset X is said to be a no-arbitrage asset if it keeps the same value as time passes.*

Let us discuss some examples to better understand the definition of no-arbitrage assets. An example of an arbitrage asset is the US dollar, since one could short the asset and buy a money market asset, thus creating an arbitrage opportunity in terms of dollars. This idea is nicely illustrated in a famous saying that today's dollar is worth more than a dollar tomorrow. However, when one considers a money market account that continuously reinvests the generated interest, it is a no-arbitrage asset. Another example of an arbitrage asset is a stock that does not reinvest its dividends.

To formally define the price of an asset, consider assets X and Y. The price of an asset X is expressed in another asset Y, which we shall denote X_Y. Asset Y is called a numeraire or reference asset. The typical choice of Y is a currency or a money market account. Mathematically,

$$X = X_Y(t) \cdot Y. \tag{2.1}$$

The symbol "=" used in (2.1) has to be understood as an equivalence relation because X and Y are not numbers, but assets. We will write $X(t) = Y(t)$ in the sense of assets when $X_Y(t) = 1$ in the sense of numbers. The numeraire approach can look a bit redundant at first, but it often leads to significantly simplified calculations for asset pricing problems, which we will demonstrate when deriving the Black-Scholes formula (Black and Scholes (1973)). From the equation (2.1) easily follows two properties of the numeraire pricing approach. Firstly, the inverse price $Y_X(t)$ to $X_Y(t)$, has to be defined as

$$Y_X(t) = \frac{1}{X_Y(t)},$$

otherwise it would be possible to short one of the assets, go long on the other one, and make a risk-free profit. Secondly, it is easy to change the numeraire used in pricing.

Theorem 2.1.2 (Change of numeraire formula)**.** *Let X,Y,Z be assets. The prices satisfy a change of numeraire formula*

$$X_Y(t) = X_Z(t)Z_Y(t).$$

Proof. It follows from

$$X = X_Z(t) \cdot Z = X_Z(t) \cdot Z_Y(t) \cdot Y.$$

□

Finally, using the definition of the no-arbitrage asset, we can formulate the First Fundamental Theorem of Asset Pricing.

Theorem 2.1.3. *(First Fundamental Theorem of Asset Pricing) If there exists a probability measure $\mathbb{P}^Y$ such that the price processes $X_Y(t)$ are $\mathbb{P}^Y$–martingales, where X is an arbitrary no-arbitrage asset, and Y is an arbitrary no-arbitrage asset with a positive price, then there is no arbitrage in the market.*

Proof. Fix an asset Y. Suppose that there is an arbitrage in the market. Thus, one can start with a zero price portfolio $P_Y(0) = 0$ and obtain a portfolio $P_Y(T)$ such that the random variable $P_Y(T)$ satisfies $P_Y(T) \geq 0$ and $\mathbb{P}^Y(P_Y(T) > 0) > 0$. This is in contradiction with the martingale property of the process P_Y, since $\mathbb{E}^Y[P_Y(T)] > 0 = P_Y(0)$. □

To demonstrate the usage of the First Fundamental Theorem of Asset Pricing and the numeraire approach, we now derive the Black-Scholes formula for European options. We recall here that the European option contract is written on two assets X resp. Y, typically representing a stock resp. currency. At the expiration time T of the option, the buyer of the call (put) option has the right to buy (sell) the asset X for $K \cdot Y$, where K is defined a priori and is called the strike price. That is the payoff for call, resp. put option in terms of the asset Y is $(X_Y(T) - K)^+$ resp. $(K - X_Y(T))^+$. When pricing European option contracts, a standard assumption in finance is that prices follow a geometric Brownian motion with volatility parameter σ, i.e., we assume that there exists a martingale measure $\mathbb{P}^Y$ such that

$$X_Y(t) = \sigma X_Y(t) dW^Y(t),$$

where W^Y is a $\mathbb{P}^Y$–Brownian motion. The existence of the probability measure $\mathbb{P}^Y$ implies the existence of the probability measure $\mathbb{P}^X$ such that the price process Y_X is a $\mathbb{P}^X$–martingale. Denote Φ the cumulative distribution function of standardized normal distribution. Then, we can formulate and prove the Black-Scholes formula.

Theorem 2.1.4. *(Black-Scholes formula) Suppose that the price process $X_Y = \{X_Y(t), t \geq 0\}$ follows a geometric Brownian motion with volatility σ. Then the price of the European call option $C_Y^{BS}(t, X_Y(t), K)$ with strike K and expiration time T at time t is*

$$C_Y^{BS}(t, X_Y(t), K) = \Phi(d_+) \cdot X_Y(t) - K\Phi(d_-), \tag{2.2}$$

where

$$d_\pm = \frac{1}{\sigma\sqrt{T-t}} \log\left(\frac{X_Y(t)}{K}\right) \pm \frac{1}{2}\sigma\sqrt{T-t}.$$

Proof. We follow Večeř (2011). Note that the European call option payoff in terms of assets is a combination of two Arrow-Debreu securities

$$(X(T) - K \cdot Y(T))^+ = \mathbb{1}_{[X_Y(T) \geq K]} \cdot X(T) - K \cdot \mathbb{1}_{[X_Y(T) \geq K]} \cdot Y(T).$$

Thus, the price of the European call option is

$$C_Y^{BS}(t, X_Y(t), K) = \mathbb{P}^X(X_Y(T) \geq K | X_Y(t)) \cdot X_Y(t) - K\mathbb{P}^Y(X_Y(T) \geq K | X_Y(t)).$$

One can easily show that

$$\mathbb{P}^X(X_Y(T) \geq K | X_Y(t)) = \Phi\left(\frac{1}{\sigma\sqrt{T-t}} \log\left(\frac{X_Y(t)}{K}\right) + \frac{1}{2}\sigma\sqrt{T-t}\right)$$

and

$$\mathbb{P}^Y(X_Y(T) \geq K | X_Y(t)) = \Phi\left(\frac{1}{\sigma\sqrt{T-t}} \log\left(\frac{X_Y(t)}{K}\right) - \frac{1}{2}\sigma\sqrt{T-t}\right)$$

which yields (2.2). □

It is important to note that the premium C_Y^{BS} also depends on the volatility parameter σ, even though we do not explicitly state it as one of its arguments. We stress that, unlike other variables, the parameter σ is not directly observable from the market. Note that higher volatility yields higher option premia due to the convexity of the payoff.

In the case where one wishes that the reference asset Y is an arbitrage asset, for example, the US dollar, one can use the change of numeraire formula in the form $C_Y^{BS} = C_M^{BS} M_Y$ with asset M representing the money market account which is a no-arbitrage asset. With a constant interest rate r, this leads to the formula

$$C_Y^{BS}(t, X_Y(t), K) = \Phi(d_+) \cdot X_Y(t) - Ke^{-r(T-t)}\Phi(d_-). \tag{2.3}$$

Using put-call parity by Stoll (1969) one can immediately show that the price P_Y^{BS} for the put option is

$$P_Y^{BS}(t, X_Y(t), K) = Ke^{-r(T-t)}\Phi(-d_-) - \Phi(-d_+) \cdot X_Y(t) \tag{2.4}$$

To simplify the numeraire notation in the rest of the text, we often omit the reference asset Y in the X_Y price process if Y is either a currency or money market.

2.2 Optimal distributional trading gain problem

Specifying and deriving optimal strategies for utility-maximizing agents has been studied widely in many forms. Historically, its origins may be found in a 1738 article of Bernoulli, later republished in Bernoulli (1954). A more modern formulation of a related problem appeared in Kelly (1956) whose main result is commonly referred to as the Kelly criterion. This problem is typically understood in the specific context of a logarithmic utility-maximizing agent trading on a binary outcome, where the subjective belief of the agent differs from that of the broader market. For example, binary outcomes appear in betting markets, where the Kelly criterion determines the optimal bet size, given the agent's bankroll, on both possible outcomes. In the financial setting, the digital outcomes can be understood as Arrow-Debreu securities, and the corresponding prices as state prices introduced in Arrow (1964) and Debreu (1959).

Following Večeř (2020), we assume that there are two agents in the market. One represents a market taker with a distributional opinion $\mathbb{P}$ and strictly increasing concave utility function U, and the other represents a market maker with a distributional opinion $\mathbb{Q}$. The goal of the market taker is to find the optimal payoff B_1 that maximizes her expected utility. This market taker can construct an arbitrary payoff B_1 as long as its expected payoff from the perspective of the market measure $\mathbb{Q}$ is the initial wealth B_0. Mathematically, the market taker faces the following optimization problem

$$\begin{aligned} &\max_{B_1} \mathbb{E}^{\mathbb{P}}\left[U(B_1)\right] \\ &s.t. \;\; \mathbb{E}^{\mathbb{Q}}\left[B_1\right] = B_0. \end{aligned} \tag{2.5}$$

The optimal payoff B_1 of the optimization problem (2.5) is given by the following Theorem.

Theorem 2.2.1. *Let $U(x)$ be a utility function satisfying $U'(x) > 0$ and $U''(x) < 0$. Assume that p resp. q are the densities associated with $\mathbb{P}$ resp. $\mathbb{Q}$. Denote I to be the inverse of U'. Then the optimal random variable $B_1^\star$ from the optimal distributional gain problem* (2.5) *is given by*

$$B_1^\star(x) = I\left(\lambda \frac{q(x)}{p(x)}\right), \tag{2.6}$$

where λ solves

$$\mathbb{E}^{\mathbb{Q}}\left[I\left(\lambda \frac{q(x)}{p(x)}\right)\right] = B_0. \tag{2.7}$$

Proof. We follow Večeř (2020). Consider Lagrange-type functional associated with the constrained problem (2.5)

$$J[B_1] = \int [U(B_1(x))p(x) - \lambda B_1(x)q(x)]\, dx + \lambda B_0.$$

The optimal F must satisfy

$$\frac{\partial J}{\partial B_1} = 0,$$

which leads to

$$U'(B_1(x))p(x) - \lambda q(x) = 0. \tag{2.8}$$

Solving (2.8) for B_1, we can immediately see that

$$B_1(x) = I\left(\lambda \frac{q(x)}{p(x)}\right),$$

where λ solves

$$\mathbb{E}^{\mathbb{Q}}\left[I\left(\lambda \frac{q(x)}{p(x)}\right)\right] = B_0.$$

□

There are two things worth mentioning about the previous Theorem. First, notice that we only need to know the likelihood ratio $\frac{q}{p}$ to find the optimal $B_1^\star$. This can be useful not only in some applications, where one can only find p and q multiplied by some unknown constant c, but it also provides a direct link to the likelihood ratio between q and p. Second, both the expected utility gain and the expected profit are statistical divergences.

The solution of the above Theorem, under different conditions, has also appeared in Kramkov and Schachermayer (1999). However, their result is limited to positive random variables and utility functions satisfying Inada conditions. They approached the problem using the Legendre transform-based optimization technique.

In finance, the most common utilities are logarithmic utility, exponential utility, and power utility, and therefore it is worth showing the formula for the optimal payoff $B_1^\star$ for these utilities.

Example 2.2.1. (Logarithmic Utility) Let $U(x) = \log(x)$, then one can easily compute that

$$B_1^\star(x) = B_0 \frac{p(x)}{q(x)}.$$

Note that the expected utility $\mathbb{E}^{\mathbb{P}}[U(B_1^\star)] = \log(B_0) + D_{KL}(\mathbb{P}||\mathbb{Q})$, where D_{KL} is a Kullback-Leibler divergence, which is also called relative entropy. For more information see Kullback and Leibler (1951).

Example 2.2.2. (Exponential Utility) Let $U(x) = 1 - \exp(-x)$, then

$$\begin{aligned} B_1^\star(x) &= \left[\log\left(\frac{p(x)}{q(x)}\right) + \int \log\left(\frac{q(x)}{p(x)}\right) q(x)dx\right] + B_0 \\ &= \left[\log\left(\frac{p(x)}{q(x)}\right) + D_{KL}(\mathbb{Q}||\mathbb{P})\right] + B_0. \end{aligned}$$

Thus, the expected profit is the sum of two Kullback-Leibler divergences and the invested initial wealth B_0. The expected utility can be written in the form

$$\mathbb{E}^{\mathbb{P}}\left[U(B_1^\star)\right] = 1 - \exp\left(D_{KL}(\mathbb{Q}||\mathbb{P}) - B_0\right).$$

Example 2.2.3. (Power Utility) For $a > 0$, let $U(x) = \frac{x^{1-a}-1}{1-a}$. This leads to

$$B_1^\star(x) = \frac{B_0 \left(\frac{p(x)}{q(x)}\right)^{\frac{1}{a}}}{\int \left(\frac{p(x)}{q(x)}\right)^{\frac{1}{a}} q(x)dx}. \tag{2.9}$$

Clearly, for $a \to 1$, the power utility converges to the logarithmic utility.

The relationship of logarithmic utility and power utility with Kullback-Leibler divergence was first observed by Večeř (2020). This relationship is remarkable. In model selection theory, an information theory approach is to select a model with the lowest Akaike criterion Akaike (1974). Since the Akaike criterion is based on Kullback-Leibler divergence, the criterion tries to select the model with the lowest information loss with respect to the data. For utility-maximizing agents, this means that the larger the divergence between the market measure and the market taker's measure, the larger the opportunity for the market taker. Intuitively, this makes sense, as one would expect a more significant discrepancy to yield larger gains for the market taker.

For the specific choice of logarithmic utility and binary outcome variable, we can replicate the Kelly criterion.

Remark 2.2.1. (Kelly Criterion) Assuming that the subjective probability $\mathbb{P}$ assigned a value $\mathbb{P}(X = 1) = p$ to an event X and the market probability, given by $\mathbb{Q}$ assigned $\mathbb{P}(X = 1) = q$, the optimal payoff $B_1^\star$ for $U(x) = \log(x)$ and initial wealth B_0 is

$$B_1^\star = \begin{cases} B_0 \cdot \frac{p}{q} & X = 1 \\ B_0 \cdot \frac{1-p}{1-q} & X = 0. \end{cases}$$

The Kelly criterion is typically stated in terms of the fraction of the bankroll that is lost on the outcome of $X = 0$, or in other words, the value $1 - \frac{1-p}{1-q} = \frac{p-q}{1-q} = \frac{p(b+1)-1}{b}$, where $b = \frac{1}{q} - 1$.

Let us return to Merton's problem. Following Večeř (2020), we reformulate the problem in terms of optimal distributional gain. We again assume that the market taker uses a power utility. The distributional opinion $\mathbb{P}$ of the market taker about the stock price process S is

$$dS(t) = \mu S(t)dt + \sigma S(t)dW^{\mathbb{P}}(t)$$

while the market maker believes in $\mathbb{Q}$ such that

$$dS(t) = rS(t)dt + \sigma S(t)dW^{\mathbb{Q}}(t),$$

where r represents the risk-free rate. Defining the discounted price process X as

$$dX(t) = \frac{d(e^{-rt}S(t))}{e^{-rt}S(t)} = (\mu - r)dt + \sigma dW^{\mathbb{P}}(t) = \sigma dW^{\mathbb{Q}}(t),$$

we can immediately see that the market taker believes that the increment dX has a distribution

$$dX \sim N((\mu - r)dt, \sigma\sqrt{dt}).$$

On the other hand, the opinion of the market maker is simply

$$dX \sim N(0, \sigma\sqrt{dt}).$$

Using (2.9) and initial bankroll $B_0 = 0$, we can see that the optimal payoff is just the discounted final value of the portfolio P,i.e., we have

$$B_1^\star(X(T)) = e^{-rT}P(T) = \frac{\left(\frac{p(X(T))}{q(X(T))}\right)^{\frac{1}{a}}}{\int \left(\frac{p(x)}{q(x)}\right)^{\frac{1}{a}} q(x)dx} = \exp\left(\frac{\mu - r}{a\sigma^2}X(T) - \frac{1}{2}\frac{(\mu - r)^2}{(a\sigma)^2}T\right). \tag{2.10}$$

Clearly, the optimal terminal wealth (2.10) is a geometric Brownian motion with volatility $\frac{\mu-r}{a\sigma^2}$ and drift $\frac{\mu-r}{2a\sigma^2}(\frac{1-a\sigma^2}{a\sigma^2})$. Note that since the market is complete, the optimal payoff $B_1^\star$ is replicable by actively trading in the underlying asset. From the perspective of the market taker the replication strategy Δ is a constant position in the risky asset

$$\Delta(t) = \frac{\mu - r}{a\sigma^2}. \tag{2.11}$$

This result can be easily extended either to multiple assets or to Merton's problem with a single Poisson jump, see Večeř (2020). Note that Theorem 2.2.1 can be used for any distributional opinion of the agent $\mathbb{P}$ and any distributional opinion $\mathbb{Q}$ of the market. Thus, it provides a more general approach to determine the optimal trading behavior of utility maximizers than that considered in Merton (1975), which is restricted to the normal distribution. Therefore, having a subjective opinion about the drift μ gives an optimal trading strategy of a power utility-maximizing agent in terms of the well-known Merton ratio (1.8). We note that one significant difference between the likelihood and Merton approaches is that the likelihood approach allows for dynamic updating of the drift instead of taking this to be a constant parameter as in the Merton model. Moreover, we note that the optimality of repeated updating of the drift parameter is justified by the likelihood method, which further extends Merton's model.

We now return to the logarithmic utility. The choice of logarithmic utility is natural to many agents since the optimal strategy also dominates any other strategy in the long run, see Leo (1961). Večeř (2020) studied the equilibrium of the market when a possibly infinite number of agents are present and showed the relationship of the agents' bankrolls to the Bayesian statistics. We restate below both the equilibrium distribution and link to Bayesian statistics.

Suppose that there are agents on the market $(A_\theta)_{\theta\in\Theta}$, where Θ is a possibly infinite index set. We suppose that each agent A_θ has logarithmic utility, bankroll $B_{0,\theta}$, and a distributional opinion $\mathbb{P}_\theta$ with density $f(\cdot|\theta)$. Aggregating these agents can be viewed as an agent representing the whole market with distribution $\mathbb{M}$ associated with density m and some bankroll B^M. The natural question is, of course, what is the density m. To answer this question, we set the market bankroll

$$B^M = \int_\Theta B_{0,\theta}\mu(d\theta) = \int_\Theta B_{1,\theta}^\star\mu(d\theta), \tag{2.12}$$

which we assume to be finite. The measure μ is typically a counting measure in case that the index set Θ is finite and the Lebesgue measure otherwise. If μ is a Lebesgue measure, then the impact of each agent is weighted only by his or her bankroll.

Theorem 2.2.2. *(Equilibrium Distribution) The equilibrium density m is given by*

$$m(x) = \frac{1}{B^M} \int_\Theta B_{0,\theta} f(x|\theta) \mu(d\theta). \tag{2.13}$$

Proof. Using (2.12), we have

$$B^M = \int_\Theta B^\star_{1,\theta} \mu(d\theta) = \int_\Theta B_{0,\theta} \frac{f(x|\theta)}{m(x)} \mu(d\theta) = \frac{1}{m(x)} \int_\Theta B_{0,\theta} f(x|\theta) \mu(d\theta).$$

And formula (2.13) follows. □

From the definition of market bankroll B^M, it is evident that m is indeed a density function. Furthermore, since the density m is a mixture distribution weighted by the bankrolls and measure μ, one can compute the expected value and the variance of the underlying process knowing the distributional opinions of the individual agents.

Let us now show the link to Bayesian statistics. Let f denote the density of a prior on some parameter space Θ. We assume that for each $\theta \in \Theta$ there is an agent on the market with initial bankroll $f(\theta)$, distributional opinion $f(x|\theta)$ using utility function $U(x) = \log(1 + x)$. The distributional opinion $f(x|\theta)$ is known in Bayesian statistics as likelihood. Market equilibrium density m is in this case simply

$$m(x) = f(x) = \int_\Theta f(\theta) f(x|\theta) \mu(d\theta),$$

since $B^M = 1$. Assume that the observation x_1 is realized on the market. Then, the updated bankroll for each agent is a posterior distribution of θ

$$B^\star_{1,\theta}(x_1) = f(\theta) \frac{f(x_1|\theta)}{f(x_1)} = f(\theta|x_1).$$

Using mathematical induction, it can be easily shown that for an arbitrary number of observations $x_1, \ldots, x_n$ on the market, the bankroll of the agents evolves according to Bayesian updating, i.e. $B_\theta(x_1, \ldots, x_n) = f(\theta|x_1, \ldots, x_n)$. Since Bayesian statistics is an actively researched area, the properties of the posterior are well known. The above relationship also provides an economic interpretation of Bayesian updating.

3. Static replication and SVI model

The optimal distributional trading framework provides a powerful tool for utility-maximizing agents. However, in general, there is no traded instrument with a payoff that corresponds to the optimal payoff. This chapter shows that it is theoretically possible to statically replicate the optimal payoff by trading in bonds, forwards, and vanilla option contracts, which is a topic of the first section. To be able to use static replication, one has to know the risk-neutral density seen by the market. This density can be obtained from the price of vanilla option contracts with the same underlying asset. However, the price depends on the volatility of the price process of the underlying asset, which is not observable from market data. Thus, the implied volatility obtained by inverting the Black-Scholes formula for a given strike and maturity is used, which is only available for strikes and maturities that are traded and have reasonable quotations. For this reason, we need a model that allows us to obtain the implied volatility outside of the traded strikes and maturities that satisfies a common financial assumption, namely the efficient market hypothesis. In other words, we need a model that does not allow for arbitrage opportunities. In section two of this chapter, we introduce the stochastic volatility-inspired model introduced by Gatheral (2004) that tackles this issue.

3.1 Static replication

Typically, there is no traded instrument on the market with the optimal payoff $B_1^\star$. Therefore, it is desirable to approximate $B_1^\star$ using the liquid assets available on the market. Under the assumption that the payoff $B_1^\star$ is path-independent and occurs at time T, Breeden and Litzenberger (1978) observed that static replication of the payoff $B_1^\star$ is possible using bonds, forwards, and European style options on the underlying asset. This result was later rigorously proved in Green and Jarrow (1987) and Nachman (1988).

Theorem 3.1.1. *Let $f(X(T))$ be twice differentiable payoff, then for any fixed constant $\kappa \geq 0$*

$$f(X(T)) = f(\kappa) + f'(\kappa)(X(T) - \kappa) + \int_0^\kappa f''(K)(K - X(T))^+ dK + \int_\kappa^\infty f''(K)(X(T) - K)^+ dK \quad (3.1)$$

Proof. We follow the proof in Carr and Picron (1999). The Fundamental Theorem of calculus implies that for any fixed κ, we have

$$f(X) = f(\kappa) - \mathbb{1}_{[X<\kappa]} \int_X^\kappa f'(u)du + \mathbb{1}_{[X>\kappa]} \int_\kappa^X f'(u)du.$$

Since $f'(u) = f'(\kappa) - \int_u^\kappa f''(v)dv$ we can write

$$\begin{aligned} f(X) &= f(\kappa) - \mathbb{1}_{[X<\kappa]} \int_X^\kappa \left[f'(\kappa) - \int_u^\kappa f''(v)dv \right] du \\ &\quad + \mathbb{1}_{[X>\kappa]} \int_\kappa^X \left[f'(\kappa) + \int_\kappa^u f''(v)dv \right] du \\ &= f(\kappa) + f'(\kappa)(X-\kappa) \\ &\quad - \mathbb{1}_{[X<\kappa]} \int_X^\kappa \int_u^\kappa f''(v)dvdu + \mathbb{1}_{[X>\kappa]} \int_\kappa^X \int_\kappa^u f''(v)dvdu \end{aligned}$$

Reversing the order of integration

$$f(X) = f(\kappa) + f'(\kappa)(X-\kappa) + \mathbb{1}_{[X<\kappa]} \int_X^\kappa \int_X^v f''(v)dudv + \mathbb{1}_{[X>\kappa]} \int_\kappa^X \int_v^X f''(v)dudv$$

and integrating over u we have

$$f(X) = f(\kappa) + f'(\kappa)(X-\kappa) + \mathbb{1}_{[X<\kappa]} \int_X^\kappa f''(v)(v-X)dv + \mathbb{1}_{[X>\kappa]} \int_\kappa^X f''(v)(X-v)dv.$$

Finally, moving the indicators to the integral leads to (3.1).

□

The interpretation of Theorem 3.1.1 is that we can replicate the payoff $f(X(T))$ using a static portfolio consisting of $f(\kappa)$ bonds, $f'(\kappa)$ forwards with strike κ, and a basket of call and put options on the same underlying asset. Under the efficient market hypothesis, the market price of the payoff $f(X(T))$ at time t should be

$$\begin{aligned} V_t &= \mathbb{E}^{\mathbb{Q}} \left[f(X(T)) | X(t) \right] \\ &= f(\kappa)B(t) + f'(\kappa)\mathbb{E}^{\mathbb{Q}} \left[X(T) - \kappa | X(t) \right] \\ &\quad + \int_0^\kappa f''(K) P^{BS}(t, X(t), K) + dK + \int_\kappa^\infty f''(K) C^{BS}(t, X(t), K) dK, \end{aligned}$$

where $B(t)$ is the price of the unit bond at time t under the market measure $\mathbb{Q}$.

For the particular case of $\kappa = \mathbb{E}^{\mathbb{Q}}[X(T)]$ being the forward value, we can see that it is possible to value an arbitrary payoff using bonds and European style option contracts since forward contracts are fairly valued from the market maker's perspective. Theorem 3.1.1 was extended to generalized functions in Carr and Picron (1999), where the authors showed how one could use the replication to hedge against the timing risk of American binary options.

In order to use the optimal distributional trading gain in practice, one has to specify the market measure $\mathbb{Q}$. We will show now how one can use market prices of European vanilla options to extract the market-implied distribution. First of all, the existence of the risk-neutral market density follows from the no-arbitrage assumption Duffie (2010). Denote by r the risk-free rate. From the no-arbitrage assumption, it must hold

$$C^{BS}(t, X(t), K) = e^{-r(T-t)} \mathbb{E}^{\mathbb{Q}} \left[(X(T) - K)^+ | X(t) \right].$$

Differentiating with respect to the strike price K, we have the following

$$\frac{\partial C^{BS}(t, X(t), K)}{\partial K} = -e^{-r(T-t)} \int_K^\infty q(x)dx.$$

Differentiating once again with respect to K yields

$$\frac{\partial^2 C^{BS}(t, X(t), K)}{\partial^2 K} = e^{-r(T-t)} q(x),$$

thus we have Breeden and Litzenberger (1978) result

$$q(x) = e^{r(T-t)} \frac{\partial^2 C^{BS}(t, X(t), K)}{\partial^2 K}. \tag{3.2}$$

Formula (3.2) implies that the market density is the second derivative of a call option price divided by the discount factor. Using put-call parity, one can get a similar result using the prices of put options. This result suggests that theoretically, it is possible to get the distributional opinion implied by the market. Using the Black-Scholes formula for option premium, one could directly compute the market density q. However, the volatility σ of the underlying asset is not observable from the market data. Thus, the implied volatility is used to match the Black-Scholes theoretical formula with market prices. This is possible since the market participants observe all other variables needed for the Black-Scholes formula. Unfortunately, the implied volatility is not constant across various strikes and often follows a volatility smile pattern. In particular, for a given expiration, options that are either deep out of money or deep in the money have higher market premiums and hence implied volatility than options around the spot price. If we knew the volatility surface implied by the market, we could reconstruct the market distributional opinion via the Black-Scholes formula. Note that Dupire et al. (1994) showed that there exists a unique diffusion process (given by a state-dependent diffusion $\sigma(S, t)$) that is consistent with the risk-neutral distribution.

A significant estimation error is typically encountered when one attempts to empirically interpolate and differentiate market option prices. To mitigate this issue, many refinements of this idea have been developed. Two notable examples include Jackwerth and Rubinstein (1998); Aït-Sahalia and Lo (1998) where in the first reference, the authors utilize a non-parametric quadratic programming techniques for risk-neutral density estimation purposes, and in the second, the authors consider smoothing kernel regression methods for the sample problem. Non-parametric methods have the advantage of capturing potentially nuanced structures in the implied risk-neutral density that parametric counterparts may overlook. However, they are also prone to considerable estimation error and practical issues such as the possibility of butterfly arbitrage.

This work will focus on a method called the stochastic volatility-inspired (SVI) parametric model. The SVI parametric model summarized in Gatheral (2011) has the advantage that it is generic enough to capture a wide range of market-implied volatility smiles, as well as having a natural interpretation of its parameters and is relatively straightforward to fit market data. In addition, there are known constraints that one may place on the model parameters to ensure that the associated best-fit smiles are arbitrage-free, c.f. Gatheral and Jacquier (2014); Ferhati (2020b). We will utilize these techniques for implied risk-neutral density estimation in chapter 5 to extract the market's view of the underlying asset price distribution. Moreover, additional practical issues include the illiquidity of option data. For example, some strikes could have no bid quotations at all.

Finally, market prices are not continuous and are given by bid-ask quotations. The spread size often depends on the option's price and is typically smaller for options with lower bid offers.

3.2 Stochastic volatility inspired model

When estimating the market density q from the option prices, it is necessary to ensure that the estimate $\hat{q}$ is well defined. Trivially, it must hold that $\hat{q} \geq 0$ and $\int_0^\infty \hat{q}(x)dx = 1$ so it is indeed a density. Furthermore, the fitting procedure must ensure no arbitrage opportunity on the market. By varying the expiration date, one can model the market's perspective on how the underlying asset price density will evolve. Thus, one must ensure that there is no arbitrage using different expirations. This type of arbitrage is called calendar spread arbitrage, and for European options often refers to the monotonicity of option premia with respect to maturity, see Carr and Madan (2005); Cousot (2007). The second type of arbitrage that should not be possible is butterfly arbitrage. Butterfly arbitrage is an arbitrage for options with the same maturity when one buys a single call option contract with strike $K - \epsilon$ and $K + \epsilon$ while at the same time selling two call options with strike K.

We start this section by introducing the notation required by the SVI model. Then, we formulate and prove Theorems that specify constraints on the SVI parameterization so that it is free of both calendar spread and butterfly arbitrage. Finally, we mention the calibration procedure to obtain the SVI parameters.

In the following, let $S = \{S(t), t \geq 0\}$ be a price process. Denote $F = \{F(t), t \geq 0\}$ by $F(t) = \mathbb{E}[S(t)|\mathcal{F}_0]$ the forward price process. By $\sigma_{impl}(k, T)$ we denote the implied volatility.

Definition 3.2.1. *We define*

- *The total implied variance* $w(k, T) = T\sigma_{impl}(k, T)$
- *The implied variance* $v(k, T) = \sigma_{impl}(k, t)$
- *The map of volatility surface* $(k, T) \mapsto w(k, T)$
- *The slice function* $k \mapsto w(k, T)$ *for fixed maturity* $T > 0$.

Definition 3.2.2. *We say that a volatility surface w is free of static arbitrage (arbitrage without rebalancing positions) if and only if*

- *w is free of calendar spread arbitrage*
- *each slice function is free of butterfly arbitrage*

To ensure no calendar spread arbitrage, one has an intuitive condition on the volatility surface w given by Gatheral and Jacquier (2014).

Theorem 3.2.3. *Suppose that the dividends are proportional to the stock price and w is continuously differentiable. Then, the volatility surface w is free of calendar spread arbitrage if and only if for all $k \in \mathbb{R}$ and $T > 0$*

$$\frac{\partial w(k, T)}{\partial T} \geq 0.$$

Proof. Let us now consider two call options with prices C_1, C_2 and strikes K_1, K_2 and maturity times t_1, t_2 respectively, such that the options have the same moneyness, i.e.

$$\frac{K_1}{F(t_1)} = \frac{K_2}{F(t_2)} =: e^k,$$

and $t_1 < t_2$. Process $Y = \{Y(t), t \geq 0\}$ defined by $Y(t) = \frac{S(t)}{F(t)}$ is a martingale by the dividend proportionality assumption. Note that we can write

$$C_1 = \mathbb{E}^{\mathbb{Q}}\left[(S(t_1) - K_1)^+\right] = \frac{1}{F(t_1)}\mathbb{E}^{\mathbb{Q}}\left[(X(t_1) - e^k)^+\right],$$

and similarly for the second option. Using this relationship and standard martingale inequality we have

$$\frac{C_1}{K_1}e^k = \mathbb{E}^{\mathbb{Q}}\left[(Y(t_1) - e^k)^+\right] \leq \mathbb{E}^{\mathbb{Q}}\left[(Y(t_2) - e^k)^+\right] = \frac{C_2}{K_2}e^k.$$

Thus, by keeping the moneyness constant and dividends proportional to the underlying asset price, the option premia in the Black-Scholes model are non-decreasing in time to maturity. Thus, it must hold that for fixed k we have $\frac{\partial w(k,T)}{\partial T} \geq 0$. □

We now consider the second type of arbitrage discussed above, i.e., the butterfly arbitrage. It is well known that the absence of this arbitrage corresponds to the existence of the risk-neutral measure, see, for example, Cox and Hobson (2005). In contrast to the calendar spread arbitrage, butterfly arbitrage is studied for the slice function, i.e., we fix time t to maturity.

Theorem 3.2.4. *Assume that the slice function is in $\mathcal{C}^2(\mathbb{R})$. Then, the slice function is free of butterfly arbitrage if and only if*

$$g(k) := \left(1 - \frac{k\frac{\partial w(k,t)}{\partial k}}{2w(k,t)}\right)^2 - \frac{1}{4}\frac{\partial w(k,t)^2}{\partial k}\left(\frac{1}{w(k,t) + \frac{1}{4}}\right) + \frac{1}{2}\frac{\partial^2 w(k,t)}{\partial k^2} \geq 0.$$

and

$$\lim_{k \mapsto \infty} d_+(k) = -\infty.$$

Proof. Twice differentiating the Black-Scholes formula (2.2) with respect to k yields

$$q(k) = \frac{g(k)}{\sqrt{2\pi w(t,k)}} \exp\left(-\frac{d_-(k)^2}{2}\right).$$

To ensure that q integrates to one, we need additional boundary conditions. One can show that if call prices converge to zero for $k \mapsto \infty$, which is equivalent to $\lim_{k \mapsto \infty} d_+(k) = -\infty$, then q is indeed a density. For more information about this step, see Rogers and Tehranchi (2010). □

Putting these two Theorems together, we have the result of Roper (2010).

Theorem 3.2.5. *If the volatility surface w satisfies*

- $w(t,\cdot)$ *is of class* $\mathcal{C}^2(\mathbb{R})$ *for each* $t \geq 0$
- $w(t,k) > 0$ *for all* $(t,k) \in \mathbb{R}^+ \times \mathbb{R}$
- $w(\cdot,k)$ *is non-decreasing for each* $k \in \mathbb{R}$
- *for all* $(t,k) \in \mathbb{R}^+ \times \mathbb{R}$ *the risk neutral density is non-negative*
- $w(0,k) > 0$ *for all* $k \in \mathbb{R}$
- $\lim_{k \mapsto \infty} d_+(k) = -\infty$ *for each* $t > 0$

Finally, since we know the conditions on the volatility surface to be free of static arbitrage, we can formulate the SVI parameterization of the volatility surface. Note that there exist multiple parameterizations of the SVI model. In order to be consistent with the literature, we slightly abuse the notation for the volatility surface w in the following definition.

Definition 3.2.6. *(Raw parameterization) Let* $\chi_R = \{a, b, \rho, m, \sigma\}$ *denote the parameters of the SVI model. For a fixed time to maturity* T*, by SVI raw parameterization of the total implied variance* w *we mean*

$$w(k; \chi_R) = a + b\left[\rho(k-m) + \sqrt{(k-m)^2 + \sigma^2}\right], \tag{3.3}$$

where k *is the logarithmic forward moneyness and the parameters satisfy the constraints* $a \in \mathbb{R}, b \geq 0, |\rho| < 1, m \in \mathbb{R}$ *and* $a + b\sigma\sqrt{1-\rho^2} \geq 0$.

See Lemma 3.3 in Gatheral and Jacquier (2014) for sufficient condition for raw parameterization (3.3) to be free of calendar spread arbitrage. Similarly, see Theorem 4.1 for sufficient and necessary condition for the parameterization to be free of butterfly arbitrage. We note that there exist equivalent parametrizations of the SVI model, namely the natural SVI parameterization and the SVI Jumps-Wings parametrization, c.f., Gatheral and Jacquier (2014).

Let us briefly explain the meaning of the SVI model parameters. Increasing the parameter a increases the volatility on the whole surface. Parameter b is the slope parameter of the volatility smile. The increase in parameter ρ increases the slope of the left-wing while simultaneously increasing the slope of the right-wingy, that is, counter-clockwise rotation. The parameter m is a horizontal shift parameter, and, finally, the parameter σ determines the curvature of the smile near the at-the-money strike. Note that in the Black-Scholes model, the volatility is flat, which means that $b = 0$.

4. Equity Market Inefficiency During the COVID-19 Pandemic

This chapter is based on the article Navrátil et al. (2021) in which we studied market inefficiency during the COVID-19 pandemic. The disruption of global financial markets caused by the COVID-19 pandemic is an event seldom considered in typical risk scenarios. Governments imposed strict stay-at-home orders worldwide, which resulted in a sudden decline in economic activity. The reaction in international equity markets was swift and severe; for example, the S&P 500 lost approximately one-third of its value in the span of only one month starting on February 20, 2020, cf. Baker et al. (2020). In this chapter, we show that during the market's initial reaction to the COVID-19 pandemic, the market was inefficient and that utility-maximizing agents could generate statistically significant profits using only historical price data and virus-related data forecast ETF returns using Merton's optimal portfolio problem.

The effect of COVID-19 and consecutive interventions on the properties of American equity markets, including performance and volatility, has been actively investigated in the scientific community. In Azimli (2020), using quantile regression, the authors demonstrate how tail dependence structures between equity sectors were altered during the pandemic period. The efficient market hypothesis during the COVID-19 pandemic and an associated comparison with the global financial crisis is studied in Choi (2021). Similarly, DIMA et al. (2021) investigated the response of VIX to the COVID-19 pandemic in the context of information efficiency. The impact of news coverage for the six most affected countries during COVID-19 on different quantile ranges of equity indices is examined in Cepoi (2020). Furthermore, the author found a positive correlation between gold and stock market returns. Cross-country studies of the equity market impact are considered in Frezza et al. (2021). Here, the authors analyzed the effect of COVID-19 on fifteen equity markets from Europe, the US, and Asia using the tools of fractal analysis to find that even though Asian markets have regained efficiency, European and US markets still have inefficient components and have been slower to rebound to pre-pandemic efficiency. In related work, Nguyen et al. (2021) examines the international equity market effects of COVID-19. In particular, they study how volatility spillover effects propagated from the United States and Chinese equity markets to other major international analogs. Structural changes to volatility and their resulting impact on returns are examined in Baek et al. (2020); Just and Echaust (2020). Thorough performance analysis of the American equity sectors and associated connections with asymmetric volatility is studied in Mazur et al. (2021). We confirm and further the results of several of these authors by considering the market inefficiency problem from the perspective of utility-maximizing agents, showing that it naturally extends the Merton optimal portfolio framework to the dynamic trading setting, cf. Merton (1975). Namely, we construct portfolios that trade only in single-risk security, taken to be a broad-based ETF and a treasury bill. We note that dynamic generalizations of the Merton optimal portfolio have been previously considered, cf. Campbell and Viceira (1999). This offers a new

approach to defining and testing market efficiency. Namely, if a portfolio produces a statistically significant profit over a benchmark, then the market is inefficient. However, we note that the market may not necessarily offer any statistically efficient means to monetize such inefficiency through trading.

In addition, the development of emerging market forecasting methods has been the focus of several recent studies. ARIMA-based forecasting methods during the initial Covid-19 crisis period were shown to be effective in Ahmar and Boj del Val (2020). Daily growth in new Covid-19 cases and deaths is shown to be a predictor of future negative returns in Al-Awadhi et al. (2020). The impacts of the European and Asian market are contrasted in Topcu and Gulal (2020), and it is shown that the size and timing of national fiscal stimulus programs differentiate recovery times. Finally, the price reaction of European investment funds' during Covid-19 is considered in Mirza et al. (2020).

The central theme of this chapter is that the returns of index securities became predictable to the point that the profitability of certain utility-maximizing trading strategies was statistically significant. We use a likelihood-based derivation of optimal trading rules for utility-maximizing agents introduced in the optimal distributional trading gain section. This result is utilized to document market inefficiency during the 2020 COVID-19 pandemic. This inefficiency is demonstrated numerically in the case of broad-based market and GICS sector ETFs. Finally, we note that one may monetize market inefficiency by executing a trading strategy that is optimal for a power utility-maximizing agent.

The remainder of this chapter aims to estimate μ on a daily basis, rebalance a portfolio consisting of a single risky and riskless asset, and finally, check whether the associated trading strategy has statistically significant profits. Note that we have two representations of the optimal profit, one that is based on the likelihood (2.10) and one that is based on the replication of the optimal portfolio (2.11). We finally note that the optimal portfolio representation in terms of the likelihood ratio is exact. The two representations should be identical in the complete market situation, but we can see some minor discrepancies from discrete hedging, where we rebalance the positions on a daily basis rather than continuously.

This chapter is organized into two parts. We start with data description and methodology to create out-of-sample forecasts for the parameters μ and σ by combining multiple linear models. Then, using the developed optimal trading strategy for power utility-maximizing agents, we show that such optimal trading strategy has a strong Sharpe ratio, desirable risk statistics, and statistically significant profitability during the weeks following the initial spread of COVID-19 for various sector ETFs.

4.1 Statistical Model and Data

We now discuss a regression-based model used to estimate the drift and volatility parameters μ and σ in Merton's formula (2.11). Specifically, we describe a mechanism to generate out-of-sample predictions for the return μ and volatility σ of several ETFs by combining multiple univariate linear regressions that utilize other liquid securities and virus-related data as predictors. We then discuss the end-of-day price dataset and the associated period on which these models are estimated.

4.1.1 Estimating the Drift and Volatility

We utilize a combination of univariate ordinary least squares linear regression models to estimate the drift parameter on a daily basis. Here, the target excess return of the j-th ETF is denoted by μ_{t+1}^j and the i-th predictor is x_t^i, where the subscripts indicate that all predictors are lagged one day prior to the target time series. We consider linear models of the form

$$\mu_{t+1}^j = \beta^{ij} x_t^i + \epsilon_{t+1}, \quad \text{for} \quad t = 1, \ldots, T-1, \tag{4.1}$$

where here we assume that the residuals ϵ_{t+1} are i.i.d. draws from a random variable that satisfies $\mathbb{E}(\epsilon_{t+1}) = 0$ and $\mathrm{Var}(\epsilon_{t+1}) = \sigma^2 < \infty$. Here the excess returns are defined in terms of the difference of an ETF and the three month treasury bill yield.

We reestimate μ_{t+1}^j on a rolling basis when testing market efficiency during the COVID-19 crisis. That is to say, at time t we train the model on N consecutive prior observations $((x_{t-N}, \mu_{t-N+1}), \ldots, (x_{t-1}, \mu_t))^T$ yielding an estimate $\hat{\beta}_t^{ij}$ of the regression coefficient. Then we create a single out-of-sample prediction $\hat{\mu}_{t+1} = \hat{\beta}_t x_t$ of the unobserved variable μ_{t+1}. During the next trading day, we observe the actual value μ_{t+1} and refit the model by adding the observation (x_t, μ_{t+1}) and omitting the first observation (x_{t-N}, μ_{t-N+1}) from the training set. Repeating this procedure, we obtain a vector of sample forecasts $(\hat{\mu}_{t+1}, \ldots, \hat{\mu}_T)$. In addition, the volatility parameter σ_t is estimated directly from the empirical standard deviation of the historical excess returns $(\mu_{t-N+1}, \ldots, \mu_{t-1}))^T$. In the empirical results section, we will show the dependence of the final portfolio value on the specific choice of the hyperparameter N. Even as we vary the hyperparameter N greatly, the market still shows inefficiency.

4.1.2 Combining Predictions

Multiple economic indicators have been shown to be a useful tool for enhancing the predictive power of the equity risk premium, c.f. Neely et al. (2014). In particular, the combination approach of utilizing the predictive power of several different models has proven successful in this application, e.g., Dangl and Halling (2012) and Rapach et al. (2010). To improve the robustness of the forecast and out-of-sample performance, we utilize a similar model combination technique by fitting several individual univariate linear regression models, which comprise a single forecasting model for future excess returns. Mathematically, this method is specified by taking a weighted sum of individual drifts to construct an aggregate model,

$$\hat{\mu}_t^i = \sum_j w_t^{ij} \hat{\mu}_t^{ij}. \tag{4.2}$$

Here $\hat{\mu}_t^i$ is a predictor of μ_t for the j-th model, and w_t^{ij} is the weight of this model at observation t for the i-th ETF whose excess returns are being estimated.

Common choices for the weights include the mean, median, and trimmed mean, c.f. Zhang et al. (2018) or Balcilar et al. (2015). We select uniform weights $w_{j,t} = \frac{1}{M}$, where here M is the number of statistical models. In addition, we note that there are many additional techniques to improve further the out-of-sample forecasting performance, such as constraining predictors as in Pan et al. (2020)

or adding new low correlation predictors, c.f. Zhang et al. (2019). However, our main purpose is to demonstrate market inefficiency during the COVID-19 crisis, and we found that using a simple uniform weighting scheme is sufficient for this task.

4.1.3 Dataset Construction

We aim to focus on examining market inefficiency shortly after the emergence of COVID-19 and restrict our dataset to include daily data from February 2020 through May 2020. We consider excess returns of several ETFs, including an S&P 500 ETF SPY, as well as eleven ETFs that cover each of the GICS sectors; namely, VCR, VDC, VDE, VGT, VNQ, XLB, XLC, XLF, XLI, XLU, and XLV. These will all serve as target variables within the regressions considered below.

In addition, we construct a dataset of one-day time-lagged predictors, which consist of daily returns from highly liquid securities, as well as information related to the severity and spread of the virus. Specifically, we consider daily excess returns of the VIX volatility index, gold futures, and bitcoin. In addition, a fixed income component is incorporated with daily two-year US treasury data, and market loss risk aversion is captured through the short interest index (c.f. Rapach et al. (2010)) of SPY. Finally, we incorporate the daily COVID-19 related case count and death rates from the United States into the predictor data set.

Data was obtained from multiple public sources. Specifically, end of day ETF and VIX data was obtained from Yahoo finance, treasury data was obtained from the United States Department of the Treasury website (treasury.gov), bitcoin prices were obtained from coinmarketcap.com, gold futures data was gathered from investing.com, and the data used in the SSI index was downloaded from http://regsho.finra.org/regsho-Index.html. Additionally, the COVID-19 data was downloaded from ourworldindata.org. When available, we utilized Python APIs to download data and the pandas package to align and prepare data for subsequent modeling.

We restrict our focus to the period starting in late February 2020, when the equity market began to react to the global spread of COVID-19. During this time, equity markets in the United States exhibited strong mean reversion, as can be seen, for example, by fitting an $AR(1)$ process to the excess daily return time series of the SPY ETF. Specifically, assume that excess daily returns follow mean reversion process $y_t = \alpha y_{t-1} + \epsilon_t$. Then over the two-month period under consideration, we estimate $\hat{\alpha} = -0.40$ with an in-sample R^2 of 13.7%. Noting that the market exhibited extreme volatility during this time, the R^2 for this simple mean reversion indicator is quite strong. Next, We seek to understand whether similar behavior is present in the out-of-sample dataset.

4.2 Empirical results

We now consider a simple trading technique based on determining the optimal investment strategy of an agent who wishes to maximize the utility $\mathbb{E}^{\mathbb{P}}[U(F)]$, where we take U to be the previously described power utility $U(x) = \frac{x^{1-a}}{1-a}$ for $a \geq 0$ and where F is the final portfolio value. The agent assumes that the equity market or ETF price evolves according to a geometric Brownian motion

with parameters μ and σ. Using the combination approach described above, the agent estimates the drift μ and the volatility σ parameters from historical data. The optimal position π_t at time t in the risky asset is then defined by Merton's fraction in equation (2.11) while the remainder of the capital is invested in the three-month treasury bill. We also impose a single trading constraint; specifically, we do not allow for leveraged portfolios, i.e., $\pi_t \in [-1, 1]$. We will assume that the agent rebalances this position on a daily basis at the close and that there are no transaction costs given the strong liquidity of the securities under consideration.

To demonstrate the inefficiency of the entire market as well as individual sectors, we suppose the agent invests independently in each of the target ETFs. First, we note that the agent realizes a positive bankroll for all ETFs under consideration. The final bankroll depends on the specific choice of hyperparameters; N for the training window size and the utility risk aversion parameter a. While the parameter N requires some statistical insight to properly select, the parameter a is given according to the personal preference of the agent. We examine the performance of the trading strategy in more detail below as a function of N and a, and initially select $N = 10$ and $a = 0.8$ in the examples below to demonstrate market inefficiency.

We plot the agent's bankroll assuming an initial unit amount of capital for all ETFs on the left subplot of Figure 4.1. On the right subplot, we display the evolution of the agent's bankroll benchmarked to the respective ETF, i.e., the right panel compares Merton's portfolio against a long-only buy and hold strategy. During the first month prior to the spread of COVID-19, the data supports the hypotheses that markets were efficient given that the bankroll oscillates around the starting capital value. Then, the market's inefficiency becomes prominent during late February, independent of the specific choice of the ETF, the agent realizes a significant profit. Finally, during the final month and a half of the period under consideration, the efficiency returns as ETF profits again resemble noise.

Trading strategy performance and risk statistics for all ETFs are given in Table 4.1. Notice that the profit for all ETFs is positive. The greatest profit is found in VDE, the Vanguard Energy ETF, while the smallest profit is in XLU, the Utilities Select Sector ETF. The annualized Sharpe ratio of trading in SPY, the market ETF, is 3.02, with a final bankroll of 1.58. The maximum drawdown statistics range from 7.9% to 27.4%. Although the maximum drawdown of this strategy is quite large, note that the drawdowns of the respective ETFs range from 25% (VDC) to 57% (VDE), so the portfolio allocation strategy dramatically reduces the drawdown. The value and the conditional value at risk statistics are calculated at the 95% level, and the out-of-sample R^2 is given according to

$$R^2_{OOS} = 100 * \left(1 - \frac{(r - \hat{r})^2}{(r - \bar{r})^2}\right),$$

where here $\bar{r}$ denotes the mean excess daily return r of the respective ETF.

Benchmarking by the underlying ETF, we find that the largest trading opportunity resides in the Vanguard Energy ETF and in the financial select sector ETF (XLF), while the rest of the considered ETFs behaved similarly from the perspective of the utility-maximizing agent. Using multi-fractal detrended fluctuation analysis, a method developed in Kantelhardt et al. (2002) was used

to study sector-level efficiency, Choi (2021) found that during the COVID-19 pandemic, the consumer discretionary (VCR) and energy sector (VDE) ETFs were the most efficient while the financial sector (XLF) and the utilities sector (XLU) were the least efficient. Our results suggest that in an inefficient market, the degree of market inefficiency of a utility maximizing agent plays a more minor role than, for example, the volatility of the traded asset.

Figure 4.1: The left subplot displays the evolution of an agent's bankroll in terms of the dollar value for each ETF under the Merton fraction portfolio described above over the COVID-19 crisis. The right subplot depicts the evolution of the agent's bankroll in terms of relative value against the respective ETF.

	Final Bankroll	SR	R^2_{OOS} %	Profitable %	DD %	VaR %	CVaR %
VDE	2.25	3.57	1.97	59.76	27.43	12.60	14.48
XLC	2.01	4.96	16.35	60.98	9.38	7.10	10.77
XLF	1.94	3.50	12.52	57.32	16.87	11.33	13.05
VGT	1.77	3.37	15.53	54.88	11.14	9.15	13.02
XLV	1.73	3.90	11.88	60.98	7.92	7.02	12.38
XLB	1.61	3.18	5.68	58.54	11.50	9.03	10.63
SPY	1.58	3.02	12.90	56.10	9.72	9.20	12.85
VCR	1.56	2.91	6.47	63.41	13.81	9.02	13.57
XLI	1.53	2.50	7.00	59.76	14.21	11.56	15.07
VNQ	1.48	1.97	6.40	52.44	12.70	9.52	14.65
VDC	1.42	2.60	11.22	59.76	14.74	4.98	12.09
XLU	1.37	1.71	4.54	50.00	18.74	10.51	15.61

Table 4.1: Trading strategy risk and performance metrics for GICS sector ETFs during the period from the beginning of February 2020 to the end of May 2020. The Sharpe ratio (SR) is annualized. VaR and CVaR are calculated at the 95% level.

To illustrate the behavior of Merton's portfolio in more detail, we plot the estimate of the drift parameter μ in Figure 4.2. Note the relatively large estimated

values during mid-March for all ETFs. Similarly, we plot the evolution of the agent's position in the respective ETFs in Figure 4.3. Notice that in this volatile period, the agent's position is, in most cases, either fully long or fully short. This resembles a bang-bang type strategy where it is always optimal to switch from one extreme to another. This implies that the influence of the risk aversion parameter a will have a small effect on the portfolio's final value.

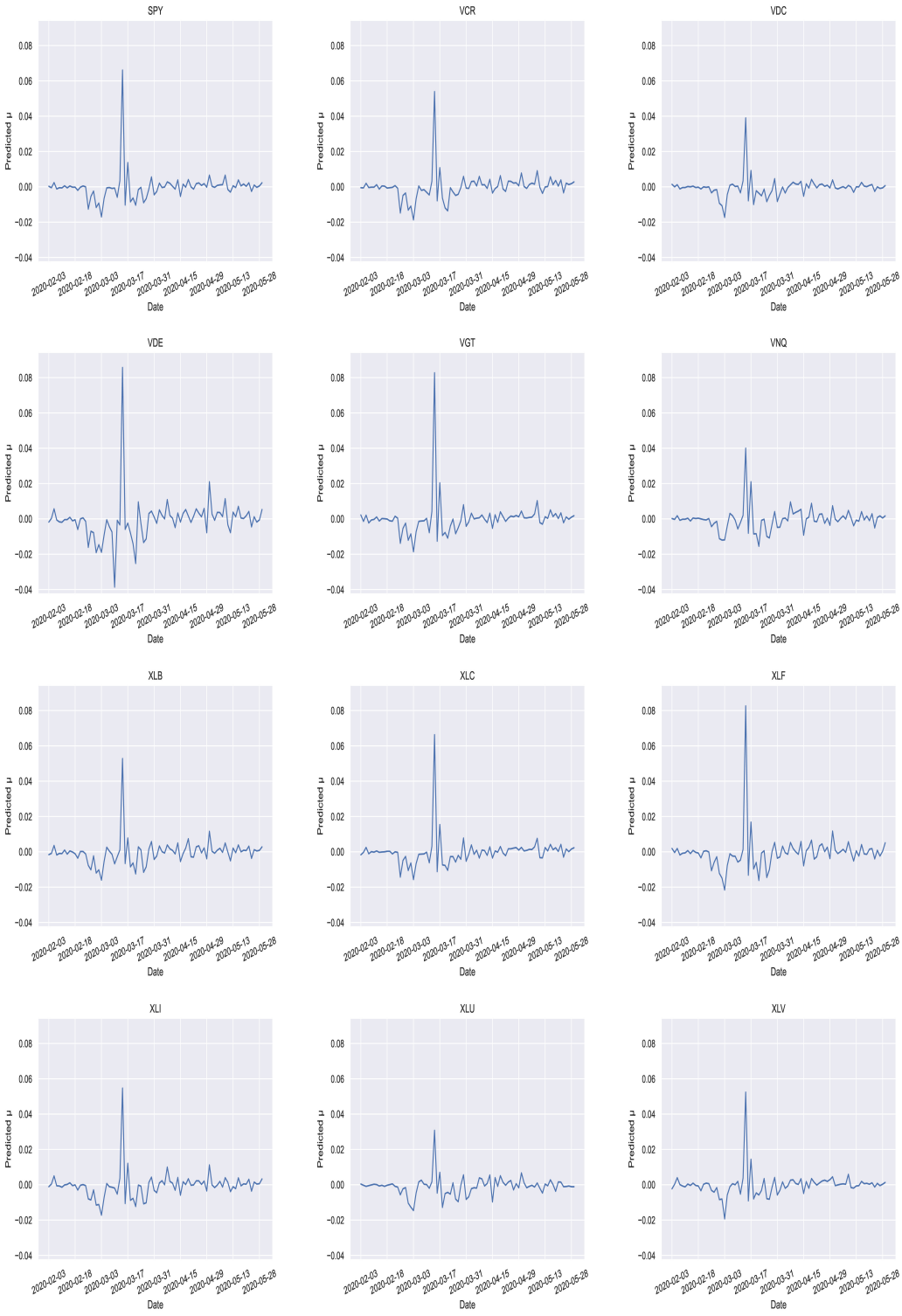

Figure 4.2: Evolution of the estimated drift parameter μ for the respective ETFs during the COVID-19 crisis period.

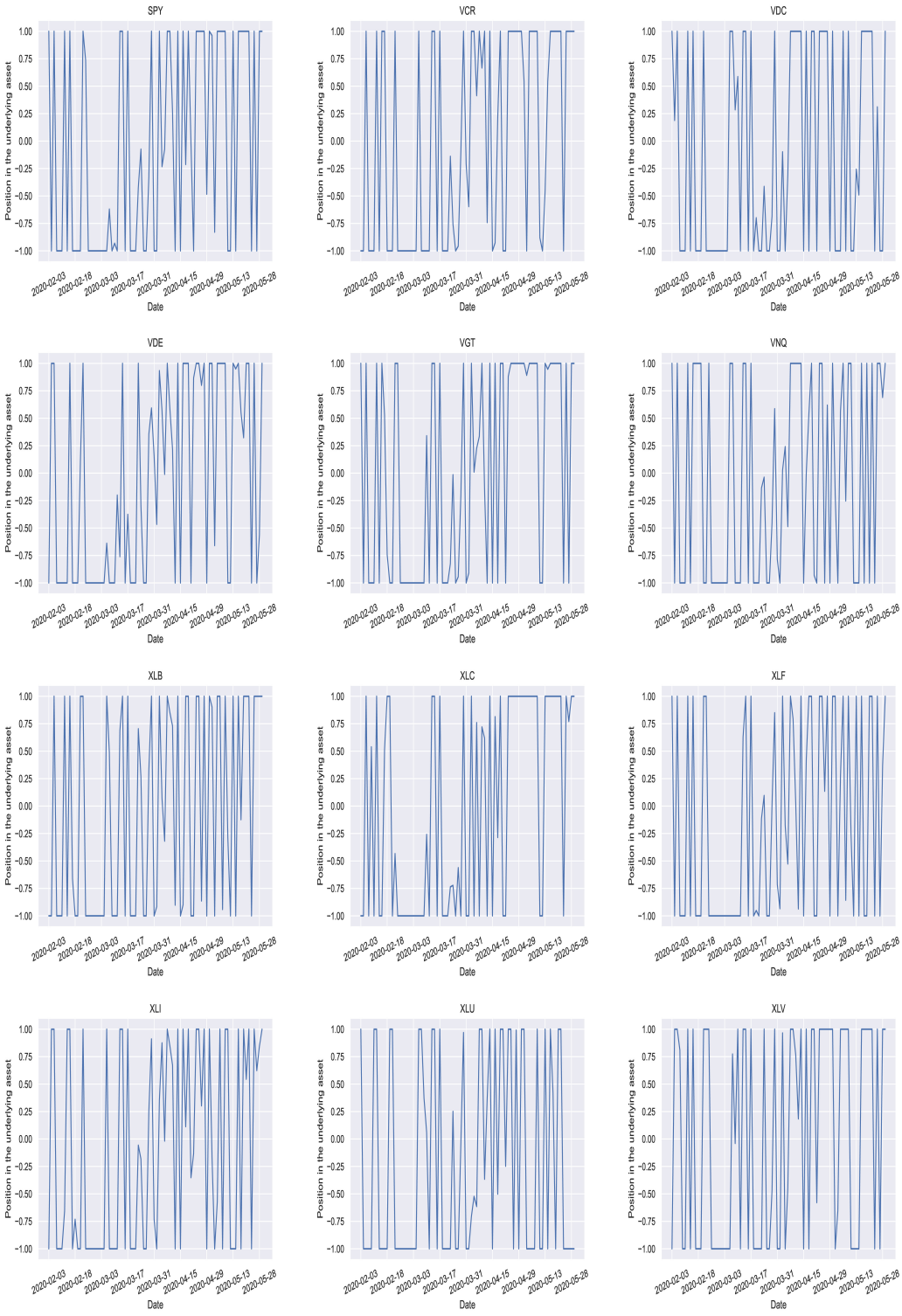

Figure 4.3: Evolution of the portfolio position π_t in the risky asset during the COVID-19 crisis period.

To further study the properties that allowed Merton's portfolio to generate excess returns due to the market inefficiency, we now focus on the individual constituents of the S&P 500. We are interested in studying the effect of the market beta, leverage, P/E ratio, and cash assets of individual firms on the final value of Merton's portfolio constructed from groups of stocks with similar values

for these fundamental quantities. The market beta of each stock is computed using excess returns in the year 2019. To ensure a uniform comparison, we exclude stocks that entered the S&P 500 index during the year 2019. We define leverage by summing the short-term and long-term debt over each firm's balance sheet assets, P/E ratio as the share price divided into earnings, and cash assets as the percentage of cash and marketable securities of total assets.

Using the previous trading strategy, we compute the evolution of the bankroll for each stock using the same hyperparameters and regressors as above. We then cluster the S&P 500 constituents into five equally sized groups based on quintile buckets of their market beta, leverage, P/E ratio, or cash assets as they were known at the pre-pandemic time in December 2019. The results are plotted in Figure 4.4. From the plot we conclude that regardless of the studied property, Merton's portfolio was able to, on average, generate excess returns over the market index. Only market beta seems to have a positive effect on the final value of Merton's portfolio. Intuitively, this makes sense as one would expect that larger movements in the price of securities in an inefficient market present greater opportunities for the utility maximizing agent. We statistically confirm this result using a linear model of the form

$$Y^i \sim \beta_0 + \beta_1 \text{P/E ratio}^i + \beta_2 \text{Leverage}^i + \beta_3 \text{Cash assets}^i + \beta_4 \text{Market beta}^i, \quad (4.3)$$

where Y_i is the predicted final bankroll of Merton's portfolio for i-th company. Moreover, to easily compare the estimated coefficients, we center and normalize the regressors. The results are summarized in Table 4.2. We find that the market beta is statistically significant and positively affects the final bankroll of the portfolio. Cash assets and leverage have a statistically negative effect on the final bankroll. Finally, we have not found statistical evidence for the effect of the P/E ratio on the final value of Merton's portfolio. The R^2 of the linear regression is 0.152. This result corresponds to Ramelli and Wagner (2020) who studied non-financial companies in the Russel 3000 index and found statistical evidence between the company's leverage, cash holdings, and the cumulative return of the company during the COVID-19 pandemic.

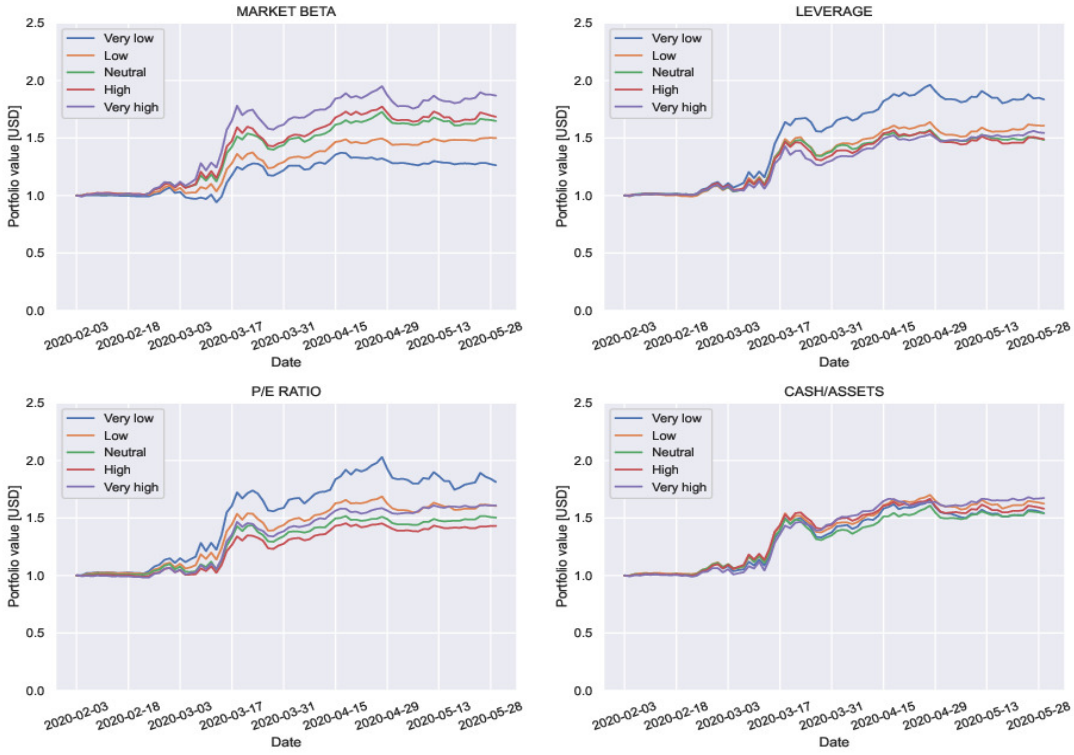

Figure 4.4: Evolution of the dollar value of Merton's portfolio for constituents in the S&P 500 index. For each studied property, the constituents of the S&P 500 are divided into five equally sized groups based upon their quintile buckets. For each group, we compute Merton's portfolio and plot the respective group mean.

	coef	**std err**	**t**	**P> |t|**	**[0.025**	**0.975]**
Intercept	1.5930	0.023	70.747	0.000	1.549	1.637
P/E ratio	-0.0301	0.023	-1.328	0.185	-0.075	0.014
Leverage	-0.0612	0.023	-2.645	0.008	-0.107	-0.016
Cash assets	-0.0499	0.024	-2.059	0.040	-0.097	-0.002
Market beta	0.2013	0.025	8.158	0.000	0.153	0.250

Table 4.2: This table shows results of OLS regression (4.3).

We finally demonstrate that Merton's portfolio does not outperform during a regular efficient market. Specifically, consider the one-year period prior to the market reaction to the global spread of COVID-19, i.e., February 2019 through May 2019. We follow the same methodology as before to estimate the μ and σ parameters of each ETF except that no COVID-19 related data is included. In Figure 4.5, we gain display the evolution of the agent's bankroll in both dollar value and ETF relative value. The average loss in dollar value is approximately 10%, while the average loss against a simple buy and hold strategy is, on average, 12%.

4.2.1 Hyperparameter Selection

We next offer suggestions on choosing the estimation window size N and the risk aversion parameter of the utility function a. We note that the length of the fitting

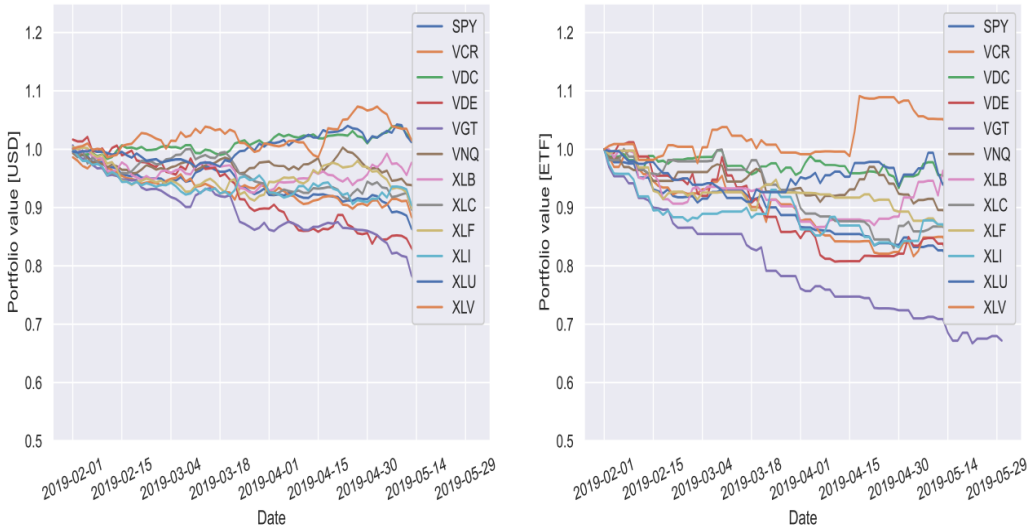

Figure 4.5: The left subplot displays the evolution of an agent's bankroll in terms of the dollar value for each ETF under the Merton fraction portfolio described above one year prior to the COVID-19 crisis. The right subplot depicts the evolution of the agent's bankroll in terms of the relative value of the respective ETF.

window N has a large effect on the final portfolio value while the risk aversion parameter a has a relatively small impact on performance. This is due to the fact that we do not allow for leverage, and Merton's optimal portfolio allocation will usually be either fully long or short.

We demonstrate the effect of N and a by examining the performance of the trading strategy for all combinations of $N \in \{5, 6, \ldots, 50\}$ and $a \in \{0.01, 0.02, \ldots, 1\}$. We are interested in the average final bankroll for all ETFs. In Figure 4.6, note that varying the a parameter for a fixed N value only has a marginal effect on performance. In contrast, varying the N parameter significantly impacts the final value of the portfolio. Note that extremely low values of N underperform in comparison with other choices. For example, relatively small N values, i.e. $N = \{8, \ldots, 15\}$ yield the strongest performing strategies as such values allow one to quickly capture the changes in the market and provide sufficient data in the rolling window to estimate the drift and volatility parameters to a sufficient accuracy. Large values of N behave similarly, since they do not allow the model to react sufficiently quickly to market changes. Note that for all choices of N, the final portfolio realizes a net gain. The highest profit obtained with a final bankroll value of 1.79 has parameters $N = 9$ and $a = 0.48$.

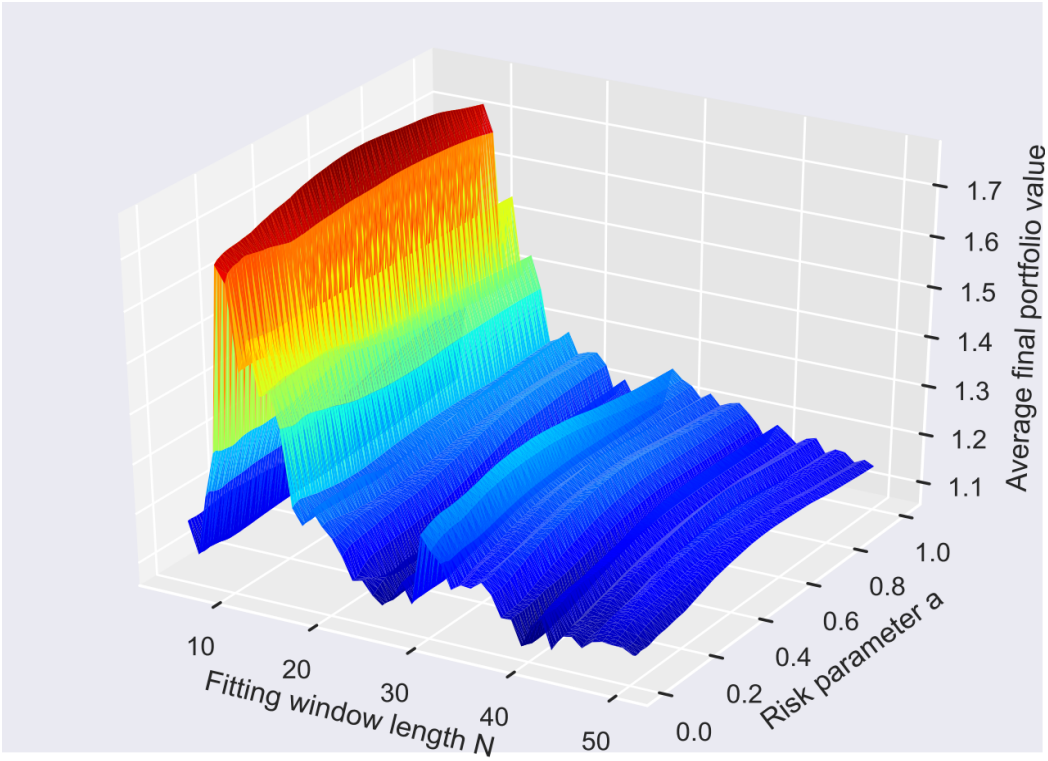

Figure 4.6: Plot of the final bankroll of the Merton optimal trading strategy as a function of the fitting window length N and risk aversion parameter a during the COVID-19 timeframe described above.

4.3 Conclusion

This whole chapter is based on Navrátil et al. (2021) where we examined the inefficiency of the United States equity market during the initial spread of the COVID-19 pandemic during 2020. We have shown that even the relatively simple Merton optimal portfolio trading strategy has strong out-of-sample performance during this period. The results were applied to S&P 500 and eleven GICS sector ETFs. Furthermore, the profitability of the trading strategy was shown to be robust to the choice of the risk aversion parameter of the utility function and the size of the lookback window.

We finally note that it would be of interest to examine further the performance of asset allocation techniques and the multivariate extension of Merton's optimal portfolio ratio during the COVID-19 timeframe. In addition, it would be of interest to develop extensions of these results in the case where the portfolio follows an extension of geometric Brownian motion, i.e., jump processes, that more closely reflect market price movements. In particular, the likelihood approach offers a considerably simplified framework over known stochastic control-based methods to derive optimal trading rules in the case of more general stochastic processes.

5. Utility Maximization of the Discrepancy between a Perceived and Market Implied Risk Neutral Distribution

This chapter covers the results that appeared in Navrátil et al. (2022). Securities trading provides a mechanism for agents to express a view on a forecast of the future price of an asset. For example, if one feels that a security price is undervalued, a natural way to express such a view would be to purchase the security, hold it until its perceived market value is realized, and then generate a profit by selling. However, binary views on whether a security price will increase or decrease seldom capture the entirety of an agent's opinion. For example, equity analysts often establish future price targets in terms of a view on the expected value of a given security price based on their opinion of the likelihood of occurrence of multiple future price evolution scenarios. This results in an individual agent effectively forecasting a discretized future price distribution for the security price. Additionally, one may consider the market-implied distributions from associated derivative contracts whose underlying is the security being considered by individual analysts. Risk neutral pricing theory provides a means to estimate such implied distributions from a collection of call and put option prices with varying strikes but fixed expiration dates in a model-free manner. When any discrepancy between a forecasted and market distribution exists, one may develop a profitable portfolio in the event that the current market distribution transitions towards the forecasted distribution. Our main aim is to develop techniques that allow one to construct the optimal portfolio to realize these gains in the sense that it will maximize the utility of the agent prescribing the forecasted distribution.

Option markets are inherently forward-looking in the sense that the current values of put and call contracts reflect the market expectation of the future price and volatility of the underlying security price. Given the recent rapid growth in both trading volume and available options markets, considerable data is available to develop estimation methods for the option market implied future price distribution of the underlying security. The seminal result in option implied risk neutral density estimation was presented in Breeden and Litzenberger (1978), where it is demonstrated that one may represent this density as the second derivative of a chain of call option prices with respect to the strike for a fixed maturity value. Significant estimation error is typically encountered when one attempts to interpolate and differentiate market option prices empirically. To mitigate this issue, many refinements of this idea have been developed. Two notable examples include Jackwerth and Rubinstein (1998); Aït-Sahalia and Lo (1998) where in the first reference, the authors utilize nonparametric quadratic programming techniques for risk-neutral density estimation purposes, and in the second, the authors consider smoothing kernel regression methods for the sample problem. Nonparametric methods have the advantage of capturing potentially nuanced structures in the implied risk-neutral density that parametric

counterparts may overlook. However, they are also prone to considerable estimation error and practical issues such as the removal of butterfly arbitrage. The stochastic volatility inspired (SVI) parametric model summarized in Gatheral (2011) has the advantage that it is generic enough to capture a wide range of market implied volatility smiles as well as having a natural interpretation of its parameters and being relatively straightforward to fit to market data. In addition, there are known constraints that one may place on the model parameters to ensure that the associated best-fit smiles are arbitrage-free, c.f. Gatheral and Jacquier (2014); Ferhati (2020b). We will utilize these techniques for implied risk-neutral density estimation to extract the market's view of the underlying asset price distribution.

Given an implied market distribution and an agent's perceived future price distribution of a security price, we develop a method to determine the optimal payoff function and associated options portfolio that the agent should purchase in order to maximize his benefit from the discrepancy. Rüschendorf and Vanduffel (2019) studied a similar problem independently using a different setup with extensions to investor's preferences following the cumulative prospect theory and Yaari's dual theory. They studied the optimal payoff using quantile formulation of the portfolio selection problem, while in our approach, we work directly with the densities of the risk-neutral measure $\mathbb{Q}$ and the subjective agent's measure $\mathbb{P}$. We next consider the question of what portfolio of tradeable securities the agent may construct in order to replicate such a payoff as precisely as possible. There is considerable literature on the replication of complex derivatives in terms of simpler tradeable securities. Static hedging techniques to replicate exotic options are developed in Carr et al. (1998); Leung and Lorig (2016). Targeted applications to volatility derivatives and barrier options are examined in Carr and Madan (2001); Carr and Lee (2008); Carr et al. (2017). In Bossu et al. (2021), the authors showed that the static replication formula is part of an integral equation framework. We examine related techniques that focus on replicating the optimal payoff function with increasing number of vanilla call and put options. In particular, we first consider strangle portfolios and then extend to include additional securities in order to construct more accurate replicating portfolios. Our results suggest that portfolios consisting of ten option contracts provide a precise replication of the optimal payoff function. From this point, increasing the number of option contracts in the replicating portfolio provides only a marginal decrease in replication error.

This chapter presents several novel contributions including, to our knowledge, the first constructive method to create an options portfolio that maximized the expected utility of an agent based upon the difference between his view on the future price distribution of an underlying asset price and that of the associated options market. First, explicit formulae for the optimal payoff function are developed in the cases of logarithmic and power utility functions. In addition, a replicating portfolio is developed for the utility-maximizing portfolio, and associated hedging applications are discussed. Next, a method is developed to approximate the optimal payoff function with a collection of call and put options. Finally, this underlying model assumption of a geometric Brownian motion is lifted. In particular, the SVI model is used to estimate the option implied market risk-neutral density. This is integrated into the prior framework to determine

the corresponding utility maximizing option portfolio and integer programming techniques are used to solve associated optimization problems.

This chapter is organized as follows. In Section 2, we derive explicit formulae for the optimal payoff function in the case of a geometric Brownian motion and logarithmic and power law utilities. In addition, a pricing formula for the optimal hedging strategy and an associated replicating hedging portfolio are given. In Section 3, we discuss the estimation of the risk neutral density using the SVI formula. In Section 4, the kernel search integer programming method is outlined and applied to the construction of the utility maximizing portfolio. Section 5 contains several numerical examples of the construction of optimal payoff functions and examination of the tradeoff between the number of securities in the approximation portfolio and the precision of the replication. Finally, in Section 6, we conclude and provide future research considerations.

5.1 Pricing with a Logarithmic Utility within a Geometric Brownian Motion Model

Similarly to the previous chapter, we will again utilize the Optimal Distributional Trading Gain problem with $B_0 = 0$. A common assumption for asset price evolution is the geometric Brownian motion model with a drift μ and volatility parameter σ; we examine this case in further detail. Note that other models, like the Heston stochastic volatility model, may also be considered. In the cases where explicit closed formulas exist for the density of the price process, we can compute the optimal payoff (2.6) directly. On the other hand, cases like the Heston model considered in, del Baño Rollin et al. (2010) do not exhibit a closed-form density in terms of elementary functions, which leads to additional challenges that need to be considered. If there is no such closed formula for the density of the price process, then one may approximate the optimal payoff numerically. The thorough investigation of such techniques alongside the development of associated numerical optimization methods would be interesting to explore in further detail. In addition, we note that there are a number of additional techniques one can utilize in the time-varying volatility case to assess the accuracy of a given density forecast. In particular, Diebold et al. (1998) develop methods along these lines and provide applications to GARCH and related volatility models. Similarly, it would be of interest to adapt these methods to continuously varying stochastic volatility models.

In the following, let g denote the density of a geometric Brownian motion, i.e. for parameters μ and σ the density at time t is given by

$$g(x, \mu, \sigma, t, S(0)) = \frac{1}{\sqrt{2\pi}} \frac{1}{x\sigma\sqrt{t}} \exp\left(-\frac{\left(\log x - \log S(0) - (\mu - \frac{1}{2}\sigma^2)t\right)^2}{2\sigma^2 t} \right).$$

where here $S(0)$ denotes the initial asset price. In addition, we define its growth parameter by $\gamma = \mu - \frac{1}{2}\sigma^2$.

Theorem 5.1.1. *Suppose that the market taker with utility* $U(x) = \frac{(1+\frac{x}{B})^{1-a}-1}{1-a}$ *believes the market behaves like a geometric Brownian motion with parameters*

(μ_1, σ_1) *whereas a market maker holds the view that the parameters are given by* (μ_2, σ_2)*. Assume that* $\sigma_2^2 - \sigma_1^2(1-a) \neq 0$*, then the optimal payoff* $B_1^\star$ *is given by*

$$B_1^\star(x) = B\left(\frac{\sigma_2 \exp\left(-\frac{\left(\log\frac{x}{S(0)}-\gamma_1 T\right)^2}{2\sigma_1^2 aT} + \frac{\left(\log\frac{x}{S(0)}-\gamma_2 T\right)^2}{2\sigma_2^2 aT}\right)}{\tilde{\sigma}\exp\left(-\frac{(\log S(0)+\gamma_1 T)^2}{2\sigma_1^2 aT} + \frac{(\log S(0)+\gamma_2 T)^2\left(\frac{1}{a}-1\right)}{2\sigma_2^2 aT} + \frac{\tilde{\mu}^2}{2\tilde{\sigma}^2}\right)} - 1\right), \tag{5.1}$$

where

$$\tilde{\mu} = \frac{(\log S(0)+\gamma_1 T)\sigma_2^2 - (\log S(0)+\gamma_2 T)\sigma_1^2(1-a)}{\sigma_2^2 - \sigma_1^2(1-a)}, \tag{5.2}$$

and

$$\tilde{\sigma} = \sqrt{\frac{\sigma_1^2\sigma_2^2 aT}{\sigma_2^2 - \sigma_1^2(1-a)}}. \tag{5.3}$$

Proof. We compute $\int_0^\infty \left(\frac{p(x)}{q(x)}\right)^{\frac{1}{a}} q(x)dx$ directly by factoring out terms in the integrand that do not depend on x which is then rewritten in terms of the transition density of a scaled geometric Brownian motion. To simplify notation, define

$$u = \log S(0) + \gamma_1 T \quad \text{and} \quad v = \log S(0) + \gamma_2 T. \tag{5.4}$$

Substituting the densities p and q leads to

$$\int_0^\infty \left(\frac{p(x)}{q(x)}\right)^{\frac{1}{a}} q(x)dx = \frac{\sigma_2}{\sigma_1}\int_0^\infty \exp\left(-\frac{(\log x - u)^2}{2\sigma_1^2 aT} + \frac{(\log x - v)^2}{2\sigma_2^2 aT}\right) \times \frac{1}{\sqrt{2\pi}}\frac{1}{x\sigma_2\sqrt{T}}\exp\left(-\frac{(\log x - v)^2}{2\sigma_2^2 T}\right). \tag{5.5}$$

Under the assumption $\sigma_2^2 - \sigma_1^2(1-a) \neq 0$, using (5.2) and (5.3) the term in the exponential of (5.5) may be rewritten in the form

$$\begin{aligned}
\ldots &= -\frac{u^2}{2\sigma_1^2 aT} + \frac{v^2\left(\frac{1}{a}-1\right)}{2\sigma_2^2 aT} - \frac{\log^2(x)(\sigma_2^2 - \sigma_1^2(1-a))}{2\sigma_1^2\sigma_2^2 aT} \\
&\qquad + \frac{2\log(x)(u\sigma_2^2 - v\sigma_1^2(1-a))}{2\sigma_1^2\sigma_2^2 aT} \\
&= -\frac{u^2}{2\sigma_1^2 aT} + \frac{v^2\left(\frac{1}{a}-1\right)}{2\sigma_2^2 aT} - \frac{\log^2(x) + 2\log(x)\frac{u\sigma_2^2 - v\sigma_1^2(1-a)}{\sigma_2^2-\sigma_1^2(1-a)}}{2\frac{\sigma_1^2\sigma_2^2 aT}{\sigma_2^2-\sigma_1^2(1-a))}} \\
&= -\frac{u^2}{2\sigma_1^2 aT} + \frac{v^2\left(\frac{1}{a}-1\right)}{2\sigma_2^2 aT} + \frac{\tilde{\mu}^2}{2\tilde{\sigma}^2} - \frac{(\log x - \tilde{\mu})^2}{2\tilde{\sigma}^2}.
\end{aligned}$$

Thus the term containing an x can be written as a scaled geometric Brownian motion which leads to

$$\begin{aligned}
&\int_0^\infty \left(\frac{p(x)}{q(x)}\right)^{\frac{1}{a}} q(x)dx \\
&\quad = \frac{\tilde{\sigma}}{\sigma_1}\exp\left(-\frac{(\log S(0)+\gamma_1 T)^2}{2\sigma_1^2 aT} + \frac{(\log S(0)+\gamma_2 T)^2\left(\frac{1}{a}-1\right)}{2\sigma_2^2 aT} + \frac{\tilde{\mu}^2}{2\tilde{\sigma}^2}\right).
\end{aligned}$$

Finally, using (2.9) we conclude the proof. □

The special case of logarithmic utility in Theorem 5.1.1 may be written in the following more elegant form.

Theorem 5.1.2. *Suppose that the market taker with utility $U(X) = \log(1 + \frac{x}{B})$ believes the market behaves like a geometric Brownian motion with parameters (μ_1, σ_1) and the market maker views the true parameters as (μ_2, σ_2). The optimal payoff $B_1^\star$ is given by*

$$B_1^\star(x) = B\left(\frac{\sigma_2}{\sigma_1}\exp\left(-\frac{\left(\log\frac{x}{S(0)} - \gamma_1 T\right)^2}{2\sigma_1^2 T} + \frac{\left(\log\frac{x}{S(0)} - \gamma_2 T\right)^2}{2\sigma_2^2 T}\right) - 1\right). \quad (5.6)$$

Moreover, F is in $L^2_{\mathbb{P}}$ if and only if either of $\sigma_1^2 < \frac{3}{2}\sigma_2^2$ or both $\sigma_1^2 = \frac{3}{2}\sigma_2^2$ and $2\sigma_1^2\gamma_2 - 3\sigma_2^2\gamma_1 \geq 0$ hold.

Proof. Formula (5.6) follows from Theorem 5.1.1 and setting $a = 1$. To show when F is in $L^2_{\mathbb{P}}$, we compute the second moment of the shifted payoff $F + B$. For simplicity, suppose that $S(0) = 1, T = 1$ and $B = 1$ as one may construct generic parameter values through rescaling and translation. We compute

$$\begin{aligned}\mathbb{E}^{\mathbb{P}}(F+B)^2 &= \int_0^\infty \frac{\sigma_2^2}{\sigma_1^2}\exp\left(-\frac{(\log x - \gamma_1)^2}{\sigma_1^2} + \frac{(\log x - \gamma_2)^2}{\sigma_2^2}\right) g(x, \mu_1, \sigma_1, 1, 1)dx \\ &= \int_0^\infty \frac{\sigma_2^2}{\sqrt{2\pi}}\frac{1}{x\sigma_1^3}\exp\left(-\frac{3(\log x - \gamma_1)^2}{2\sigma_1^2} + \frac{(\log x - \gamma_2)^2}{\sigma_2^2}\right)dx, \quad (5.7)\end{aligned}$$

and rewrite the exponential term in (5.7) as

$$\begin{aligned}&-\frac{3(\log x - \gamma_1)^2}{2\sigma_1^2} + \frac{(\log x - \gamma_2)^2}{\sigma_2^2} \\ &\qquad = \frac{(2\sigma_1^2 - 3\sigma_2^2)\log^2 x - (4\sigma_1^2\gamma_2 - 6\sigma_2^2\gamma_1)\log x + 2\sigma_1^2\gamma_2^2 - 3\sigma_2^2\gamma_1^2}{2\sigma_1^2\sigma_2^2}.\end{aligned}$$

Clearly, if $2\sigma_1^2 > 3\sigma_2^2$, the random payoff F has infinite variance. In the case $2\sigma_1^2 = 3\sigma_2^2$ the $\log^2$ term vanishes, so convergence is determined by the sign of the log term. Finally, if $\sigma_1^2 < \frac{3}{2}\sigma_2^2$, the function after the integral in (5.7) can be written as a lognormal density modulo a constant; hence the integral converges. □

Formula (5.6) represents the likelihood ratio payoff in the asset space. When $\sigma_1 < \sigma_2$, resp. $\sigma_2 > \sigma_1$, the likelihood ratio is directly, resp. inversely, proportional to a lognormal density. The optimal payoff for two sets of parameters is displayed in Figure 5.1. The first set of parameters, $\mu_1 = \mu_2 = 0.1, \sigma_1 = 0.3, \sigma_2 = 0.4$, represents a case where the forecasted and market distribution have the same drift, but the forecasted distribution assumes a reduced volatility. Thus a logarithmic utility-maximizing agent can speculate on the absence of a larger move in the underlying asset price. A popular option trading strategy that speculates on the absence of such a move is called a strangle. Specifically, a strangle consists of a put option with strike K_1 and a call option with strike $K_2 > K_1$. These options are usually out of the money, which reduces the net cost of the overall option strategy. The second set of parameters is

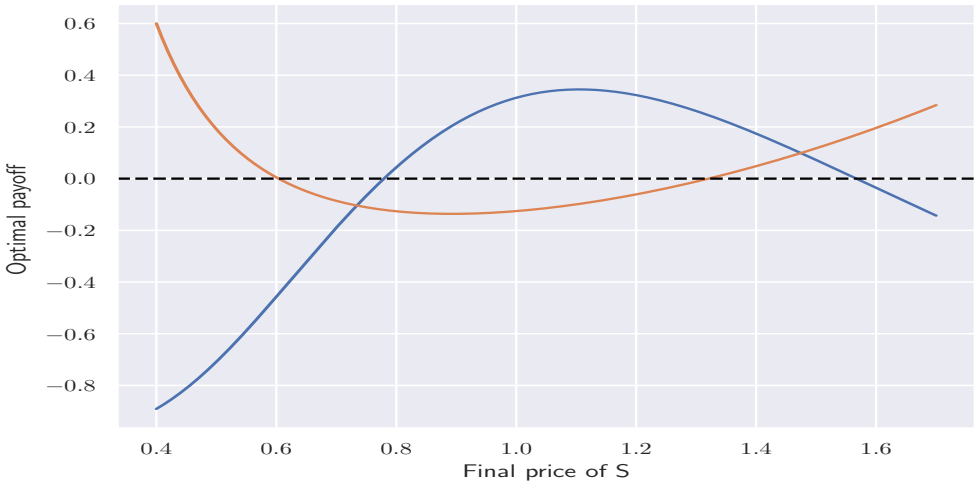

Figure 5.1: The blue line corresponds to the optimal payoff with parameters $\mu_1 = 0.1, \sigma_1 = 0.3, \mu_2 = 0.1, \sigma_2 = 0.4$ while the orange line corresponds to the optimal payoff with parameters $\mu_1 = 0.1, \sigma_1 = 0.4, \mu_2 = 0.05, \sigma_2 = 0.35$.

$\mu_1 = 0.1, \mu_2 = 0.05, \sigma_1 = 0.4, \sigma_2 = 0.35$. In this case, the forecasted distribution of the agent is more volatile than the market distribution; however, it has a greater risk premium. The optimal payoff for the agent believing in a higher volatility grows beyond any bound as the underlying asset price either goes to zero or infinity, whereas for an agent believing in the smaller volatility, the optimal payoff is bounded from above as well as from below by minus one.

The payoff function (5.6) may be replicated by a dynamic portfolio containing the underlying asset.

Theorem 5.1.3. *Under the martingale measure $\mathbb{Q}$ the price $V(t)$ of the contract that pays $B_1^\star$ assuming the underlying evolves according to a geometric Brownian motion is given by*

$$V(t) = B\left[\frac{\tilde{\sigma}}{\sigma_1\sqrt{T-t}}\exp\left(-\frac{(\log S(0)+\gamma_1 T)^2}{2\sigma_1^2 T}+\frac{(\log S(0)+\gamma_2 T)^2}{2\sigma_2^2 T}\right.\right.$$
$$\left.\left.-\frac{(\log S(t)+\gamma_2(T-t))^2}{2\sigma_2^2(T-t)}+\frac{\tilde{\mu}^2}{2\tilde{\sigma}^2}\right)-1\right], \quad (5.8)$$

and the associated delta hedging strategy is

$$\Delta(t) = (V(t)+B)\left[-\frac{\log S(t)+\gamma_2(T-t)}{\sigma_2^2(T-t)S(t)}\right.$$
$$\left.+\frac{\sigma_1^2 T\left(\frac{\sigma_1^2 T}{T-t}(\log S(t)+\gamma_2(T-t))-\sigma_1^2(\gamma_2 T+\log S(0))+\sigma_2^2(\gamma_1 T+\log S(0))\right)}{\tilde{\sigma}^2(T-t)\left(\frac{\sigma_1^2 T}{T-t}+\sigma_2^2-\sigma_1^2\right)^2 S(t)}\right],$$

where here

$$\tilde{\mu} = \frac{(\log S(0)+\gamma_1 T)\sigma_2^2-(\log S(0)+\gamma_2 T)\sigma_1^2+(\log S(t)+\gamma_2(T-t))\sigma_1^2\frac{T}{T-t}}{(\sigma_2^2-\sigma_1^2)+\sigma_1^2\frac{T}{T-t}}, \quad (5.9)$$

and

$$\tilde{\sigma} = \sqrt{\frac{\sigma_1^2\sigma_2^2 T}{(\sigma_2^2 - \sigma_1^2) + \sigma_1^2 \frac{T}{T-t}}}. \tag{5.10}$$

Proof. The price $V(t)$ of the payoff F at time t given by $X(t)$ is computed using

$$\begin{aligned} V(t) &= \mathbb{E}^{\mathbb{Q}}\left[B_1^\star | X(t)\right] \\ &= \int_0^\infty B\left(\frac{\sigma_2}{\sigma_1}\exp\left(-\frac{\left(\log\frac{x}{S(0)} - \gamma_1 T\right)^2}{2\sigma_1^2 T} + \frac{\left(\log\frac{x}{S(0)} - \gamma_2 T\right)^2}{2\sigma_2^2 T}\right) - 1\right) \\ &\qquad \times \frac{1}{\sqrt{2\pi}}\frac{1}{x\sigma_2\sqrt{(T-t)}}\exp\left(-\frac{\left(\log\frac{x}{S(t)} - \gamma_2(T-t)\right)^2}{2\sigma_2^2(T-t)}\right) dx \end{aligned}$$

To simplify notation, denote

$$u = \log S(0) + \gamma_1 T, \quad v = \log S(0) + \gamma_2 T, \quad w = \log S(t) + \gamma_2(T-t). \tag{5.11}$$

The exponential term can be now be expressed as

$$\begin{aligned} &-\frac{u^2}{2\sigma_1^2 T} + \frac{v^2}{2\sigma_2^2 T} - \frac{w^2}{2\sigma_2^2(T-t)} - \frac{\log^2(x)\left[(\sigma_2^2 - \sigma_1^2)(T-t) + \sigma_1^2 T\right]}{2\sigma_1^2\sigma_2^2 T(T-t)} \\ &\qquad + \frac{\log(x)\left[2u\sigma_2^2(T-t) - 2v\sigma_1^2(T-t) + 2w\sigma_1^2 T\right]}{2\sigma_1^2\sigma_2^2 T(T-t)}. \end{aligned}$$

Since the term $-\frac{u^2}{2\sigma_1^2 T} + \frac{v^2}{2\sigma_2^2 T} - \frac{w^2}{2\sigma_2^2(T-t)}$ does not depend on x, it can be factored out of the integral. Using (5.9) and (5.10), we can rewrite the remaining terms as

$$-\frac{\log^2(x) - 2\log(x)\frac{2u\sigma_2^2(T-t) - 2v\sigma_1^2(T-t) + 2w\sigma_1^2 T}{(\sigma_2^2 - \sigma_1^2)(T-t) + \sigma_1^2 T}}{\frac{2\sigma_1^2\sigma_2^2 T(T-t)}{(\sigma_2^2 - \sigma_1^2)(T-t) + \sigma_1^2 T}} = -\frac{(\log(x) - \tilde{\mu})^2}{2\tilde{\sigma}^2} + \frac{\tilde{\mu}^2}{2\tilde{\sigma}^2}.$$

Once again, the term $\frac{\tilde{\mu}^2}{2\tilde{\sigma}^2}$ does not depend on x and can be factored out of the integral. The portion with the logarithm can be scaled to a log-normal density, thus yielding

$$V(t) = B\frac{\tilde{\sigma}}{\sigma_1\sqrt{T-t}}\exp\left(-\frac{u^2}{2\sigma_1^2 T} + \frac{v^2}{2\sigma_2^2 T} - \frac{w^2}{2\sigma_2^2(T-t)} + \frac{\tilde{\mu}^2}{2\tilde{\sigma}^2}\right) - B. \tag{5.12}$$

Substituting u, v, w into (5.12) results in equation (5.8).

Finally, the fraction of capital invested in the risky asset S is given by $\Delta(t) = \frac{\partial V(t)}{\partial S(t)}$. □

Remark 5.1.1. In the special case that $\sigma = \sigma_1 = \sigma_2$, the hedging strategy Δ simplifies to

$$\Delta(t) = \frac{\mu_1}{\sigma^2}\frac{V(t) + B}{S(t)},$$

while in the classical Merton's portfolio problem, the replication strategy is a constant fraction $\Delta(t) = \frac{\mu_1}{\sigma^2}$. The difference in the replication formula comes from the fact that in the optimal distributional trading gain problem, the market taker is maximizing an expected utility under the $\mathbb{P}$ measure, whereas the market's distributional opinion is expressed in the $\mathbb{Q}$ measure.

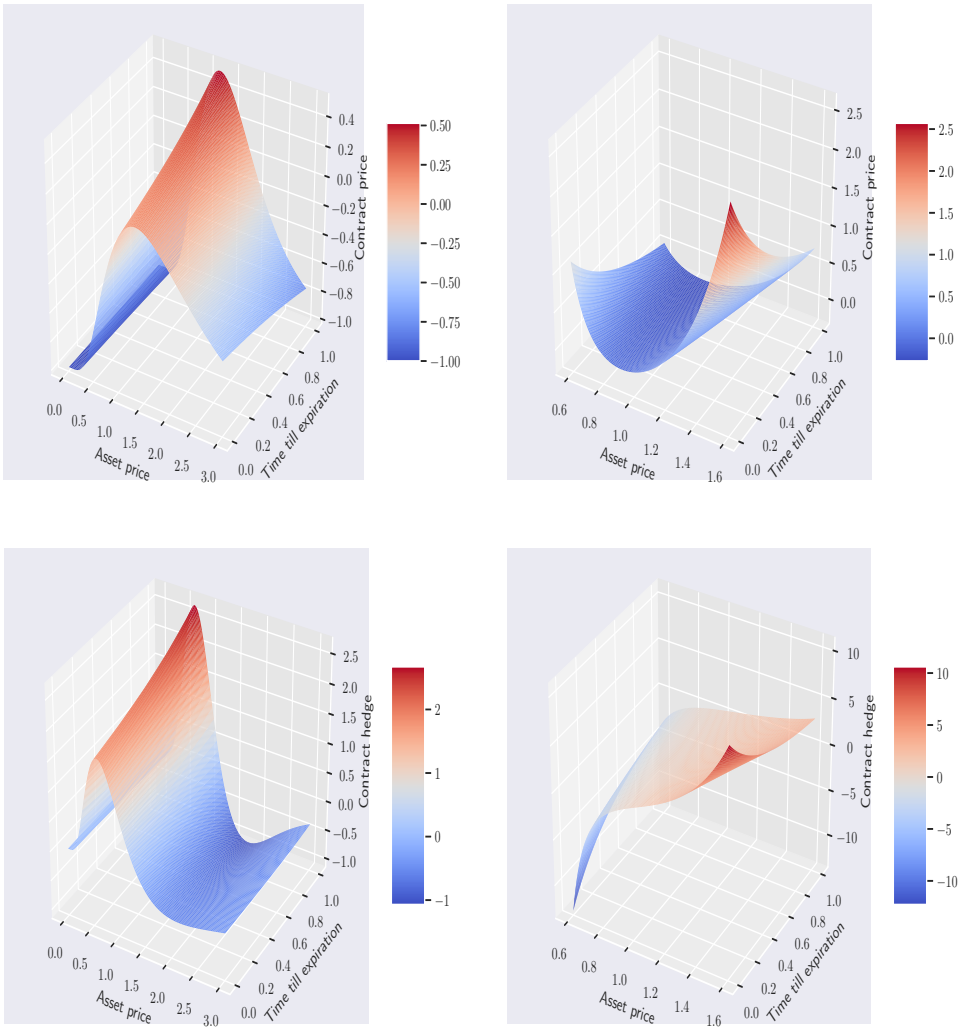

Figure 5.2: The upper two plots depict the price of the contract based upon the underlying asset price and option time until expiration for parameter sets $\mu_1 = 0.1, \sigma_1 = 0.3, \mu_2 = 0.0, \sigma_2 = 0.4$ (left) and $\mu_1 = 0.1, \sigma_1 = 0.4, \mu_2 = 0.0, \sigma_2 = 0.3$ (right). The lower plots display the hedging position in the underlying asset.

We plot the price of the contract with respect to the price of the underlying asset and expiration time in Figure 5.2 for both sets of previously described parameters.

5.1.1 Approximation of the optimal payoff

Suppose that an agent seeks to replicate the payoff $f(X(T))$. From (3.1) we know that one can replicate the payoff $f(X(T))$ by a static portfolio consisting of $f(x_0)$ bonds, $f'(x_0)$ forwards, and a basket of call and put options on the same underlying asset. For the special case $x_0 = \mathbb{E}^{\mathbb{Q}}[X(T)]$ being the forward value, we note that the forward contracts are fairly valued from the market maker's perspective. Leung and Lorig (2016) studied situations when the perfect replication is not available given a set of hedging instruments. They derived

a model-free expression for the optimal static hedge that minimizes the mean squared error subject to a cost constraint for entering into the positions in the bond and option contracts.

We study the problem from a different perspective. Instead of minimizing the mean squared error of the replication subject to a cost constraint we incorporate the cost of the replication into the static portfolio. Specifically, let $\mathbb{P}$ and $\mathbb{Q}$ represent probabilities measures of a forecasted and market distribution, respectively. Then for a payoff X we seek a static portfolio Π such that $\mathbb{E}^{\mathbb{P}}[(X-\Pi)^2]$ is minimized under the condition that $\mathbb{E}^{\mathbb{Q}}[\Pi]=0$. Moreover, to minimize both the impact of the strategy on the market and liquidity risks, we minimize over a fixed number of option contracts.

Let us illustrate the optimization procedure on options with fixed time until expiration $T=1$. We assume that the market's distributional opinion about the underlying asset's price is a lognormal process with drift μ_2 and volatility σ_2. The option's premiums are priced via the Black-Scholes formula, which is now fully determined by the type of option and strike price. First, we fix the number of different option strikes N we intend to use for the approximation. Denote by K_i and m_i the strike of the i-th option and its type (put or call) for $i=1,\ldots,N$. Similarly, by n_i we denote the position in the i-th option with negative n_i indicating a short position. Finally, by $p(K_i,m_i)$ we denote the Black-Scholes $\mathbb{Q}$–option's premium for strike K_i and option type m_i.

To ease notation, we define the function

$$g(X,K,m)=\begin{cases}(x-K)^+-p(K,m) & \text{for } m=\text{call option}\\ (K-x)^+-p(K,m) & \text{for } m=\text{put option}\end{cases}$$

For all $K>0$, we have $\mathbb{E}^{\mathbb{Q}}g(X,K,m)=0$, where X is the value of the underlying asset at the expiration time of the option. For a fixed N, we consider the following mean squared minimization optimization problem for the market taker

$$\min_{n_i}\mathbb{E}^{\mathbb{P}}\left[\left(F(X)-\sum_{i=1}^{N}n_i g(X,K_i,m_i)\right)^2\right]. \tag{5.13}$$

In other words, we want to minimize the L^2 error from the perspective of the market taker. Note that the problem (5.13) is a quadratic optimization problem. Let us define the matrix $\mathbf{C}(K,m)$ by

$$\mathbf{C}_{i,j}=\mathbb{E}^{\mathbb{P}}\left[g(X,K_i,m_i)g(X,K_j,m_j)\right]\quad \text{for } 1\le i,j\le N,$$

and the vector $D(K,m)$ by the expectation,

$$D_i=\mathbb{E}^{\mathbb{P}}\left[F(X)g(X,K_i,m_i)\right]\quad \text{for } 1\le i\le N.$$

The optimization problem (5.13) can be written in the usual quadratic form

$$\min_{n_i}\left[\frac{1}{2}n^T\mathbf{C}(K,m)n-n^TD(K,m)\right]. \tag{5.14}$$

To solve the optimization problem (5.14) we utilize the Python programming language, in particular the cvxpy (c.f. Diamond and Boyd (2016); Agrawal

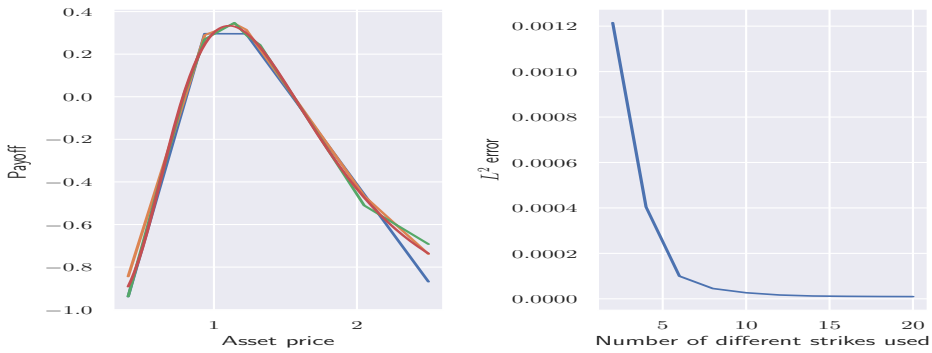

(a)

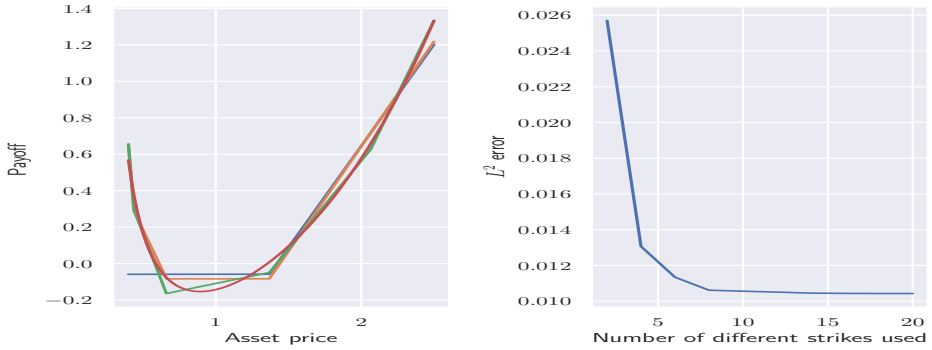

(b)

Figure 5.3: (a) The optimal payoff for parameters $\mu_1 = 0.1, \sigma_1 = 0.3, \mu_2 = 0.1, \sigma_2 = 0.4$ and its approximation error. (b) The optimal payoff for parameters $\mu_1 = 0.1, \sigma_1 = 0.4, \mu_2 = 0.05, \sigma_2 = 0.35$ and its approximation error.

et al. (2018)) and pandas packages for convex optimization and data preparation, wrangling, and plotting purposes, respectively.

The dependence on K in (5.14) does not permit one to solve this optimization problem directly. To remedy this situation, we introduce a set of strikes $(K_1^{test}, \ldots, K_{100}^{test})$ chosen to be uniformly spaced quantiles of the lognormal distribution under the $\mathbb{P}$ measure which we optimize. The matrix $\mathbf{C}$ and vector D are then estimated using Monte Carlo techniques. Note that a brute-force search through all asset weight combinations for large N is computationally very extensive given the problem becomes equivalent to the feature selection question involving the construction of a performance maximizing feature subset, which is known to be NP hard. Thus, iterating over all possible combinations quickly becomes computationally infeasible. To overcome this issue, we use a greedy algorithm since it is easy to implement and, as we will see, provides a good approximation of the replication. That is, in the first step, we start by finding the optimal strikes K_1 and K_2 and their types m_1 and m_2 with position sizes determined by solving this optimization problem with the cvxpy package. For the next step, we fix strikes K_1, K_2 and the option types m_1, m_2 and find the next two optimal strikes, option types, and then recalculate the position for all other options. We repeat this procedure until we determine n_{N-1} and n_N.

On the left side of Figure 5.3, we display the increasingly accurate approximate payoffs with $N = 2, 4$ and 6 options for two sets of parameters. Notice that even

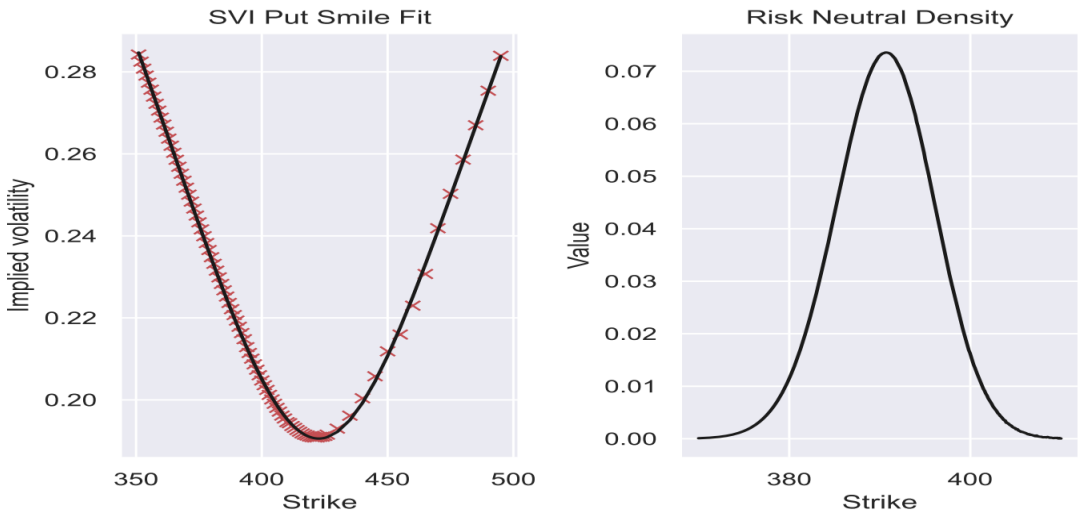

Figure 5.4: In the left subplot, we plot the SVI fit of the implied volatility values of a three month option chain of the S&P 500 ETF SPY. On the right plot we plot the associated risk neutral density.

in the case $N = 2$, the approximation fits well for the first set of parameters $\mu_1 = 0.1, \sigma_1 = 0.3, \mu_2 = 0.1, \sigma_2 = 0.4$. The options have strikes resp. types $K_1 = 0.93, K_2 = 1.22$ resp. $m_1 = \text{put}, m_2 = \text{call}$ and thus one should expect that in practice both of these strikes should be liquid enough to enter the strangle. Enlarging the number of options used results in adding options with strikes $K_3 = 1.14, K_4 = 2.04, K_5 = 0.78, K_6 = 1.32$ and option types $m_3 = \text{put}, m_4 = \text{put}, m_5 = \text{call}, m_3 = \text{put}$. For the second set of parameters $\mu_1 = 0.1, \sigma_1 = 0.4, \mu_2 = 0.05, \sigma_2 = 0.35$ the approximation of $N = 2$ options fails to capture the optimal payoff when the underlying asset goes bankrupt, as the optimal options are two call options with strikes $K_1 = 1.36$ and $K_2 = 2.8$. For $N = 4$ the additional options are two put options with strikes $K_3 = 0.44$ and $K_4 = 0.66$ that allow us to capture the left tail of the payoff. On the right side of Figure 5.3, we plot the mean squared error of the approximation. Note that when using $N \geq 8$ options, the approximation error only marginally decreases.

5.2 Risk Neutral Density Estimation with the SVI Parameterization

In practice, a lognormal assumption in the form of an asset price return distribution is too rigid. This section will estimate the implied market distribution directly from option price data using the SVI model. We will follow the implementation of the SVI model presented in Ferhati (2020b) which uses a sequential quadratic programming algorithm to obtain a risk-neutral density free of static arbitrage, i.e., an arbitrage that does not require position rebalancing.

In Figure 5.4, we plot the risk-neutral density and SVI fit of the model using SPY options as an example. The calibrated parameters found via the sequential least-squares quadratic programming algorithm are $a = -0.003, b = 0.001, \rho =$

$-0.017, m = 421.78$ and $\sigma = 52.32$. One can easily check that the resulting density is indeed a density and is free of both calendar spread and butterfly arbitrage, see, for example, Ferhati (2020a).

We will take this risk-neutral density as the option market's view on the distribution of the underlying asset price at the expiration time of the option. It will be integrated into the above results to determine an optimal replicating portfolio for a static trading strategy to maximize the expected utility of an agent seeking to benefit from the difference between this distribution and his own forecasted distribution. Next, we discuss how one may determine such a portfolio through optimization techniques.

5.3 Optimal Option Portfolio Determination via Kernel search

We seek to determine the optimal portfolio of call and put options an agent should hold to maximize an expected utility based upon the difference between a forecasted and actual market risk-neutral distribution. To avoid computational costs related to integer programming problems, we utilize a kernel search heuristic framework introduced by Angelelli et al. (2010, 2012). The idea of the kernel search heuristics is to select a kernel $\Lambda \subset M$ of promising securities and then solve the associated integer programming problem by considering securities only in Λ. The remaining securities are then divided into buckets B_i, and the algorithm solves a sequence of restricted integer programming problems constructed from the original objective to create a progressively refined solution.

Formally, the kernel search consists of two phases, the initialization phase, and the extension phase. In the initialization phase, the kernel Λ is selected, and then the rest of the assets are divided into buckets. A smaller Λ may result in a low-accuracy solution but usually requires significantly lower computational cost to obtain than the optimal solution on this set. One method to select Λ is to use the optimal solution of the continuous relaxation of the initial problem, see Angelelli et al. (2012). Their approach relies on sorting all assets in non-decreasing order using some criterion based on the weights in the relaxed problem. First, C assets are chosen as the kernel Λ, where C is the heuristic parameter. The rest of the assets are then divided in sorted order into buckets of fixed length L_b, where L_b is chosen apriori, with the possibility that the last bucket is smaller. Finally, the integer programming problem for the kernel Λ is solved to obtain the initial solution of the problem. This concludes the *initialization phase*.

The extension phase tries to improve the solution obtained in the initialization phase and consists of iterating over buckets B_i and solving the integer problem for $\Lambda \cup B_i$ with two additional natural constraints. The first constraint is that we need to improve the optimal value of the current solution, and the second condition is that at least one of the assets in B_i has to be used, which reduces the computational complexity of the problem. If the solution is feasible, i.e. it improved our optimal value, we update our optimal value and set $\Lambda := \Lambda \cup \Lambda_i$, where $\Lambda_i \subset B_i$ is the subset of assets in B_i that are used in the new optimal solution. To control the size of the kernel Λ, Guastaroba and Speranza (2012)

introduced the removal of assets that have not been used in the last p iterations. The kernel search heuristics algorithm is summarized below.

Algorithm 1: Kernel search

Initialization phase

1. Solve the continuous relaxation of the original problem
2. Determine a kernel Λ and sequence of buckets B_i
3. Solve the integer problem for Λ

Extension Phase

while $i \leq$ *number of buckets* **do**

1. Solve the integer problem for $\Lambda_i = \Lambda \cup B_i$
2. **if** *model* Λ_i *is feasible* **then**
   Update kernel with newly selected securities Λ_i from B_i, i.e. $\Lambda := \Lambda \cup \Lambda_i$
   Update the optimal value
3. Remove non-promising securities from the kernel Λ

end

The theoretical replication formula (3.1) implies that one only needs a subset of call and put options depending on the choice of x_0. In our numerical study we choose x_0 to be the forward value, i.e. $x_0 = S(0)e^{rT}$. To illustrate the solution of the relaxed problem, we plot the approximated payoff and individual weights in the options contracts in Figure 5.5 for SPY. Notice that the approximation visually corresponds to the theoretical payoff for smaller movements in the underlying asset price. For larger movements, the approximation starts to differ from the theoretical payoff, which is caused by sparsity of the out-of-the-money strikes. Moreover, the position in each option contract is rather small which poses a problem since the position in the option contracts can only be integer valued in practice. Finally, trading a large selection of option contracts poses a significant risk to the market taker. For example, once other market participants notice heavy market activity from the market taker, the price of the option contracts is likely to move against the market taker, and thus the price for entering the position would be higher.

5.4 Numerical Examples

In this section, we consider several numerical examples related to the optimization problem (5.13). We start by listing deviations from the above theoretical approach, which are essential for practical applications. Next, we briefly describe the actual market data used in these experiments and estimate the risk-neutral measure $\mathbb{Q}$ via the SVI model. Finally, using integer programming techniques, we consider examples that approximate the theoretical payoff (5.6) with option portfolios.

5.4.1 Differences from the theoretical approach

From the practitioner's point of view, the following are differences from the above theoretical approach that should be taken into consideration:

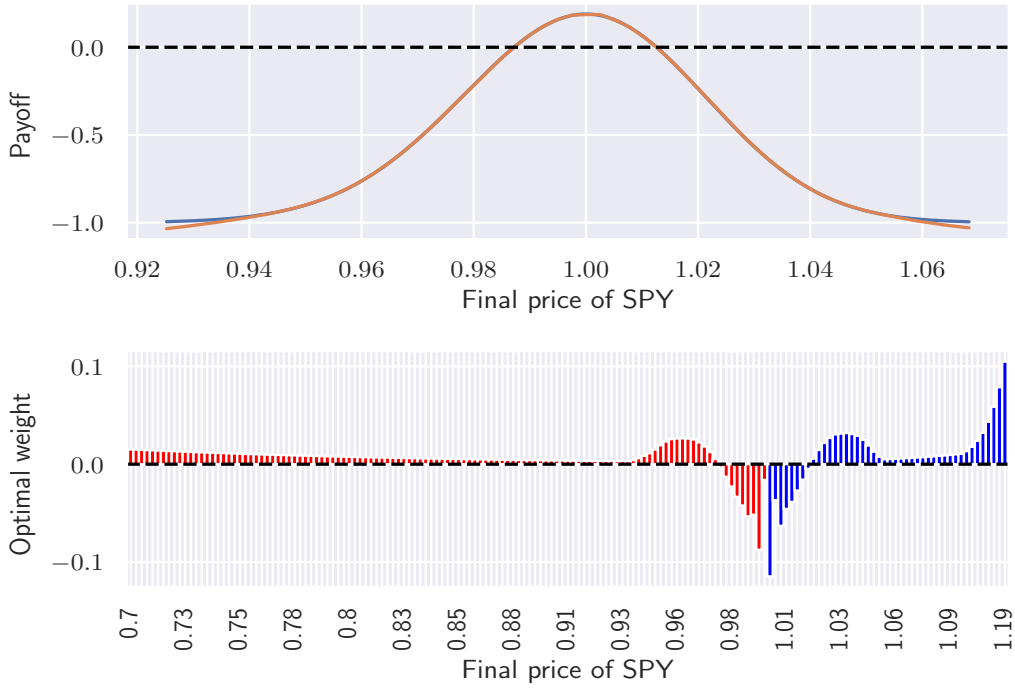

Figure 5.5: The upper plot is the theoretical payoff (blue) along with its approximation using fractional asset positions (orange) in put and call options for SPY. In the lower plot, positions in individual put (red) and call (blue) options are displayed.

- The position sizes n_i are integer-valued as one cannot buy or sell a fractional share of an option contract. Thus, the optimization problem (5.13) has to be reformulated in the integer programming optimization setting.
- A single option contract covers 100 shares of the underlying asset.
- The strikes available on the market comprise a discrete set, e.g. one cannot select an arbitrary strike value. Moreover, deep-out-of-the-money options may have liquidity problems.
- The distributional opinion measure $\mathbb{Q}$ of the market is not readily available and needs to be estimated in order to calculate (5.6).

5.4.2 Market Data and Software

We now discuss the market data used in these numerical studies and related software relevant to their implementation. We use the tia and blpapi Python packages to construct end-of-day put and call option market data using Bloomberg's API. We consider end-of-day closing prices for call and put options written on two equity indices: SPY and DAX. To minimize liquidity risk, we filter out options whose bid price is lower than \$0.01.

To illustrate the data, we shall focus on the SPY options. We examine the options on February 19th, 2021, and consider an end-of-quarter expiration on June 18th, 2021. The prices of the call and put options are displayed on Figure

5.6. Note that the closing price of the underlying asset was \$390.7. Using the three-month Treasury yield as a risk-free rate proxy, we use the Newton-Raphson technique to calculate the implied volatility of the options from their prices.

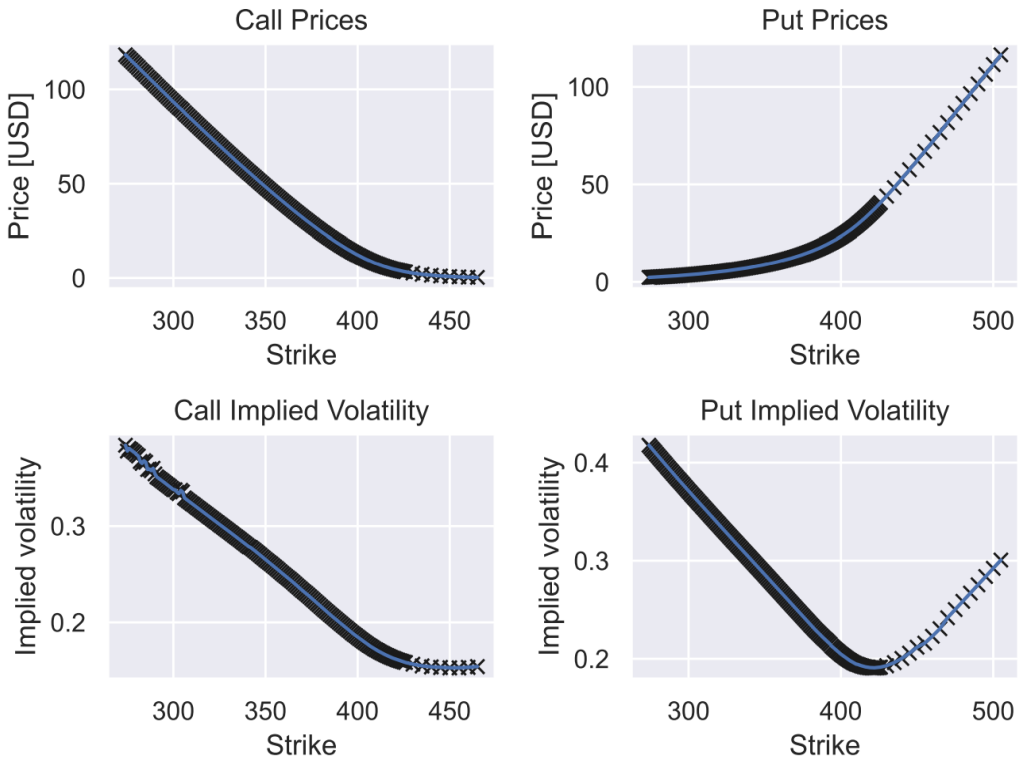

Figure 5.6: February 19th, 2021 end of day prices and implied volatilities for SPY put and call options with maturity June 18th, 2021. The plot data represent implied volatility values for different strikes.

5.4.3 Approximation of the Payoff

Using the risk-neutral density obtained from the SVI model, we can compute the optimal payoff (5.6) and its approximation. Note that we allow the distributional opinion of the market to be any probability measure $\mathbb{P}$ such that F is continuous. We start by rewriting the optimization problem (5.13) to reflect real market conditions. Suppose there are M sufficiently liquid hedging assets available for the optimization; each of the assets can be identified by its strike K_i and its type m_i for $i \in \{1, \dots, M\}$. The position in the option contracts can only be integer-valued. Thus the optimization problem (5.13) can be written in the following form:

$$\min_{n_i} \mathbb{E}^{\mathbb{P}} \left[\frac{1}{2} n^T \mathbf{C}(K, m) n - n^T D(K, m) \right], \tag{5.15}$$
$$n_i \in \mathbb{Z}, \qquad \sum_{i=1}^{M} |n_i| \leq N.$$

To solve the optimization problem (5.15), we utilize the Gurobi optimization library (Gurobi Optimization (2021)), the cvxpy convex optimization Python

Symbol	No. call options	No. put options	Spot
SPY	161	169	$ 390.72
DAX	106	113	13 886.93 €

Table 5.1: Description of the filtered option data set.

package, and a kernel search heuristic. Note that the above is an integer quadratic problem and is inherently non-convex. In its full generality, integer quadratic problems are NP-complete problems, see Vavasis (1990).

5.4.4 Numerical Experiment Results

In this subsection, we apply the proposed methodology to a historical financial dataset. All numerical experiments were conducted on a Windows machine with an Intel Core i5-3470 CPU with 3.20GHz and 16 GB of RAM.

We illustrate the approximation procedure for two choices of the market taker's measure $\mathbb{P}$ for logarithmic, exponential, and power utility functions. Our first choice is that the market taker believes that the implied volatility on option contracts should be 50% lower than the market price. The second choice is that the implied volatility should be 50% higher. The matrix $\mathbf{C}$ and vector D are then estimated using Monte Carlo. Finally, to make assets comparable, we modify the option's payoffs and premiums so that they are not denominated in dollars, but in the underlying asset. This allows us to compare different options quickly.

Single maturity

Our choice of studied symbols are SPY and DAX as options on indices are highly liquid, and thus one can assume that the approximation of the theoretical payoff will be sufficiently good. We study the options on February 19th, 2021, focusing on the quarter expiration on June 18th, 2021. Moreover, to make the indices SPY and DAX comparable, we normalize them by the spot price of the underlying asset. As mentioned in the data section, we filter out options with small bid prices and bid-ask spreads greater than 10% of the bid price to reduce the liquidity risk. The number of options considered and the associated spot prices are summarized in Table 5.1.

On the left side of Figure 5.7, we plot the market-implied density where associated option market implied volatility values were estimated using the SVI model. In addition, we also display the density of the market taker who believes that the implied volatility of each option on the market should be 50% higher or 50% lower. Notice that the market density for SPY and DAX are very similar. In the middle of Figure 5.7, we plot the optimal payoffs for the logarithmic utility (blue), power utility with $a = 0.75$ (orange) and exponential utility (green). Similarly, the higher volatility case is plotted on the right. For the lower volatility case, note that the market taker realizes a profit only for small moves in the price of the underlying asset, and in the case of bigger moves, his loss is bounded for logarithmic and power utility, which behave similarly. For the higher volatility case, the market taker can realize multiple units of the underlying asset in case

of more significant moves, which is due to the fact that the market assumes that these events are extremely unlikely.

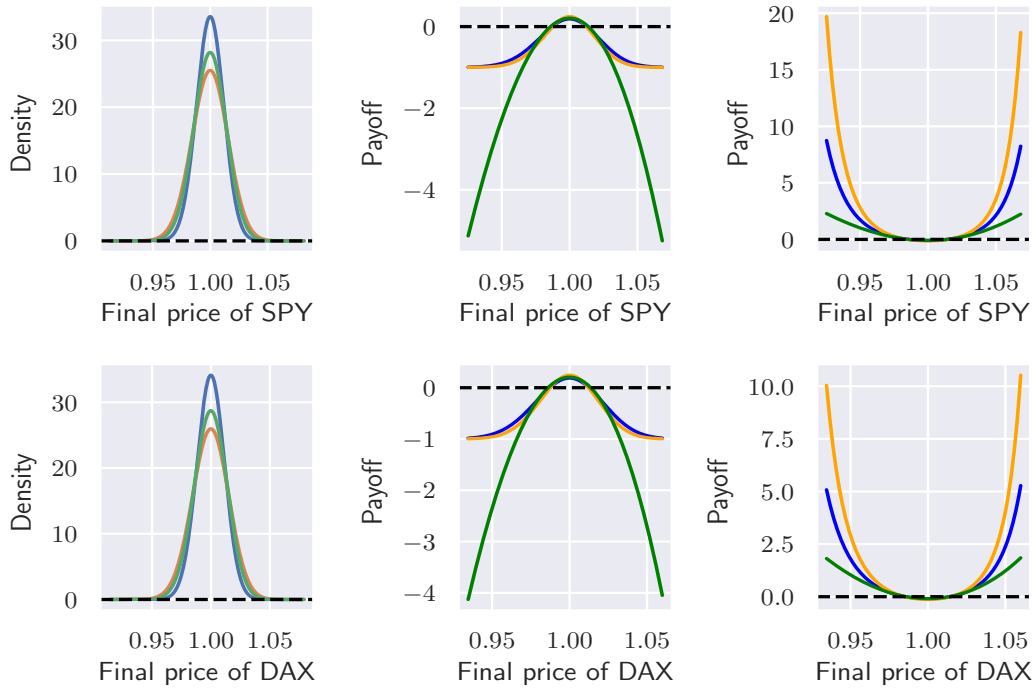

Figure 5.7: The left subplot contains estimated risk neutral densities (blue) along with the density of the market taker believing in smaller (orange) resp. higher (green) volatility. On the middle plots (lower volatility) resp. right plots (higher volatility) are associated with optimal payoffs in the asset space for logarithmic utility (blue), power utility with $a = 0.75$ (orange) and exponential utility (green) for the market taker.

For the implementation of kernel search heuristics, we choose the parameter $C = 20$ for the size of the initial kernel Λ. For the choice of the bucket length L_b, we follow Guastaroba et al. (2017) where the authors recommend to use $L_b = C$. Finally, we set the removal parameter $p = 3$ as this choice leads to significant computational speedup while having only a minor effect on the quality of the solution found.

To illustrate the behavior of the kernel search heuristics, we plot the approximation for $N = 10$ and $N = 20$ in Figures 5.8 and 5.9 for the SPY and DAX indices. In the higher volatility case, the kernel search fit captures the optimal payoff (2.6) in both cases. For the lower volatility case, the kernel search algorithm reasonably captured the center of the payoff curve, but it fails to capture payoffs for larger movements in the price of the underlying asset. This is because a one-contract option covers one hundred shares of the underlying asset and, more importantly, the lower volatility model believes that these outcomes are extremely unlikely, and thus their contribution to the density-weighted L^2 error from the market taker's perspective is minuscule.

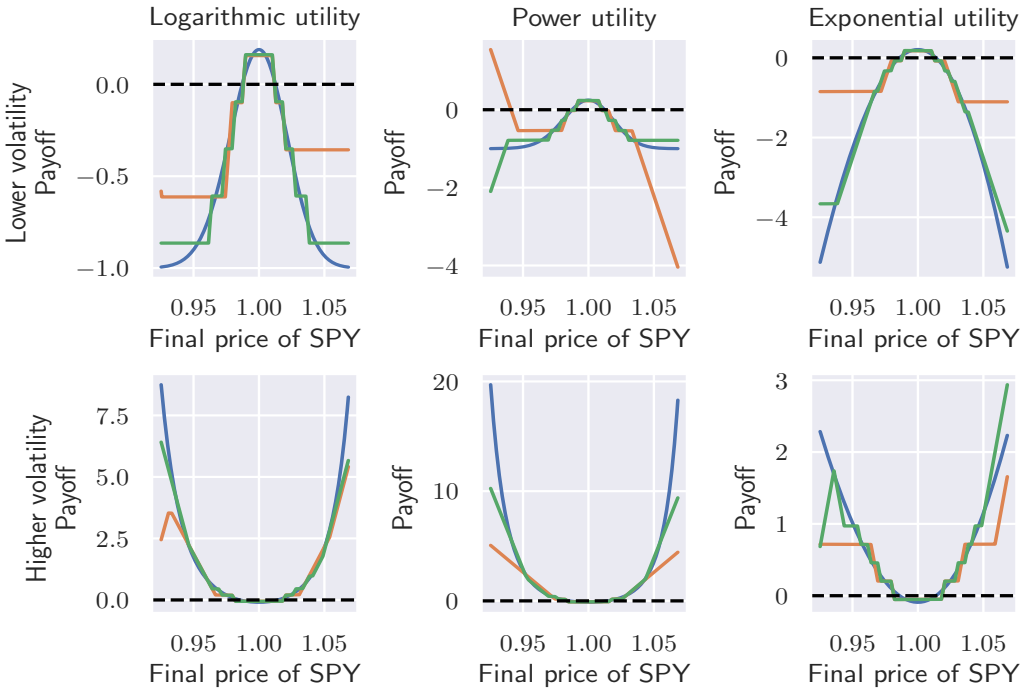

Figure 5.8: Approximation of the optimal payoff for the SPY ticker using $N = 10$ (orange) resp. $N = 20$ (green) options.

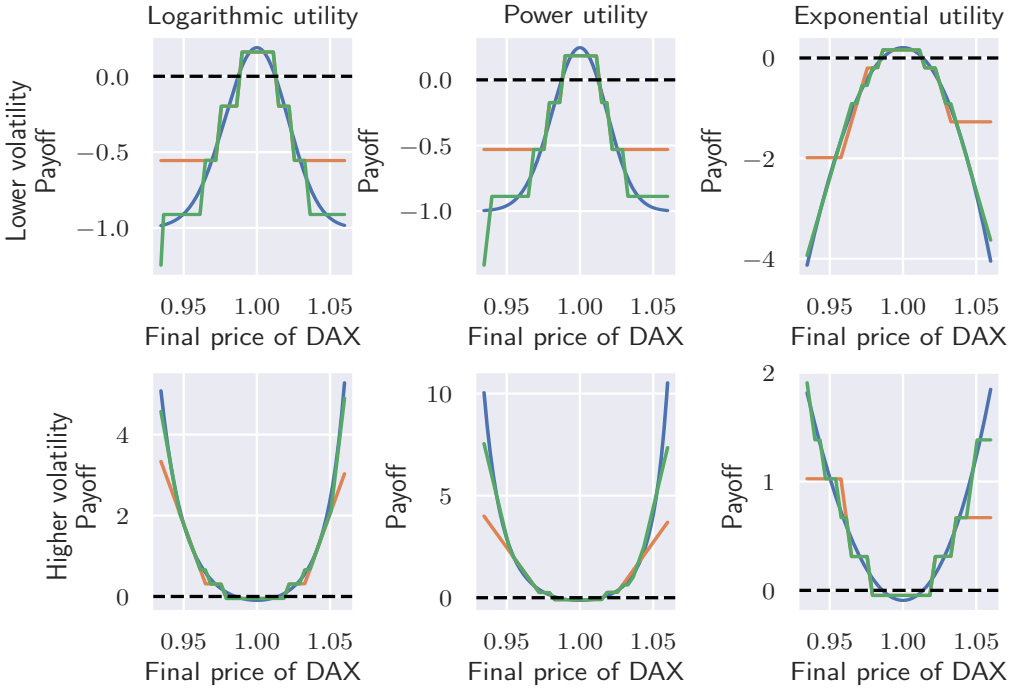

Figure 5.9: Approximation of the optimal payoff for the DAX ticker using $N = 10$ (orange) resp. $N = 20$ (green) options.

Errors for the kernel search heuristics are plotted in Figure 5.10. Note that using twelve or more options for the approximation procedure has only a small marginal impact on the L^2 error and that the SPY and DAX error functions behave similarly. The fact that the approximation error does not decrease monotonically in the number of options can be contributed to the removal part of the kernel search algorithm.

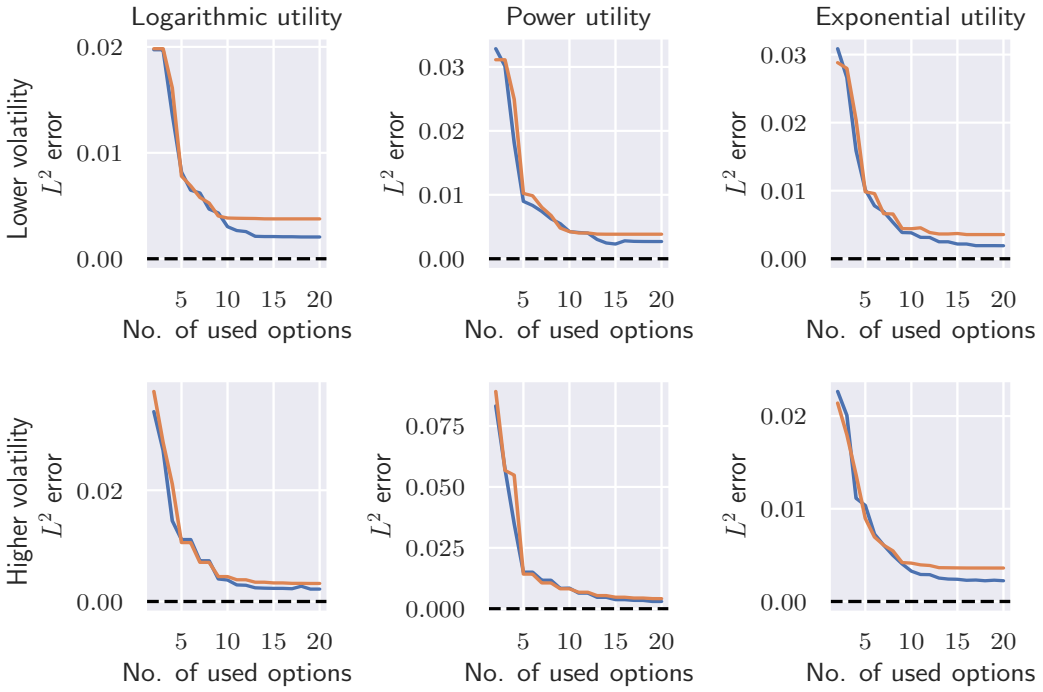

Figure 5.10: Error for the approximation of SPY (blue) and DAX (orange).

Finally, we note that one could be interested in enriching the option data set used for replication by options that were filtered due to the specific choice of x_0 in the replication formula (3.1). The intuition is that by enriching the option data set, one could achieve a better approximation of the optimal payoff at the cost of larger computational time. To study this problem, we ran the approximation procedure five times on both the entire option price dataset and on the filtered version for the lower volatility case with logarithmic utility in the case of the SPY ticker. In Figure 5.11, we plot the average computational time on a logarithmic scale and the average approximation error. Using the entire option data set significantly increases computational time, but does not improve the quality of the replication procedure. To better illustrate the difference in computational time, note that using ten options for the replication provides a relatively good approximation of the optimal payoff. The computational time using ten options for the replication in the filtered data set case was 2.9 seconds, while for the whole data set, it was 214.6 seconds.

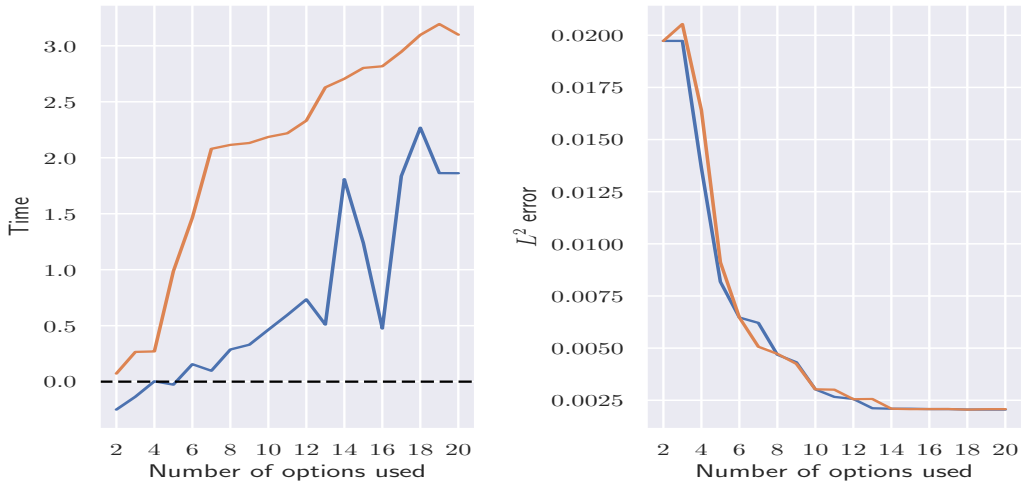

Figure 5.11: Comparison of runtime on logarithmic scale (left) and approximation error (right) for lower volatility case with logarithmic utility and SPY ticker using all options on the market (orange) versus using filtered option data set (blue).

5.4.5 Multiple maturities

In this subsection, we focus on constructing replicating portfolios during time periods of increased levels of market uncertainty. Specifically, during the end of November 2021, a new variant of COVID-19 called omicron was discovered. Since this variant appears to be more contagious than the current prevalent COVID-19 delta variant, equity and commodity markets reacted to an anticipation of lockdowns and the halt of international travel. For example, WTI crude oil lost around 10% of its value on November 26th. Similarly, airline industry stocks have declined significantly.

In addition to the SPY and DAX ETFs, we also examine the USO (United States Oil Fund) and GLD (SPDR Gold Shares) funds. USO may be seen as a particularly risky asset during the omicron uncertainty period, while GLD can be viewed as a relatively stable one. We use the same methodology as in the previous subsection. We run the replication procedure for various maturities for each symbol but only focus on the logarithmic utility function. The list of option maturities differs for each ticker and can be seen in Figure 5.12. The SPY ticker has the greatest number of option strikes available on the market. The quantity of option contracts available for other tickers varies greatly by maturity. For example, for USO, we can see that the number of options available for the March 18th 2022 maturity is very limited, which indicates a potential problem when replicating the portfolio.

Symbol	Spot	Δ_1	Δ_2	Δ_3	Δ_4	Δ_5
SPY	$ 470.74	1.0	1.0	1.0	1.0	5.0
DAX	15623.31 €	50.0	50.0	50.0	100.0	100.0
USO	$ 52.03	0.5	1.0	1.0	1.0	0.5
GLD	$ 166.58	1.0	1.0	1.0	1.0	1.0

Table 5.2: Spot option price at December 10th, 2021 together with minimal option strike distances Δ between neighboring options available at the market for maturities as in Figure 5.12.

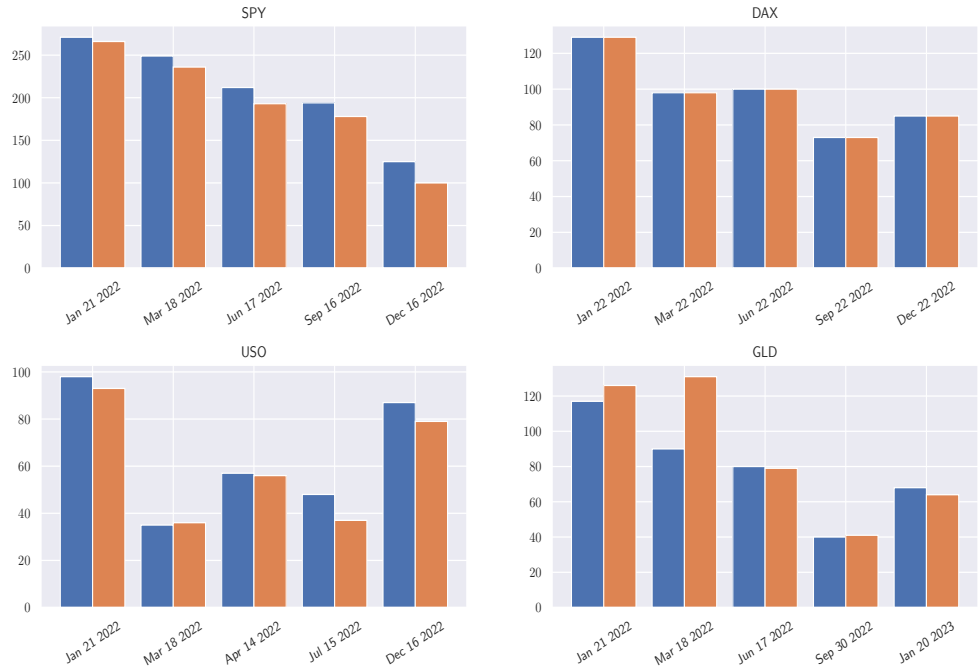

Figure 5.12: Number of analyzed call (blue) and put (orange) options for various tickers and maturities.

To achieve an accurate replication of the theoretical payoff, it is crucial to both have a large number of options available and to consider strikes as close together as possible. Naturally, the greater the minimal distance between two strikes the rougher the approximation of the payoff. In Table 5.2, we describe the spot price of the underlying ETF and the minimum distance Δ between two neighboring option strikes. As the minimal distance for SPY, DAX, and USO is relatively small, in terms of the spot price of the underlying asset, one could hope to achieve a strong replicating portfolio. In contrast, option strikes on USO are minimally about 2% of the spot price apart from each other, thus one can expect a lower quality fit.

The replication error for the logarithmic utility as a function of maturity is plotted in Figure 5.13. Let us briefly describe the results. From the considered tickers, the replication error for SPY is the lowest for both the lower volatility and the higher volatility case. For SPY, the option maturity with highest replication

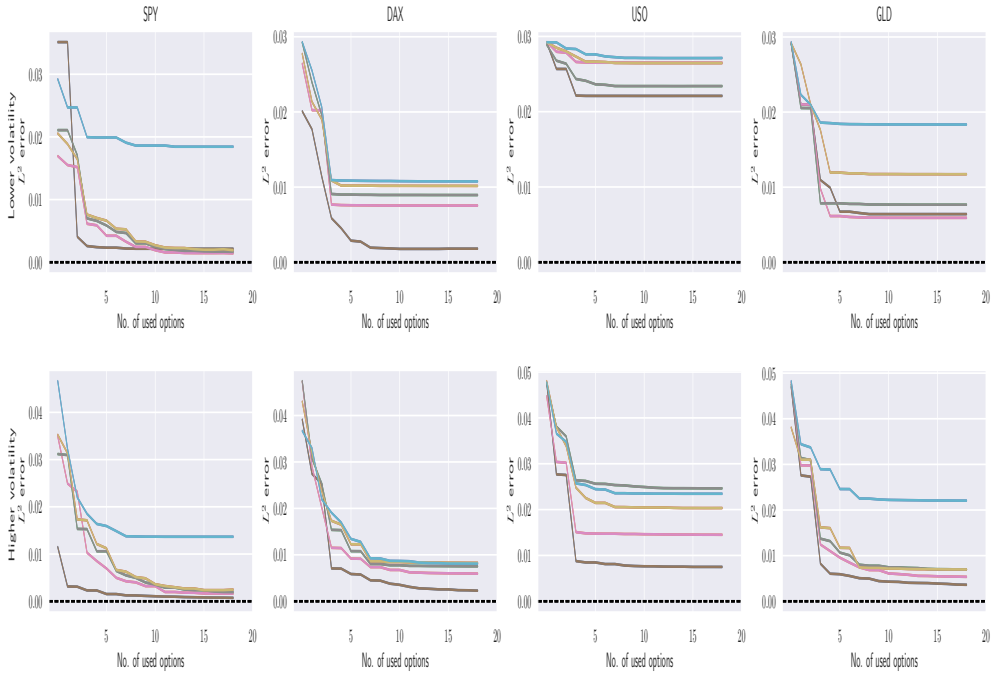

Figure 5.13: Error for the approximation of SPY, DAX, USO and GLD. Colors correspond to maturities as given in Figure 5.12 in the same order: brown, pink, gray, ochre, blue.

error is December 16th, 2022. This is because the minimal distance between neighboring option strikes increases from 1 to 5, which naturally yields a poorer replication. For DAX we see that in the lower volatility case, the lowest replication error is achieved by options that expire on January 22, 2022. This is because there is a denser set of options available on the market for the replication and the discrepancy between the distributional opinions of the market taker and market maker is lower since the time until expiration is the least of the considered maturities. For other maturity times, we note that in the low volatility case, there is only a minor improvement in the L^2 error of the replication when using five or more option contracts. USO achieves the worst replication, which is due to the sparse option data set available. GLD achieves a similar replication error as the DAX, with the exception that the replication when using options with a January 20, 2023 expiration achieves poor performance. This is due to the sparsity of the options available around the spot price.

In Figure 5.14 we plot the approximation for USO and GLD with maturities July 15th, 2021, respectively for March 18th, 2021 using $N = 6$ option contracts. For the lower volatility case, the replicating portfolio for GLD seems to capture the theoretical payoff around the spot price, however, for USO, the fit is of lower quality which can be contributed to sparsity of available strikes on the market.

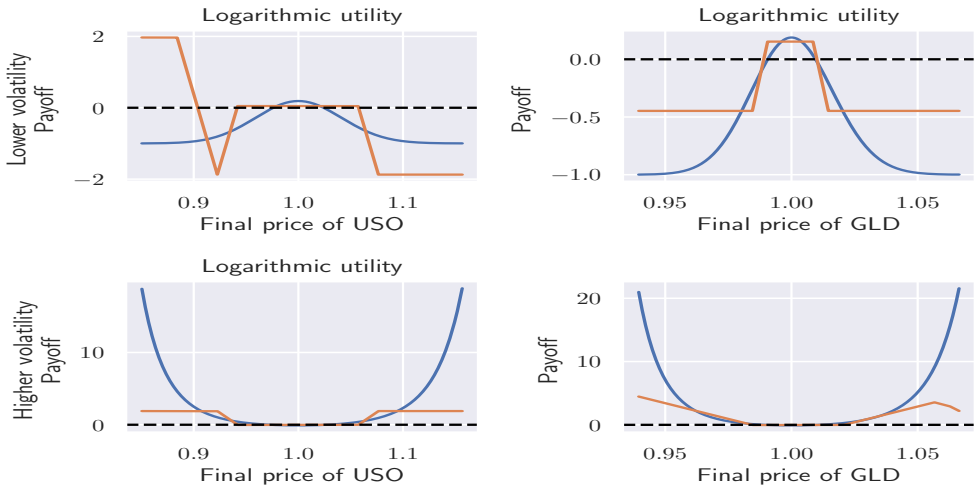

Figure 5.14: Approximation of the optimal payoff for the USO resp. GLD using options with maturity July 15, 2021 resp. March 18, 2021 using $N = 6$ options.

5.5 Conclusion

In this chapter, we have examined a utility-maximizing portfolio from the perspective of an agent who believes in the distributional discrepancy between the risk-neutral and market-implied densities of an underlying asset. Under a geometric Brownian motion assumption, we provided exact formulas for the price and delta hedge for this portfolio. In the general case, we use integer programming and kernel search heuristics for the static replication of the optimal gain of the agent under the assumption that the price of the replicating portfolio from the market's perspective is trivial. We show that the replicating portfolio consisting of ten options provides a good approximation of the optimal payoff for various utility functions using historical market data. Moreover, according to our numerical results, it is sufficient only to use a subset of the options available on the market for the replication procedure, which significantly reduces the computational time of integer programming methods while having no impact on the replication quality.

6. Options on a traded account: symmetric treatment of the underlying assets

6.1 Introduction

This chapter is based on the article Večeř et al. (2020) in which we studied passport options with two assets. We restate the results here and mention a possible extension to an arbitrary number of assets. Options on a traded account have been widely studied in the previous literature. In the simplest setup, the client is free to trade in two underlying assets subject to specific contractual limits. At maturity, he can keep the profits from this trading strategy while his losses are forgiven, which intuitively leads to risky strategies. Some of the contracts within this family, such as passport options, have even been actively traded. However, such contracts have been unpopular so far. Arguably, the major reason is the fact that the previously studied contracts are expensive in relation to the client's portfolio, which we will demonstrate with several examples. Moreover, these contracts treat the two underlying assets asymmetrically. In the traditional setup, the restriction of the trading position is set to one asset only, and the residual wealth is invested in the second asset. For the passport option, the restriction on the position in the first asset is $[-1, 1]$, which means that the agent can take any position between long and short. The residual wealth gives the position in the second asset. The typical starting wealth is at $X = 0$ for the traded account insured by the option, and since one position in the underlying asset is short, and the other is long, the corresponding option covers losses on heavily leveraged positions, making the resulting contract relatively expensive and speculative for any practical purposes of investment or pension funds that could naturally benefit from the existence of such products.

Passport options were introduced in the paper of Hyer et al. (1997). The authors derived the optimal strategy in the geometric Brownian motion model, which is achieved by a short position when the traded account is positive and a long position when the traded account is negative. They also found the corresponding option value by solving the corresponding pricing partial differential equation. Andersen et al. (1998) described a numerical algorithm for solving the pricing differential equation. Henderson and Hobson (2000) showed that the same strategy remains optimal in the presence of stochastic volatility. Shreve and Večeř (2000) considered more general trading limits on the first asset. The optimality of the solution was proved using probabilistic arguments based on a comparison theorem of Hajek (1985). Večeř (2001) later showed that Asian options are special cases of options on a traded account when the restriction on the first asset has a specific deterministic form and found a novel pricing partial differential equation. Delbaen and Yor (2002) showed that the strategy for the passport option remains optimal when the portfolio rebalancing is restricted to a discrete time. Kampen (2016) considered multivariate passport options, where the traded account consists of more than one asset. Moreover, the author observed

that optimal strategies might depend on the sign of correlations between assets. The decomposition of the passport option into a portfolio of plain vanilla contracts was studied by Buchen and Malloch (2014). The Greeks of the passport option were studied by Kanaujiya and Chakrabarty (2017).

The fact that the trading constraints on the two assets are asymmetric in the previously considered options on a traded account limits the applicability of such contracts. If we consider a foreign exchange type option with the underlying currencies, the dollar and euro, the contract with asymmetric constraints would be different from the perspective of the dollar and the euro investor. This is not the case for the plain vanilla options, where a call option from the perspective of the first currency is a put option from the perspective of the second currency. This leads to a natural question of whether we can formulate an option on a traded account with the symmetrical treatment of the two underlying assets.

The approach that treats both assets symmetrically is relatively straightforward. Instead of imposing an absolute restriction on the position in the first asset, one can simply require a relative restriction in terms of the fraction of the current wealth. The most natural restriction allows the client to invest any proportion of his wealth in the first asset, so the α fraction of the invested wealth in that asset is in the interval $[0, 1]$. Obviously, this is symmetric with respect to the second asset, as the residual wealth proportion $1 - \alpha$ invested in the second asset is restricted to the same interval $[0, 1]$. Moreover, this approach generalizes to any number of assets, so we can formulate the symmetric problem for an arbitrary number of assets I. This is a very natural approach as the investors are typically free to invest any portion of their wealth to assets of their choice, corresponding to a $[0, 1]$ fraction of their total wealth. The problem of finding the optimal strategy that maximizes the option value is rather complex for any $N > 2$, and thus we limit ourselves to a solution for $N = 2$ assets only.

Imposing symmetric trading restrictions is only the first necessary step for the symmetric treatment of the underlying assets. We also need to use the reference asset that treats the individual assets symmetrically. Here, a candidate for reference asset is an index that starts with 50% of both assets and remains static afterward. Our paper is structured as follows. In the next section, we mathematically formalize the definition of the option on a traded account that treats both assets symmetrically. This is model-independent. Next, we assume geometric Brownian motion dynamics and first derive the evolution of the asset prices with respect to the index. In the following step, we find the evolution of the actively traded account with respect to the index. In order to find the optimal strategy, we need to generalize Hajek's Comparison Theorem and adapt it to our problem. This extends a comparison result for stochastic sums published in Kampen (2016). It is still true that the optimal strategy has the largest volatility with respect to the index, which is interesting in itself as the resulting portfolio has the largest price variance. Thus it determines the maximal possible distributional departure in the sense of L^2 norm from the index that can be achieved by active trading. This is a well-known stop-loss strategy that invests all the wealth in the weaker asset. The volatility maximizing strategy also maximizes the probability of reaching the higher goal in a given time framework, which is shown at the end of our paper. A similar problem was studied in a different setup by Kulldorff (1993).

Our proposed setup may be appealing to conservative investment funds, such as pension funds. The pension funds typically face regulatory constraints that prevent significant fund losses. However, the client may want to be given a choice to move their investments to different markets, typically to the money market or the stock market. In order to prevent substantial losses resulting from switching between different markets, an insurance policy may be needed to cover such losses. In order that this insurance is possible, it should be reasonably cost-effective, costing only a small fraction of the client's wealth. The competitive costs are not expected to exceed 2% of the client's wealth annually, corresponding to typical hedge fund charges. As we show in our paper, the contract costs are indeed very small depending on the parameter $\sigma\sqrt{T}$, where σ is the relative volatility of the two markets and T is the time horizon. For instance, when $\sigma\sqrt{T} = 0.1$ which corresponds to a EUR-USD currency pair over a one-year horizon, the cost of the option is just 1.813% of the client's wealth. In contrast, the passport option on the same horizon with a trading constraint corresponding to the initial client's wealth costs 4.116% of his wealth, making it hardly competitive. The cost of the insurance for the same currency pair over $T = 20$ year horizon ($\sigma\sqrt{T} = 0.4472$) gives the cost of the option 9.746% of the client's wealth, making the total cost below 0.5% annually. The corresponding passport option costs more than double, namely 20.489% of the client's wealth. The stock market (SP500) and the money market pair has typically a larger relative volatility that takes a wide range of values in the interval [0.1,0.3], but the option contracts would still be fairly priced even for volatility $\sigma = 0.2$. A $T = 20$ year contract ($\sigma\sqrt{T} = 0.8944$) gives the option price 20.993%, which corresponds to an annual cost of around 1% of the client's wealth. The corresponding passport option costs 46.860%.

6.2 Model Free Setup

Our entire analysis is limited to only two underlying assets S and M. Asset S often represents the stock market, while asset M often represents the money market. For simplicity, we consider only assets with their martingale measure, such as stocks that reinvest dividends or the money markets. For instance, the prices expressed with respect to a reference asset M are $\mathbb{P}^M$ martingales. In particular $S_M(t)$ is a $\mathbb{P}^M$ martingale. Assets that do not have their own martingale measure, such as the currencies, can be linked to the corresponding money markets using the proper discounting.

We can further simplify the setup and introduce the following scaling

$$S_M(0) = 1.$$

At the start of the investment period, the investor creates a self-financing portfolio X by starting at $X(0) = S(0) = M(0)$ and at time t:

$$X(t) = \Delta^S(t)S(t) + \Delta^M(t)M(t), \tag{6.1}$$

where Δ^S and Δ^M represents the agent's strategy. Mathematically, we assume that these processes are progressively measurable. Moreover, we only allow long positions in the assets, i.e. we assume

$$\Delta^S(t) \geq 0, \qquad \Delta^M(t) \geq 0. \tag{6.2}$$

The constraint in Equation (6.2) means that the investor is free to invest any fraction between $[0, 1]$ of his wealth X into the asset S with the remaining fraction of his wealth going to the money market M. This follows from Equation (6.1) by using X as a numeraire:

$$1 = \Delta^S(t)S_X(t) + \Delta^M(t)M_X(t).$$

In particular, the investor may choose to fully invest in one fund, say in the stock market, so we have $\Delta^M(t) = 0$ and

$$1 = \Delta^S(t)S_X(t),$$

or

$$X_S(t) = \Delta^S(t).$$

The lower bound condition in one of the markets imposes an upper bound condition in the second market, so the positions are constrained by

$$X_S(t) \geq \Delta^S(t) \geq 0, \qquad X_M(t) \geq \Delta^M(t) \geq 0,$$

This is a very natural condition. Moreover, it treats both assets equivalently, imposing the same restriction. Note that the upper bounds are random and depend on the current value of the investor's wealth X. A trivial observation is that X must always be non-negative with zero wealth being an absorbing boundary.

Remark 6.2.1 (Relationship to passport options). The constraint for the passport option is on the position in the stock market only

$$a \leq \Delta^S(t) \leq b,$$

the position in the second market M follows from

$$\Delta^M(t) = X_M(t) - \Delta^S(t)S_M(t).$$

In particular, it can be negative even in the situation when we constrain the investor to have a positive position in $S(t)$ by requiring $\Delta^S(t) \geq a \geq 0$. The condition is not symmetric for both assets since the imposed restriction does not treat them equivalently. This is arguably one of the main reasons why such a contract is not appealing to the investors. Moreover, the traded account can become negative in contrast to the situation that treats both assets symmetrically.

Remark 6.2.2 (Trading restrictions allowing shorting). The trading restrictions can be generalized to allow shorting. The symmetric restriction is to allow the investor to have another lower bound on the stock position and the money market position in terms of the fraction of his wealth. The fraction of the wealth in the stock market is given by $\Delta^S(t)S_X(t)$, the fraction of wealth in the money market is given by $\Delta^M(t)M_X(t)$. The symmetric condition is that both fractions are limited by the same lower bound c:

$$\Delta^S(t)S_X(t) \geq c, \qquad \Delta^M(t)M_X(t) \geq c,$$

or in another words,

$$\Delta^S(t) \geq c \cdot X_S(t), \qquad \Delta^M(t) \geq c \cdot X_M(t).$$

The lower bound in one asset imposes an upper bound on the other asset:

$$(1-c)\cdot X_S(t) \geq \Delta^S(t) \geq c\cdot X_S(t), \qquad (1-c)\cdot X_M(t) \geq \Delta^M(t) \geq c\cdot X_M(t).$$

The constant c can be negative (allowing for shorting). However, the maximal allowed c is $\frac{1}{2}$ as one cannot impose to have positions in both assets above 50% of the wealth.

For preservation of the symmetry of the contract, it is necessary that the reference asset also treats both assets equally. One obvious choice is to use

$$I(t) = \tfrac{1}{2}(S(t) + M(t)). \tag{6.3}$$

The asset I can be regarded as an index consisting of the two assets, or equivalently, a basket of the two assets.

The contact on the actively traded account can be then defined by a payoff at the terminal time T

$$(X_I(T) - K)^+ \text{ units of } I(T)$$

for some contractually defined strike K. As $X_I(0) = 1$, the strike corresponding to the at the money option equals $K = 1$. In order to preserve the symmetry, the contract has to be settled in the index I rather than a single asset S or M. For instance, if the contract is written on two currencies, say dollar and euro, the contract seen from the position of the dollar investor or the euro investor is identical.

6.3 Price Evolution in the GBM Model

The seller of the option must be ready to cover any trading strategy used by the contract holder. In particular, the fair price of the contract corresponds to the trading strategy $\Delta^S(t)$ that maximizes the value of the option

$$\mathbb{E}^I\left[(X_I(T)-1)^+\right].$$

Let us assume a geometric Brownian motion model for the stock price $S_M(t)$, so

$$dS_M(t) = \sigma S_M(t) dW^M(t).$$

Any discounting is already incorporated in the money market M and the price $S_M(t)$ is $\mathbb{P}^M$ martingale. Similarly, the inverse price

$$dM_S(t) = \sigma M_S(t) dW^S(t)$$

is a $\mathbb{P}^S$ martingale. The relationship between $W^M(t)$ and $W^S(t)$ is

$$dW^S(t) = -dW^M(t) + \sigma dt.$$

From the self-financing trading assumption, the evolution of the trading portfolio X is

$$dX_M(t) = \Delta^S(t) dS_M(t)$$

and

$$dX_S(t) = \Delta^M(t) dM_S(t).$$

In order to find the optimal strategy, we need to find price evolutions with respect to the index I.

Lemma 6.3.1. *The evolution of the price $M_I(t)$ under the probability measure $\mathbb{P}^I$ is given by*

$$dM_I(t) = \frac{1}{2}\sigma M_I(t)(2 - M_I(t))dW^I(t).$$

Proof. Note that

$$M_I(t) = \frac{M(t)}{\frac{1}{2}(M(t) + S(t))} = \frac{2}{1 + S_M(t)}$$

and an application of Ito's lemma gives

$$\begin{aligned} dM_I(t) &= d\left(\frac{2}{1 + S_M(t)}\right) \\ &= \frac{1}{2}\sigma M_I(t)(2 - M_I(t))\left[-dW^M(t) + \frac{\sigma S_M(t)}{(1 + S_M(t))}dt\right] \\ &= \frac{1}{2}\sigma M_I(t)(2 - M_I(t))dW^I(t). \end{aligned}$$

The process $M_I(t)$ must be $\mathbb{P}^I$ martingale, which determines $W^I(t)$ as

$$dW^I(t) = -dW^M(t) + \frac{\sigma S_M(t)}{(1 + S_M(t))}dt = -dW^M(t) + \frac{1}{2}\sigma S_I(t)dt.$$

□

The SDE in Equation (6.3) is interesting on its own as it represents the evolution of the asset with respect to the index. From the definition of I in Equation (6.3), we have

$$2 = M_I(t) + S_I(t), \tag{6.4}$$

constraining the $M_I(t)$ process between 0 and 2:

$$0 \leq M_I(t) \leq 2.$$

One can think about $M_I(t)$ as the scaled proportion of the money market M in the index I. The price $M_I(t)$ has the largest volatility when $M_I(t) = 1$, or in other words, when $M(t) = S(t)$. The process $M_I(t)$ loses volatility in two extreme cases, when $M_I(t) = 0$ and when $M_I(t) = 2$. The first case corresponds to $S_M(t) = \infty$, so the asset M is worthless in comparison with the asset S, the second case corresponds to $S_M(t) = 0$ when the asset S is worthless in comparison with the asset M.

Note that from the symmetry of the problem, we have immediately

$$dS_I(t) = -\frac{1}{2}\sigma S_I(t)(2 - S_I(t))dW^I(t). \tag{6.5}$$

It also follows from Equation (6.4).

Now we are ready to compute the evolution of $X_I(t)$.

Lemma 6.3.2. *The evolution of the actively traded portfolio X with respect to the index I follows:*

$$dX_I(t) = \frac{1}{2}\left(X_I(t) - 2\Delta^S(t)\right)\sigma S_I(t)dW^I(t). \tag{6.6}$$

Proof. A straightforward application of Ito's lemma gives

$$dX_I(t) = d(X_M(t) \cdot M_I(t)) = \frac{1}{2}\left(X_I(t) - 2\Delta^S(t)\right)\sigma S_I(t) dW^I(t).$$

□

From $\Delta^S(t) = X_S(t) - \Delta^M(t) M_S(t)$, we also have an alternative representation

$$dX_I(t) = -\frac{1}{2}\left(X_I(t) - 2\Delta^M(t)\right)\sigma M_I(t) dW^I(t). \tag{6.7}$$

6.4 Optimal Strategy

One would intuitively expect that the optimal strategy should maximize the absolute value of the $dW^I(t)$ term $\left(X_I(t) - 2\Delta^S(t)\right)\sigma S_I(t)$. However, the mean comparison theorem of Hajek would apply only without the stochastic term $S_I(t)$, and thus we must address this problem differently. Our result indeed confirms the intuition that the $dW^I(t)$ term should be maximized in the absolute value in order to find the optimal strategy and the option value. Note that the following comparison result is not restricted to models with constant volatility. Only the boundary conditions simplify in the latter case, and therefore we mention the boundary conditions in the more general case, too.

The proof considered here is based on partial integration and the relationships between derivatives of the fundamental solution and its adjoint (forward and backward density in probabilistic terms).

Note that such an argument cannot be based on the full convexity of a suitable approximating value function: nontrivial convex functions usually are not zero everywhere at infinity, and we need such an approximation in order to do partial integration. Furthermore, it is natural to work with smoothed and strictly convex approximations of natural payoffs in finance which usually have kinks, because this 'globalizing' of a local convexity at a kink is effected for the value function by the density at any short time anyway. Note that we are interested in strict orders of value functions when determining an optimal strategy. Furthermore, the argument given here is essentially global because we evaluate finite differences of an integrated Green's identity on the boundary of large balls. Such arguments may be used to obtain full or partial convexity criteria in specific circumstances such as fixed controls in regular control spaces, univariate payoffs, and strictly elliptic operators. However, there is no general algorithm by which we could obtain local pointwise criteria about Greeks or partial convexity from this type of argument. The example of symmetric passport option considered here may serve for illustration of the latter remark: it turns out that the optimal control function is not even continuous, and in such a situation, we can not know a priori whether the value function is regular enough in order to have Greeks which exist in a pointwise sense. For this, additional reasoning is needed case by case and may hold or not.

The portfolio process related to a given stochastic strategy Δ is denoted by X_I^Δ. For each strategy Δ we define

$$v^\delta(t,x,y) := \mathbb{E}^I[(X_I^\Delta(T) - 1)^+ | S_I(t) = x, X_I^\Delta(t) = y].$$

Let us consider the transformation to normal coordinates $u^\delta(\tau, z_1, z_2) := v^\delta(t, z_1, z_2)$, where $\tau = T - t$ $z_1 = \ln(x)$ and $z_2 = \ln(y)$. The stochastic strategy Δ corresponds to a strategy δ in value space which is a function of the underlyings. The function u^δ satisfies the initial- boundary value problem

$$u^\delta_\tau - \frac{1}{8}\sigma^2(2-\exp(z_1))^2 u^\delta_{z_1 z_1} + \frac{1}{4}\sigma^2(2-\exp(z_1))(\exp(z_1)-2\delta)u^\delta_{z_1 z_2} - \frac{1}{8}\sigma^2(\exp(z_1)-2\delta)^2 u^\delta_{z_2 z_2} = 0. \quad (6.8)$$

with initial condition

$$u(0, z_1, z_2) = (\exp(z_2) - 1)^+.$$

We impose natural boundary conditions at spatial infinity and have an additional finite boundary condition at $z_1 = \log(2)$. We get

$$u^\delta_\tau - \frac{1}{8}\sigma^2(2-2\delta)^2 u^\delta_{z_2 z_2} = 0, \text{ at } z_1 = \log(2).$$

This equation corresponds to the process

$$dX_I(t) = \frac{1}{2}\left(X_I(t) - 2\Delta^S(t)\right)\sigma S_I(t) dW^I(t)$$

such that we can apply Hajek's result at the boundary where $z_1 = \log(2)$. Hence we know $\delta = 0$ at $\{(\tau, z_1, z_2) | z_1 = \log(2)\}$ a priori. We may say that δ lives in reduced control space if $\delta \in C_c := \{\delta \in \mathcal{C}^3 | \delta|_{z_1 = \ln(2)} = 0\}$. The boundary condition reduces to

$$u^\delta_\tau - \frac{1}{2}\sigma^2 u^\delta_{z_2 z_2} = 0, \text{ at } z_1 = \log(2), \quad (6.9)$$

and such a boundary condition can be considered if the volatilities are regular functions. In case of constant volatilities the latter condition simplifies to

$$u^\delta(t, \log(2), z_2) \;=\; \exp(z_2)\cdot N(d_+) - N(d_-),$$

where $d_\pm = \frac{z_2 \pm \frac{1}{2}\sigma^2\tau}{\sigma\sqrt{\tau}}$. The problem may be considered on the domain $D = [0,T] \times (-\infty, \log(2)] \times \mathbb{R}$. There are three further issues here concerning comparison: a) in which space does the strategy function δ live?; b) the problem has a boundary in finite space, and comparison has to be adapted to this situation, and c) the spatial part of the operator is not strictly elliptic. We formulate the comparison theorem in regular strategy spaces and for a regularized problem. More precisely, we modify the asset dynamics, where for small $\epsilon > 0$ we define

$$dS^\epsilon_I = -\frac{1}{2}\sigma S_I(t)\,(2 - S_I(t))\,dW^{I,\epsilon}(t) \quad (6.10)$$

where $W^{I,\epsilon}(t)$ is constructed by adding a small perpendicular process, i.e.,

$$dW^{I,\epsilon}(t) = dW^I + \epsilon dW^{\perp,I}, \;\; \left\langle dW^I, dW^{\perp,I}\right\rangle = 0$$

The corresponding equation for $u^{\delta,\epsilon}$ gets an additional factor $(1+\epsilon)^2$ in the second term of the equation (6.8) and becomes strictly elliptic. Concerning issue a) we compare $\mathcal{C}^3$ strategies in order to prove identity for derivatives of the density and its adjoint up to second order. The issue in b) is addressed in the proof of the following theorem.

Theorem 6.4.1 (Comparison Theorem)**.** *Let $\delta, \delta' \in \mathcal{C}_c^3$ and $\epsilon > 0$ be strategies of the value functions $u^{\delta,\epsilon}$, $u^{\delta',\epsilon}$ defined on the domain D. Then the order of these value functions is induced by the order of the volatility of the portfolio term alone, i.e., for $\tau \in (0, T]$*

$$\frac{1}{8}\sigma^2(x-2\delta)^2 < \frac{1}{8}\sigma^2(x-2\delta')^2 \Rightarrow u^{\delta,\epsilon}(\tau,.) < u^{\delta',\epsilon}(\tau,.).$$

Proof. See Appendix 6.7. □

The regular control space $\mathcal{C}^3$ does not contain the volatility-maximizing function $\mathbb{I}(z_1 \leq 0) = \mathbb{I}(\exp(z_1) \leq 1)$ or $\mathbb{I}(x \leq 1)$ of the portfolio term. Define the sequence of functions h^ϵ, where

$$h^\epsilon(z_1) = \begin{cases} 1 \text{ if } z_1 \leq -\epsilon, \\ \exp\left(-1 - \frac{\epsilon}{z_1}\right) \text{ if } -\epsilon \leq z_1 \leq 0, \\ 0 \text{ else.} \end{cases}$$

Let $\delta^\epsilon \in \mathcal{C}^\infty$ be defined by a convolution of h^ϵ with a smoothing Gaussian kernel which is close to the identity. Then this a sequence of functions δ^ϵ which is monotonically increasing as ϵ decreases and $\lim_{\epsilon \downarrow 0} \delta^\epsilon = \delta^{opt} = \mathbb{I}(x \leq 1)$. According to Theorem 6.4.1 we have

$$v^{\delta^\epsilon}(t,x,y) = \lim_{\epsilon \downarrow 0} \mathbb{E}^I[(X_I^{\Delta^\epsilon}(T) - 1)^+ | S_I(t) = x, X_I^{\Delta^\epsilon}(t) = y]$$

and stochastic ODE theory shows that the limit $v^{\delta^{opt}}(t,x,y)$ exists as $\epsilon \downarrow 0$.

Theorem 6.4.2 (Optimal strategy)**.** *The optimal strategy maximizing*

$$\mathbb{E}^I[X_I(T) - K]^+$$

is given by

$$\bar{\Delta}^S(t) = \bar{X}_S(t) \cdot \mathbb{I}(S_I(t) \leq 1), \qquad \bar{\Delta}^M(t) = \bar{X}_M(t) \cdot \mathbb{I}(S_I(t) \geq 1),$$

meaning that one should be fully invested in the weaker asset. The evolution of the optimal portfolio is given by

$$d\bar{X}_I(t) = \frac{1}{2}\left(S_I(t) - 2 \cdot \mathbb{I}(S_I(t) \leq 1)\right)\sigma \bar{X}_I(t) dW^I(t).$$

Proof. According to Theorem 6.4.1, the optimal strategy maximizes the absolute value of the $dW^I(t)$ term. The optimal position $\Delta^S(t)$ is attained at one of the ends of the interval for its possible range. When $\Delta^S(t) = 0$, the absolute value reduces to

$$X_I(t).$$

When $\Delta^S(t) = X_S(t)$, the absolute value is equal to

$$-X_I(t) + 2X_S(t).$$

Thus $\Delta^S(t) = 0$ is optimal when

$$X_I(t) \geq -X_I(t) + 2X_S(t),$$

which is equivalent to

$$S(t) \geq M(t).$$

$$\bar{\Delta}^S(t) = \begin{cases} X_S(t), & S(t) \leq M(t), \\ 0, & S(t) \geq M(t), \end{cases}$$

and

$$\bar{\Delta}^M(t) = \begin{cases} 0, & S(t) \leq M(t), \\ X_M(t), & S(t) \geq M(t), \end{cases}$$

More succinctly,

$$\bar{\Delta}^S(t) = \bar{X}_S(t) \cdot \mathbb{I}(S_I(t) \leq 1), \qquad \bar{\Delta}^M(t) = \bar{X}_M(t) \cdot \mathbb{I}(S_I(t) \geq 1).$$

Thus it is optimal to be fully invested in the weaker asset. The evolution of the optimal portfolio is given by

$$\begin{aligned} d\bar{X}_I(t) &= \frac{1}{2}\left(\bar{X}_I(t) - 2\Delta^S(t)\right)\sigma S_I(t) dW^I(t) \\ &= \frac{1}{2}\left(\bar{X}_I(t) - 2\bar{X}_S(t) \cdot \mathbb{I}(S_I(t) \leq 1))\right)\sigma S_I(t) dW^I(t) \\ &= \frac{1}{2}\left(S_I(t) - 2 \cdot \mathbb{I}(S_I(t) \leq 1))\right)\sigma \bar{X}_I(t) dW^I(t). \end{aligned}$$

□

Remark 6.4.1 (Volatility maximizing strategy). The above strategy

$$\bar{\Delta}^S(t) = \bar{X}_S(t) \cdot \mathbb{I}(S_I(t) \leq 1), \qquad \bar{\Delta}^M(t) = \bar{X}_M(t) \cdot \mathbb{I}(S_I(t) \geq 1),$$

also maximizes

$$\mathrm{Var}^I(X_I(T)) = \mathbb{E}^I\left[(X_I(T) - 1)^2\right],$$

and the resulting portfolio has the maximal possible variance (or volatility) with respect to the index.

Thus the resulting portfolio is as far as possible from the index in the distributional L^2 sense. It means that some mass of this portfolio is expected to be far from the index in both the positive or a negative sense. The scope of validity of this observation in the case of multiple stocks is interesting without further saying as we know that correlation signs between stocks are significant for optimal strategies, even for classical passport options.

Figure 6.1 shows two simulated scenarios with $\sigma = 0.1$ and $T = 20$. The volatility corresponds to a typical foreign exchange pair such as EUR-USD. The first-time horizon was chosen to reflect the length of the existence of the euro currency. The first graph illustrates the mechanism of how the maximum volatility portfolio increases due to frequent crosses of the asset prices of the initial par price. The second graph shows that the situation when these crosses of the par price do not happen after some small time and thus the portfolio tracks the weaker asset.

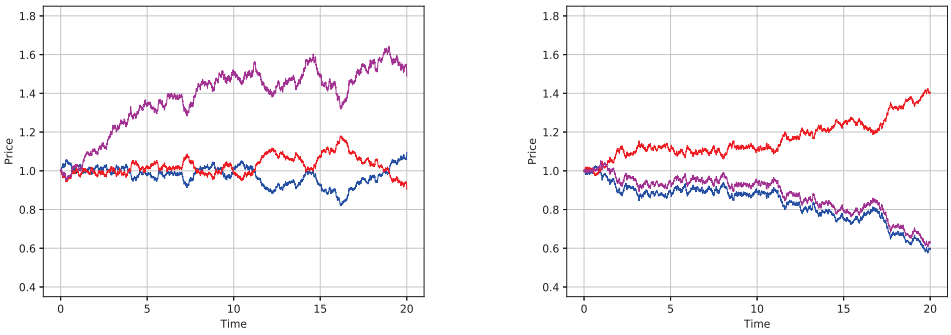

Figure 6.1: Two simulated scenarios with $\sigma = 0.1$ and $T = 20$. Red and blue graphs represent the prices of the two individual assets with respect to the index, the purple graph represents the trading strategy that maximizes the volatility. The scenario on the left represents the situation when there is a large number of crosses of the initial par price 1. These crosses push the volatility maximizing porfolio up. The right graph shows the situation when the crosses of the initial par price do not happen after year 3 and the volatility maximizing portfolio simply follows the weaker asset.

As seen in Figure 6.1, the prices of the individual assets do not depart too far from the initial price 1 even on a relatively long period of 20 years. Recall that the price evolution of the individual asset M with respect to the index I is given by

$$dM_I(t) = \frac{1}{2}\sigma M_I(t)(2 - M_I(t))dW^I(t).$$

The $dW^I(t)$ term has the maximal value when $M_I(t) = 1$ and it gets smaller with an increasing distance from 1.

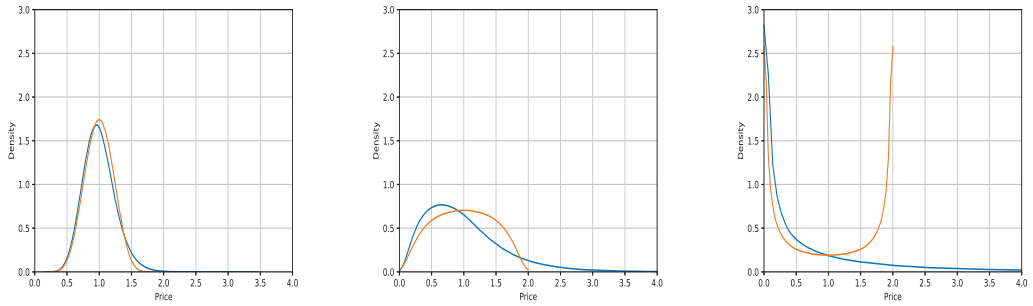

Figure 6.2: Numerically simulated densities of the optimal solution $X_I(T)$ in blue and the price of an individual asset $S_I(T)$ for $\sigma = 0.1$, $T = 20$ (left) and $T = 100$ (center) and $T = 500$ (right) in orange. The price $S_I(T)$ eventually shifts from the initial price of 1 to the two edges 0 and 2, but only very slowly.

To illustrate the distribution of the asset prices and the volatility maximizing strategy, Figure 6.2 shows the simulated densities for the optimal $X_I(T)$ and $S_I(T)$ for $\sigma = 0.1$, $T = 20$, $T = 100$ and $T = 500$. As seen from the graph, the difference between the distribution of the price of an individual asset and the distribution of the the optimal portfolio is only small even on such a long time

horizon of 20 years, meaning that the trading strategy to always invest in the weaker asset is distributionally very similar to investing in any of the two assets to start with. In other words, it is not that straightforward to move away from the index by trading in the individual components of the index and the strategies that fully invest in one asset result in a similar distribution, at least on a scale of several years.

Since the strategy that fully invests in the weaker asset also maximizes the price variance with respect to the index (index always has value 1), the distribution of this strategy has the largest dispersion among all trading strategies that do not short any of the two assets. There is a visible mass on the right side of the graphs in Figure 6.2 that produces the maximal dispersion. In order to see a larger distributional difference between the optimal strategy and the price of an asset, we show the simulated densities for the time horizon of 100 years. On an extreme time horizon of 500 years, we see that the prices of individual assets converge to 0 or 2 and the volatility maximizing strategy has the most mass around zero as it tracks the weaker asset.

Figure 6.3 shows how the volatility maximizing strategy performs in the real situation of currency pairs. The exchange rates were obtained from the European Central Bank[1] and it currently spans the period starting from January 1999 until March 2019. These data covers 18 currencies with the complete time series from 1999. We pick four major currencies, namely EUR, USD, GBP, and JPY, for illustrative purposes. We have six possible currency pairs, namely EUR-USD, EUR-GBP, EUR-JPY, USD-GBP, USD-JPY, and GBP-JPY. The graphs show the volatility maximizing portfolios' performance in all these six scenarios and the price evolutions of individual assets. The reference asset is, in every case, a basket that consists of 50% of the two corresponding currencies. It is interesting to note that each volatility maximizing strategy ended above the starting value of 1.

Figure 6.4 shows the two most extreme scenarios obtained from the pairwise comparison of 18 available currencies, namely the GBP-HUF and CHF-ZAR currency pairs. This illustrates that such scenarios do not pose any significant concern, as doubling or halving the portfolio value over 20 years in the most extreme cases from 153 currency pairs does not create a serious risk issue.

We conclude this section with a study of the value function that corresponds to the price of the option that pays off $\mathbb{E}^I[X_I(T)-1]^+$ units of the index I at expiration T. Let us assume that the holder of the option uses the optimal strategy that maximizes the value of this option. Then if we introduce a function

$$v(t,x,y) = \mathbb{E}^I[(\bar{X}_I(T)-1)^+ | S_I(t)=x, \bar{X}_I(t)=y], \tag{6.11}$$

we get the following result:

Theorem 6.4.3 (Value function)**.** *The function v defined as*

$$v(t,x,y) = \mathbb{E}^I[(\bar{X}_I(T)-1)^+ | S_I(t)=x, \bar{X}_I(t)=y],$$

satisfies the following PDE

$$v_t + \tfrac{1}{8}\sigma^2 x^2(2-x)^2 v_{xx} - \tfrac{1}{4}\sigma^2 x(2-x)y(x-2\mathbb{I}(x\leq 1))v_{xy} + \tfrac{1}{8}\sigma^2 y^2(x-2\mathbb{I}(x\leq 1))^2 v_{yy} = 0 \tag{6.12}$$

[1] https://www.ecb.europa.eu/stats/eurofxref/eurofxref-hist.zip

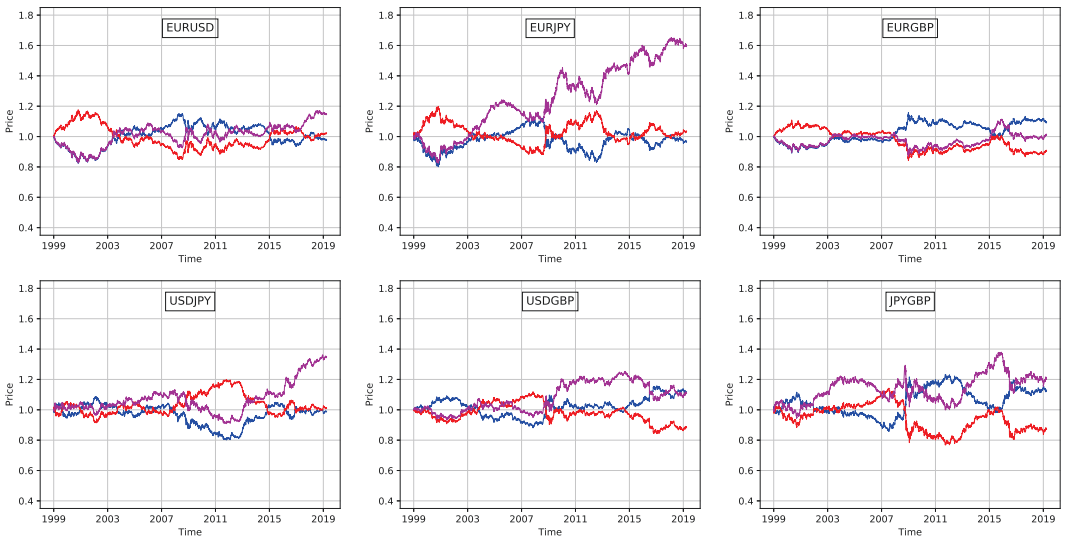

Figure 6.3: Performance of the most volatile strategy (purple) that invests in the cheaper of the two assets for all possible currency pairs of EUR, USD, GBP and JPY from 01/1999 – 03/2019. The evolutions of the two individual currencies for the specific currency pair are in blue (first listed currency) and in red (second listed currency).

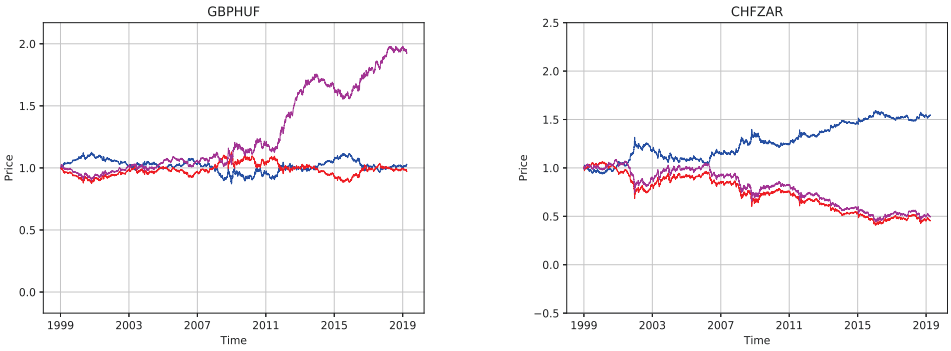

Figure 6.4: The most profitable pair for the volatility maximizing strategy is GBP-HUF that experienced frequent crosses and the resulting portfolio nearly doubled (1.925). In contrast, the worst performing currency pair was CHF-ZAR resulted in a final portfolio value of 0.507, where the volatility maximization strategy tracked the weaker currency ZAR (South African Rand) that historically depreciated.

with the terminal and the boundary conditions

$$\begin{aligned} v(T,x,y) &= (y-1)^+, \\ v(t,x,0) &= 0, \\ v(t,0,y) &= y \cdot N(d_+) - N(d_-), \\ v(t,2,y) &= y \cdot N(d_+) - N(d_-), \end{aligned}$$

where

$$d_{\pm} = \frac{\ln(y) \pm \frac{1}{2}\sigma^2(T-t)}{\sigma\sqrt{T-t}}.$$

Proof. Since $v(t, S_I(t), X_I(t))$ as a process is a $\mathbb{P}^I$ martingale, the dt term must be zero. This gives:

$$v_t + \tfrac{1}{8}\sigma^2 x^2(2-x)^2 v_{xx} - \tfrac{1}{4}\sigma^2 x(2-x)y(x - 2\mathbb{I}(x \le 1))v_{xy} + \tfrac{1}{8}\sigma^2 y^2(x - 2\mathbb{I}(x \le 1))^2 v_{yy} = 0.$$

The terminal condition and the y boundary conditions are straightforward. The x boundary condition follows from the fact that near the boundary points $S_I(t) = 0$ and $S_I(t) = 2$, the process $X_I(t)$ becomes geometric Brownian motion in a limit:

$$\begin{aligned} d\bar{X}_I(t) &= \frac{1}{2}\left(S_I(t) - 2 \cdot \mathbb{I}(S_I(t) \le 1)\right)\sigma\bar{X}_I(t)dW^I(t) \\ &\approx \pm\sigma\bar{X}_I(t)dW^I(t) \end{aligned}$$

and thus the standard Black-Scholes formula for European call option applies on the two boundaries. □

It is not difficult to see that the price of the option is a function of $\sigma\sqrt{T}$ due to the scaling property of the Brownian motion W^I. Figure 6.5 shows the price of the option as a function of $\sigma\sqrt{T}$ for fixed initial values of $S_I(0) = X_I(0) = 1$ (blue curve). The analogous passport option that uses the initial wealth as a trading constraint is plotted in red. The price of the passport option is substantially higher. The realistic values of $\sigma\sqrt{T}$ are well below 1, so the most relevant prices for practical applications are on the very left of this graph. From the previous discussion, the individual asset prices and the optimal strategy for the newly proposed contract do not tend to move away from the initial price one even on a relatively long-term horizon such as 20 years. Thus such a contract is expected to be relatively cheap. Indeed, if we take $\sigma = 0.1$ and $T = 20$, the initial price of the option that pays off $(X_I(T) - 1)^+$ is only 0.09746 units of I (so only 9.746% of any of the asset as $S(0) = M(0) = I(0)$). In comparison, an option covering a constant position in a single asset S with a payoff $(S_I(T) - 1)^+$ costs slightly less, namely 0.08853 units of I. In contrast, the passport option for the same parameters costs 20.490%, significantly more than the newly proposed option. We note that one could further reduce the option's cost by utilizing the idea in Taylor and Večeř (2021), where the authors studied plain vanilla options with maturity in years and argued that instead of focusing on simple returns, one could focus on logarithmic returns in order to reduce the fair price of the option.

For numerical illustration, Figure 6.6 shows the numerical solution of the value function as a function of both S_I and X_I for a fixed $\sigma\sqrt{T} = 1$.

6.5 Maximizing Probability of Reaching a Goal

The volatility maximization strategy also has the property that it maximizes the probability of reaching a higher goal. This section confirms that a slight modification of the volatility maximization strategy is also an optimal strategy

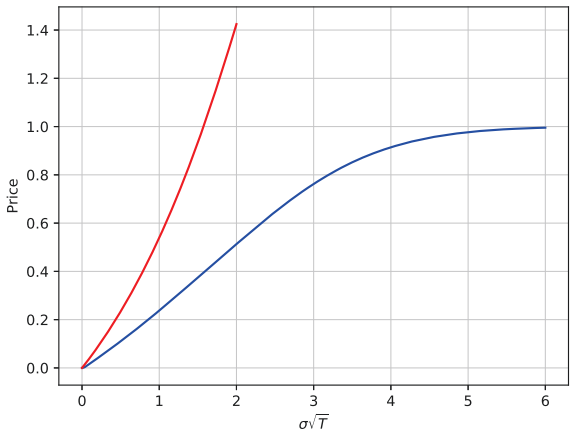

Figure 6.5: Price of the option contract as a function of $\sigma\sqrt{T}$ (blue) with fixed values $S_I(0) = X_I(0) = 1$. The price of the analogous passport options is plotted in red for comparison.

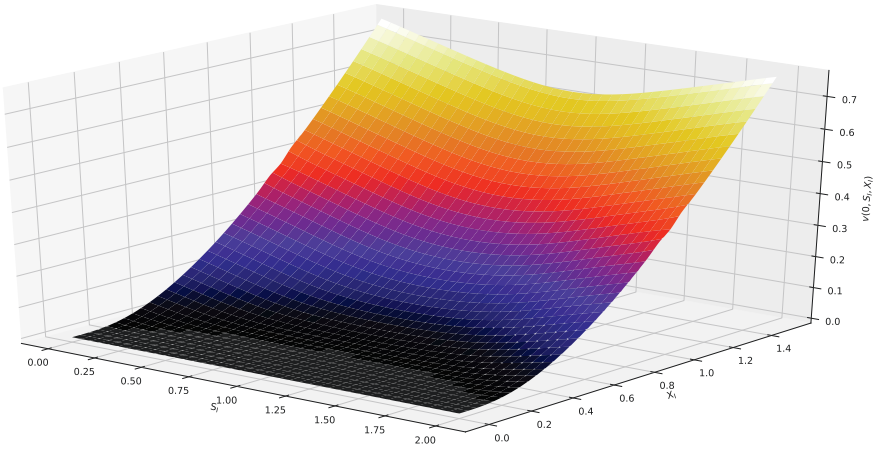

Figure 6.6: Numerical solution of the value function from Equation (6.12) with fixed parameters $\sigma\sqrt{T} = 1$ as a function of S_I and X_I.

to the problem of maximizing the $\mathbb{P}^I$ probability that the portfolio's value at time T will be at least α. We want to maximize $\mathbb{P}^I(X_I(T) \geq \alpha)$ for all possible strategies $\Delta^S(t)$ and $\Delta^M(t)$.

Theorem 6.5.1. *(The optimal strategy for reaching $\alpha > 1$) The optimal strategy for maximizing the probability of reaching a higher level $\alpha > 1$ before time T,*

$$\mathbb{P}(X_I(T) \geq \alpha),$$

is to be fully invested in the cheaper asset until level α is reached. Then it is optimal being fully invested in the asset I.

Proof. We can easily observe that for an arbitrary strategy, it is optimal to fully invest in the asset I once the value of the portfolio reaches α, thus completely eliminating the probability of ending below α. Our approach is to find a sequence of convex functions ϕ_n, $n \in \mathbb{N}$ such that their limit is an indicator at α. In order to do that, let us stop the process X_I once its value reaches α since it is optimal to fully invest in the asset I from that point. Let us denote a stopping time τ by

$$\tau = \inf\{t \in [0,T] : X_I(t) = \alpha\},$$

with the convention $\inf\{\emptyset\} = T$. From the continuity of X_I, we can see that τ is indeed a stopping time, since $\{\alpha\}$ is a closed set. Trivially, τ is bounded, hence the stopped process $X_I^\tau\ (t) = \{X_I^\tau\ (t), t \in [0,T]\}$ defined as

$$X_I^\tau(t) = \begin{cases} X_I(t), & \text{for } \ t \leq \tau, \\ \alpha, & \text{for } \ t > \tau, \end{cases}$$

is a continuous $\mathbb{P}^I$–martingale from the Optional Stopping Theorem. Thus we can use Theorem 6.4.1 with a payoff function

$$\phi_n(x) = n\left(x + \frac{1}{n} - \alpha\right)^+, \quad x \in \mathbb{R}$$

for any $n \in \mathbb{N}$. Note that for any $x \in [0,\alpha]$,

$$\lim_{n\to\infty} \phi_n(x) = \mathbb{I}_{[x=\alpha]}.$$

From the convexity of functions ϕ_n for any $n \in \mathbb{N}$, it holds for any strategy q

$$\mathbb{E}^I[\phi_n(X_{I,q}^\tau(T))] \leq \mathbb{E}^I[\phi_n(X_{I,opt}^\tau(T))],$$

where $X_{I,q}^\tau$ resp. $X_{I,opt}^\tau$ are evolutions of the portfolio value for strategy q and for the optimal strategy *opt* respectively (investing in the cheaper asset). Since the processes $X_{I,q}^\tau$ and $X_{I,opt}^\tau$ are bounded by α, we can use Lebesgue's Dominated Convergence Theorem to conclude

$$\begin{aligned} \mathbb{P}^I(X_{I,q}^\tau(T) = \alpha) &= \mathbb{E}^I[\mathbb{I}_{[X_{I,q}^\tau(T)=\alpha]}] = \mathbb{E}^I[\lim_{n\to\infty} \phi_n(X_{I,q}^\tau(T))] \\ &= \lim_{n\to\infty} \mathbb{E}^I[\phi_n(X_{I,q}^\tau(T))] \leq \lim_{n\to\infty} \mathbb{E}^I[\phi_n(X_{I,opt}^\tau(T))] \\ &= \mathbb{E}^I \lim_{n\to\infty}[\phi_n(X_{I,opt}^\tau(T))] = \mathbb{E}^I[\mathbb{I}_{[X_{I,opt}^\tau(T)=\alpha]}] \\ &= \mathbb{P}^I(X_{I,opt}^\tau(T) = \alpha). \end{aligned}$$

Hence it is optimal to invest in the cheaper asset until the goal α is reached. Then, it is optimal to switch in the asset I entirely. □

6.6 Generalization to N assets

A significant advantage of the equal treatment of the underlying assets is that we can naturally generalize the contract to N assets. Let us consider the situation when we have N assets $S_1, S_2, \ldots, S_N$. We can easily generalize the definition of the index to

$$I(t) = \frac{1}{N}\sum_{i=1}^{N} S_i(t)$$

and consider a traded account $X(t)$ with positions $\Delta^i(t)$ in the asset S_i in an obvious manner

$$X(t) = \sum_{i=1}^{N} \Delta^i(t) S_i(t),$$

subject to no shorting constraints $\Delta^i(t) \geq 0$. This in turn implies an upper bound on $\Delta^i(t) \leq X_{S_i}(t)$ corresponding to being fully invested in the asset S_i. A contract protecting the trading losses pays off $(X_I(T) - K)^+$ units of $I(T)$ at the maturity time T.

In order to treat all assets symmetrically, we need to slightly change the geometric Brownian motion model $dS_{ij}(t) = \sigma_{ij} S_{ij}(t) dW^j$ since otherwise the constraints imposed on S_{ik} by evolution of S_{ij} and S_{jk} breaks the desired symmetry. Thus, we propose a symmetric version of geometric Brownian motion

$$dS_{ij}(t) = S_{ij} \sigma_{ij}^T dW^j(t) \quad \text{and} \quad S_{ij}(0) = 1, \tag{6.13}$$

where $W^j = (W^{j1}, \ldots, W^{jn})$ is an n-dimensional Brownian motion and σ_{ij} are n-dimensional vectors. To simplify further calculations we set $\sigma_{iik}(\cdot) = 0$ for every i and k. The model is heavily overparametrized. Nevertheless, we can write

$$\begin{aligned} dS_{ji}(t) = dS_{ij}^{-1}(t) = -\frac{1}{S_{ij}^2(t)} dS_{ij}(t) + \frac{1}{S_{ij}^3(t)} d\langle S_{ij} \rangle_t \\ = -S_{ji}(t) \sigma_{ij}^T dW^j + S_{ji}(t) \sigma_{ij}^T \sigma_{ij}(t) dt, \end{aligned}$$

and at the same time, from the definition of S_{ji}, it holds

$$dS_{ji}(t) = S_{ji}(t) \sigma_{ji}^T dW^i(t).$$

To preserve the symmetry, we choose

$$\sigma_{ij} = \sigma_{ji} \quad \text{and} \quad dW^i(t) = dW^j(t) - \sigma_{ij} dt.$$

We now have a nice relation between σ_{ijk}'s, as can be seen from the calculations below

$$\begin{aligned} dS_{lj}(t) &= dS_{li}(t) S_{ij}(t) \\ &= S_{li}(t) dS_{ij}(t) + S_{ij}(t) dS_{li}(t) + dS_{li}(t) dS_{ij}(t) \\ &= S_{li}(t) S_{ij}(t) \sigma_{ij}^T dW^j(t) + S_{ij}(t) S_{li}(t) \sigma_{li}^T dW^i(t) + \sigma_{li}^T \sigma_{ij}(t) dt \\ &= S_{lj}(t) \left(\sigma_{ij}^T \left(dW^j(t) + \sigma_{li}(t) dt \right) + \sigma_{li}^T dW^i(t) \right) \\ &= S_{lj}(t) \left(\sigma_{ij}^T dW^i(t) + \sigma_{li}^T dW^i(t) \right) \\ &= S_{lj}(t) \sigma_{lj}^T dW^j(t). \end{aligned}$$

Thus we have

$$\sigma_{lj} = \sigma_{li} + \sigma_{ij}, \quad l, i, j \in \{1, \ldots, n+1\}. \tag{6.14}$$

The model is still over-parametrized even with constraints on σ parameters discussed above. For example, for three assets, it can be shown that the market can be described as four σ parameters. From the market, we can observe nine evolutions in the prices S_{ij}. Three evolutions S_{ii} are trivially constant ones. The remaining six evolutions are S_{12},S_{13},S_{23} and their inverses. Thus we have four

parameters that are described by three price processes. As it turns out, if we can estimate the volatilities of the prices from the market, then, independently of the choice of parameters, the models are equivalent. We shall need the following theorem from the theory of stochastic differential equations.

Theorem 6.6.1. *Let $g, \sigma : \mathbb{R}_+ \times \mathbb{R}^m \mapsto \mathbb{R}^{m\times d}$ be Borel measurable functions such that $\sigma\sigma^T = gg^T$ on $\mathbb{R}_+ \times \mathbb{R}^m$. Then there exists a weak solution of stochastic differential equation*

$$dX(t) = \sigma(t, X(t))dW(t), \quad X(0) = 1, \tag{6.15}$$

if and only if there exists a weak solution to stochastic differential equation

$$dY(t) = g(t, Y(t))dW(t), \quad Y(0) = 1. \tag{6.16}$$

Moreover, the solution of (6.15) *has same law as the solution of* (6.16).

Proof. This theorem is a special case of the martingale problem, first noticed by Stroock and Varadhan (1969). □

Using Theorem 6.6.1 with the system of stochastic differential equations for $S_{21}, \ldots, S_{(n+1)1}$, we can immediately see that as long as we can observe the volatilities of the prices from the market, it does not matter what are our specific estimates of σ's.

Theorem 6.6.2. *Suppose the market model is given by*

$$dS_{ij}(t) = S_{ij}(t)\sigma_{ij}^T dW^j(t) \quad \textit{and} \quad S_{ij}(0) = 1,$$

and further suppose that we are able to observe volatilities of the market prices at each time, that is at each time t we know $\sigma_{ij}^T\sigma_{ij}$ for every i and j. Then irrespectively of chosen estimates of σ parameters the model is the same.

Proof. Let $\hat{\sigma}_{ij}$ be the estimate of σ_{ij} for every i, j such that $\hat{\sigma}_{ij}^T\hat{\sigma}_{ij} = \sigma_{ij}^T\sigma_{ij}$. We will use theorem 6.6.1 for equations

$$d\left(S_{21}(t), \ldots, S_{(n+1)1}(t)\right)^T = \left(S_{21}(t)\sigma_{21}^T, \ldots, S_{(n+1)1}(t)\sigma_{(n+1)1}^T\right) dW^1(t)$$

and

$$d\left(\hat{S}_{21}(t), \ldots, \hat{S}_{(n+1)1}(t)\right)^T = \left(\hat{S}_{21}(t)\hat{\sigma}_{21}^T, \ldots, \hat{S}_{(n+1)1}(t)\hat{\sigma}_{(n+1)1}^T\right) dW^1(t)$$

Denote g resp. $\hat{g}$ the diffusion matrix of X resp. $\hat{X}$. From the assumption on estimates, $gg^T = \hat{g}\hat{g}^T$ on the diagonal, so we need to check whether $(gg^T)_{ij} = (\hat{g}\hat{g}^T)_{ij}$ for $i \neq j$. Let us fix i and j. Multiplying, we need to check $S_{i1}S_{j1}\sigma_{i1}^T\sigma_{j1} = S_{i1}S_{j1}\hat{\sigma}_{i1}^T\hat{\sigma}_{j1}$. Using (6.14) we get

$$\sigma_{ij}^T\sigma_{ij} = (\sigma_{i1} + \sigma_{1j})^T(\sigma_{i1} + \sigma_{1j}) = \sigma_{i1}^T\sigma_{i1} + 2\sigma_{i1}^T\sigma_{1j} + \sigma_{1j}^T\sigma_{1j}$$

Similarly,

$$\hat{\sigma}_{ij}^T\hat{\sigma}_{ij} = \hat{\sigma}_{i1}^T\hat{\sigma}_{i1} + 2\hat{\sigma}_{i1}^T\hat{\sigma}_{1j} + \hat{\sigma}_{1j}^T\hat{\sigma}_{1j}.$$

Thus, from the assumptions, it follows that $\sigma_{i1}^T\sigma_{1j} = \hat{\sigma}_{i1}^T\hat{\sigma}_{1j}$. Since $\sigma_{1j} = -\sigma_{j1}$ the theorem follows. □

Remark 6.6.1. Although we have not found the proof for the multivariate case, one can prove that the optimal strategy is being fully invested in one asset. The main idea is based on studying the price of the option. Denote

$$v(t,x,s_1,\dots,s_N)=\mathbb{E}\left[(X_I(T)-1)^+|X_I(t)=x,S_{1I}=s_1,\dots,S_{NI}=s_N\right]$$

be the price of the option. Then v is convex in x. To see this, fix trading strategy Δ and let

$$X_I^3(t)=\lambda X_I^1(t)+(1-\lambda)X_I^2(t).$$

Then

$$X_I^3(T)=\lambda X_I^1(T)+(1-\lambda)X_I^2(T).$$

From this we have

$$\begin{aligned}\mathbb{E}(X_I^3(T)-1)^+&=\mathbb{E}(\lambda X_I^1(T)+(1-\lambda)X_I^2(T)-1)^+\\&=\mathbb{E}(\lambda X_I^1(T)-\lambda+(1-\lambda)X_I^2(T)-(1-\lambda))^+\\&\le\mathbb{E}(\lambda X_I^1(T)-\lambda)^+\mathbb{E}((1-\lambda)X_I^2(T)-(1-\lambda))^+\\&=\lambda\mathbb{E}(X_I^1(T)-1)^+(1-\lambda)\mathbb{E}(X_I^2(T)-1))^+\\&=\lambda v(t,x^1,\dots)+(1-\lambda)v(t,x^2,\dots),\end{aligned}$$

and the convexity follows from maximizing the left hand side over all possible strategies Δ.

Since v is convex in x, we have $v_{xx}\ge 0$. Finally, if we calculate the HJB equation for the price v, then the dependence on strategy Δ is quadratic for the term v_{xx} and linear for terms v_{xs_i}. Since $v_{xx}\ge 0$ the option price is convex in Δ, and thus the optimum is found on the boundary, i.e., being fully invested in one asset only.

6.7 Proof of Theorem 6.4.1

Proof. For small positive angle θ consider the transformed coordinates

$$\begin{pmatrix}\tilde{z}_1\\ \tilde{z}_2\end{pmatrix}=\begin{pmatrix}\cos(\theta) & \sin(\theta)\\ -\sin(\theta) & \cos(\theta)\end{pmatrix}\begin{pmatrix}z_1\\ z_2\end{pmatrix}\tag{6.17}$$

Multiplying with the inverse (rotation by $-\theta$), we observe that $-\sin(-\theta)\tilde{z_1}+\cos(-\theta)\tilde{z_2}=\sin(\theta)\tilde{z_1}+\cos(\theta)\tilde{z_2}=z_2$ such that both coefficients $\sin(\theta),\cos(\theta)$ in the sum representation of z_2 are positive for θ positive and small. As z_2 lives on the whole space, the transformed coordinates live on the whole space for any small positive θ. Hence in transformed coordinates, the problem is defined on the whole space where initial data are defined as a payoff of a weighted sum $(\exp(z_2)-1)^+=(\exp(\sin(\theta)\tilde{z_1}+\cos(\theta)\tilde{z_2})-1)^+$. For a smoothed payoff f_ϵ (smoothing close to identity), define for small $\delta_0>0$ and large R an approximation (in $H^2\cap\mathcal{C}^2$) of the payoff function

$$f^R_{\epsilon,\delta_0}(w)=:\begin{cases}f_\epsilon(w)\text{ if }|w|\le R,\\ \\ f_\epsilon(w)\exp(-\delta_0|w-R|^2)\text{ if }|w|>R.\end{cases}$$

Let $u^{\delta,\theta,\epsilon,\delta_0,R}$ be a value function of the regularized (i.e., strictly elliptic approximation) form of the equation (6.8) in rotated coordinates with data $f^R_{\epsilon,\delta_0}(\sin(\theta)\tilde{z}_1+\cos(\theta)\tilde{z}_2)$, let $p^{\delta,\theta,\epsilon,\delta_0,R}$ be the corresponding fundamental solution, and let $p^{*,\delta,\theta,\epsilon,\delta_0,R}$ be its adjoint (backward and forward equation density in probabilistic terms). The approximative value function itself and the multivariate spatial derivatives of order $|\alpha|\leq 2$ have the representation

$$D^\alpha_{\tilde{z}} u^{\delta,\theta,\epsilon,\delta_0,R}(\tau,\tilde{z}_1,\tilde{z}_2)=\int_0^\tau\int_{\mathbb{R}^n} f^R_{\epsilon,\delta}(\xi)D^\alpha_{\tilde{z}}p^{\delta,\theta,\epsilon,\delta_0,R}(\tau,\tilde{z}_1,\tilde{z}_2;\sigma,\xi_1,\xi_2)d\xi_1 d\xi_2 d\sigma. \tag{6.18}$$

Next, for $w=(w_1,w_2)$ and $\sigma<s<\tau$ define

$$\overline{v}(s,w)=p^{\delta,\theta,\epsilon,\delta_0,R}(s,w;\sigma,\xi_1,\xi_2)$$

$$\overline{u}(s,w)=p^{*,\delta,\theta,\epsilon,\delta_0,R}(s,w;\tau,\tilde{z}_1,\tilde{z}_2).$$

Let $L\overline{v}=0$ and $L^*\overline{u}=0$ abbreviate the equations for $\overline{u},\overline{v}$ (approximative equations for (6.8)). We may assume that $\epsilon>0$ is small enough such that $\sigma+\epsilon<s<\tau-\epsilon$. Integrating over the domain $[\sigma+\epsilon,\tau-\epsilon]\times B_R$ (where B_R is the 2-dimensional ball of radius R around the origin) we have

$$\begin{aligned} 0 &= \textstyle\int_{\sigma+\epsilon}^{\tau-\epsilon}\int_{B_R}(\overline{u}L\overline{v}-\overline{v}L^*\overline{u})(s,w)dwds \\ &= \textstyle\int_{B_R}(\overline{u}(\tau-\epsilon,w)\overline{v}(\tau-\epsilon,w)-\overline{v}(\sigma+\epsilon,w)\overline{u}(\sigma+\epsilon,w))dw+r^*_{B_R}, \end{aligned} \tag{6.19}$$

where $\lim_{R\uparrow\infty} r^*_{B_R}=0$ for the reminder term which follows from $\mathcal{C}^3$-regularity of coefficients and an a priori estimates of the densities. Next, for directions h, consider finite difference quotients $D^+_h\overline{u}(s,w)=\frac{\overline{u}(s,w+h)-\overline{u}(s,w)}{h}$, $D^-_h\overline{u}(s,w)=\frac{\overline{u}(s,w)-\overline{u}(s,w-h)}{h}$, $D^2_h\overline{u}(s,w)=\frac{D^+_h\overline{u}(s,w)-D^-_h\overline{u}(s,w)}{h}$, and for multiindices α, let D^α_h denote the coordinate versions of these difference equations. Then from (6.19), we get for all $0\leq|\alpha|\leq 2$

$$\begin{aligned} 0 &= \textstyle\int_{\mathbb{R}^2}((D^\alpha_h\overline{u})(\tau-\epsilon,w)\overline{v}(\tau-\epsilon,w)-(D^\alpha_h(\overline{v})(\sigma+\epsilon,w)\overline{u}(\sigma+\epsilon,w))dw \\ &= \textstyle\int_{\mathbb{R}^2}((D^\alpha_h\overline{u})(\tau-\epsilon,w)p^{\delta,\theta,\epsilon,\delta_0,R}(\tau-\epsilon,w;\sigma,\xi_1,\xi_2) \\ &\quad -(D^\alpha_h\overline{v})(\sigma+\epsilon,w)p^{*,\delta,\theta,\epsilon,\delta_0,R}(\sigma+\epsilon,w;\tau,\tilde{z}_1,\tilde{z}_2))dw \end{aligned} \tag{6.20}$$

We conclude that

$$(D^\alpha_{\tilde{z}}\overline{v})(\tau,\tilde{z})=(D^\alpha_\xi\overline{u})(\sigma,\xi).$$

Hence we can do partial integration and obtain comparison for arbitrary small θ, which is preserved in the limit $\theta\downarrow 0$. □

7. Conclusion

In the thesis, we have focused on the efficient market hypothesis, utility-maximizing agents, and optimal distributional trading gain problem of the form

$$\begin{aligned} &\max_{B_1} \mathbb{E}^{\mathbb{P}}\left[U(B_1)\right] \\ &s.t. \;\; \mathbb{E}^{\mathbb{Q}}\left[B_1\right] = B_0. \end{aligned}$$

In the case of two agents, one representing a market taker and one representing a market maker, who share a geometric Brownian motion distributional assumption, we have provided exact formulas for the price and hedge of the optimal random payoff $B_1^\star$. Furthermore, we showed how one could construct a static portfolio Π with a payoff that replicates the random variable $F^\star$. To construct the static portfolio, we have used the implied market density estimated using the stochastic volatility-inspired model. For practitioners, we showed how one could use kernel search heuristics to solve the associated integer programming problem that minimizes the L^2 distance between the payoff of the random variable $F^\star$ and the payoff of the portfolio Π.

Another application of the optimal distributional trading gain that we have focused on was the study of market efficiency during the COVID-19 pandemic. We have considered a utility-maximizing agent that invests in a single ETF contract and bases his position in the ETF using Merton's portfolio. The drift required by Merton's portfolio is estimated using a combination of estimates from univariate linear regressions computed on historical price and virus-related data. We have shown that using these out-of-sample estimates, the agent realizes a substantial profit in all ETFs we have considered.

Finally, we have studied a symmetric version of a passport option. For two assets, we have found the optimal strategy and we have shown that the optimal strategy also maximizes the probability of outperforming the market index before the expiration of the option contract. Moreover, we have demonstrated the application of the passport to currency pairs and the desirability of the contract when one wishes to insure an actively traded account with a very large investment horizon.

Bibliography

Agrawal, A., R. Verschueren, S. Diamond, and S. Boyd (2018). A rewriting system for convex optimization problems. *Journal of Control and Decision 5*(1), 42–60.

Ahmar, A. and E. Boj del Val (2020). Suttearima: Short-term forecasting method, a case: Covid-19 and stock market in spain. *Science of The Total Environment 729*, 138883.

Aït-Sahalia, Y. and A. Lo (1998). Nonparametric estimation of state-price densities. *Journal of Finance 53*(2), 499–547.

Akaike, H. (1974). A new look at the statistical model identification. *IEEE transactions on automatic control 19*(6), 716–723.

Al-Awadhi, A., K. Alsaifi, A. Al-Awadhi, and S. Alhammadi (2020). Death and contagious infectious diseases: Impact of the COVID-19 virus on stock market returns. *Journal of Behavioral and Experimental Finance 27*, 100326.

Andersen, L., J. Andreasen, and R. Brotherton-Ratcliffe (1998). The passport option. *Journal of Computational Finance 1*(3), 15–36.

Angelelli, E., R. Mansini, and M. G. Speranza (2010). Kernel search: A general heuristic for the multi-dimensional knapsack problem. *Computers & Operations Research 37*(11), 2017–2026.

Angelelli, E., R. Mansini, and M. G. Speranza (2012). Kernel search: A new heuristic framework for portfolio selection. *Computational Optimization and Applications 51*(1), 345–361.

Arrow, K. J. (1964). The role of securities in the optimal allocation of risk-bearing. *The Review of Economic Studies 31*(2), 91–96.

Azimli, A. (2020). The impact of COVID-19 on the degree of dependence and structure of risk-return relationship: A quantile regression approach. *Finance Research Letters 36*, 101648.

Bachelier, L. (1900). Théorie de la spéculation. In *Annales scientifiques de l'École normale supérieure*, Volume 17, pp. 21–86.

Baek, S., S. Mohanty, and M. Glambosky (2020). Covid-19 and stock market volatility: An industry level analysis. *Finance Research Letters 37*, 101748.

Baker, S., N. Bloom, S. David, K. Kost, M. Sammon, and T. Viratyosin (2020). The unprecedented stock market reaction to covid-19. *The Review of Asset Pricing Studies 10*, 742–758.

Balcilar, M., R. Gupta, and S. M. Miller (2015). Regime switching model of us crude oil and stock market prices: 1859 to 2013. *Energy Economics 49*, 317–327.

Bernoulli, D. (1954). Exposition of a new theory on the measurement of risk. *Econometrica 22*(1), 23–36.

Black, F. and M. Scholes (1973). The pricing of options and corporate liabilities. *The journal of political economy 81*, 637–654.

Bossu, S., P. Carr, and A. Papanicolaou (2021). A functional analysis approach to the static replication of European options. *Quantitative Finance 21*(4), 637–655.

Breeden, D. T. and R. H. Litzenberger (1978). Prices of state-contingent claims implicit in option prices. *Journal of business 51*(4), 621–651.

Buchen, P. and H. Malloch (2014). CLA's, PLA's and a new method for pricing general passport options. *Quantitative Finance 14*(7), 1201–1209.

Campbell, J. and L. Viceira (1999). Consumption and portfolio decisions when expected returns are time varying. *Quarterly Journal of Economics 114*, 433–495.

Carr, P., K. Ellis, and V. Gupta (1998). Static hedging of exotic options. *Journal of Finance 53*(3), 1165–1190.

Carr, P. and R. Lee (2008). Robust replication of volatiliy derivatives. *NYU Mathematics in Finance Working Paper Series*, 1–49.

Carr, P., R. Lee, and M. Lorig (2017). Robust replication of barrier-style claims on price and volatility. Papers 1508.00632, arXiv.org, revised May 2017.

Carr, P. and D. Madan (2001). *Towards a theory of volatility trading*. Cambridge University Press Cambridge, UK.

Carr, P. and D. B. Madan (2005). A note on sufficient conditions for no arbitrage. *Finance Research Letters 2*(3), 125–130.

Carr, P. and J.-F. Picron (1999). Static hedging of timing risk. *The Journal of Derivatives 6*(3), 57–70.

Cepoi, C.-O. (2020). Asymmetric dependence between stock returns and news during COVID-19 financial turmoil. *Finance Research Letters 36*, 101658.

Choi, S.-Y. (2021). Analysis of stock market efficiency during crisis periods in the us stock market: Differences between the global financial crisis and COVID-19 pandemic. *Physica A: Statistical Mechanics and its Applications 574*, 125988.

Chopra, N., J. Lakonishok, and J. R. Ritter (1992). Measuring abnormal performance: do stocks overreact? *Journal of financial Economics 31*(2), 235–268.

Cousot, L. (2007). Conditions on option prices for absence of arbitrage and exact calibration. *Journal of Banking & Finance 31*(11), 3377–3397.

Cowles, A. (1933). Can stock market forecasters forecast? *Econometrica: Journal of the Econometric Society 1*(3), 309–324.

Cowles, A. (1944). Stock market forecasting. *Econometrica, Journal of the Econometric Society 12*(3/4), 206–214.

Cox, A. M. and D. G. Hobson (2005). Local martingales, bubbles and option prices. *Finance and Stochastics 9*(4), 477–492.

Crandall, M. G. and P.-L. Lions (1983). Viscosity solutions of hamilton-jacobi equations. *Transactions of the American mathematical society 277*(1), 1–42.

Dangl, T. and M. Halling (2012). Predictive regressions with time-varying coefficients. *Journal of Financial Economics 106*(1), 157–181.

De Bondt, W. F. and R. Thaler (1985). Does the stock market overreact? *The Journal of finance 40*(3), 793–805.

Debreu, G. (1959). *Theory of value: An axiomatic analysis of economic equilibrium*. New Haven, CT: Yale University Press.

Degutis, A. and L. Novickytė (2014). The efficient market hypothesis: A critical review of literature and methodology. *Ekonomika 93*, 7–23.

del Baño Rollin, S., A. Ferreiro-Castilla, and F. Utzet (2010). On the density of log-spot in the heston volatility model. *Stochastic Processes and their Applications 120*(10), 2037–2063.

Delbaen, F. and M. Yor (2002). Passport options. *Mathematical Finance 12*(4), 299–328.

Diamond, S. and S. Boyd (2016). CVXPY: A Python-embedded modeling language for convex optimization. *Journal of Machine Learning Research 17*(83), 1–5.

Diebold, F., T. Gunther, and A. Tay (1998). Evaluating density forecasts with applications to financial risk management. *International Economic Review 39*(4), 863–883.

DIMA, B., Ştefana Maria DIMA, and R. IOAN (2021). Remarks on the behaviour of financial market efficiency during the COVID-19 pandemic. the case of VIX. *Finance Research Letters 43*, 101967.

Duffie, D. (2010). *Dynamic asset pricing theory*. Princeton University Press.

Dupire, B. et al. (1994). Pricing with a smile. *Risk 7*(1), 18–20.

Fama, E. F. (1965). The behavior of stock-market prices. *The journal of Business 38*(1), 34–105.

Fama, E. F. (1970). Efficient capital markets a review of theory and empirical work. *Journal of Finance 25*(2), 383–417.

Ferhati, T. (2020a). Robust calibration for SVI model arbitrage free. Available at SSRN 3543766.

Ferhati, T. (2020b). Svi model free wings. Unpublished manuscript.

Fernholz, E. R. (2002). Stochastic portfolio theory. In *Stochastic portfolio theory*, pp. 1–24. Springer.

Fleming, W. H. and R. W. Rishel (2012). *Deterministic and stochastic optimal control*, Volume 1. Springer Science & Business Media.

Frezza, M., S. Bianchi, and A. Pianese (2021). Fractal analysis of market (in)efficiency during the COVID-19. *Finance Research Letters 38*, 101851.

Gatheral, J. (2004). A parsimonious arbitrage-free implied volatility parameterization with application to the valuation of volatility derivatives. Presentation at Global Derivatives & Risk Management, Madrid.

Gatheral, J. (2011). *The Volatility Surface: A Practitioner's Guide*. John Wiley and Sons.

Gatheral, J. and A. Jacquier (2014). Arbitrage-free SVI volatility surfaces. *Quantitative Finance 14*(1), 59–71.

Girsanov, I. V. (1960). On transforming a certain class of stochastic processes by absolutely continuous substitution of measures. *Theory of Probability & Its Applications 5*(3), 285–301.

Green, R. C. and R. A. Jarrow (1987). Spanning and completeness in markets with contingent claims. *Journal of Economic Theory 41*(1), 202–210.

Grossman, S. J. and J. E. Stiglitz (1980). On the impossibility of informationally efficient markets. *The American economic review 70*(3), 393–408.

Guastaroba, G., M. Savelsbergh, and M. G. Speranza (2017). Adaptive kernel search: A heuristic for solving mixed integer linear programs. *European Journal of Operational Research 263*(3), 789–804.

Guastaroba, G. and M. G. Speranza (2012). Kernel search: An application to the index tracking problem. *European Journal of Operational Research 217*(1), 54–68.

Gurobi Optimization, L. (2021). Gurobi optimizer reference manual.

Hajek, B. (1985). Mean stochastic comparison of diffusions. *Zeitschrift für Wahrscheinlichkeitstheorie und verwandte Gebiete 68*(3), 315–329.

Haugen, R. A. (1995). *The new finance: the case against efficient markets*. Prentice Hall.

Henderson, V. and D. Hobson (2000). Local time, coupling and the passport option. *Finance and Stochastics 4*(1), 69–80.

Hyer, T., A. Lipton-Lifschitz, and D. Pugachevsky (1997). Passport to success: Unveiling a new class of options that offer principal protection to actively managed funds. *Risk-London-Risk Magazine Limited 10*, 127–132.

Jackwerth, J. and M. Rubinstein (1998). Recovering probability distributions from option prices. *Journal of Finance 51*(5), 1611–1631.

Jensen, M. C. (1968). The performance of mutual funds in the period 1945-1964. *The Journal of finance 23*(2), 389–416.

Just, M. and K. Echaust (2020). Stock market returns, volatility, correlation and liquidity during the COVID-19 crisis: Evidence from the markov switching approach. *Finance Research Letters 37*, 101775.

Kampen, J. (2016). Generalisation of Hajek's stochastic comparison results to stochastic sums. *International Journal of Stochastic Analysis 2016*, 6p.

Kanaujiya, A. and S. P. Chakrabarty (2017). Pricing and estimates of Greeks for passport option: a three time level approach. *Journal of Computational and Applied Mathematics 315*, 49–64.

Kantelhardt, J. W., S. A. Zschiegner, E. Koscielny-Bunde, S. Havlin, A. Bunde, and H. E. Stanley (2002). Multifractal detrended fluctuation analysis of nonstationary time series. *Physica A: Statistical Mechanics and its Applications 316*(1-4), 87–114.

Karatzas, I. and S. Shreve (1991). *Brownian motion and stochastic calculus*, Volume 113. Springer Science & Business Media. Second edition.

Kelly, J. (1956). A new interpretation of the information rate, bell systems tech. *J 35*, 917–926.

Kramkov, D. and W. Schachermayer (1999). The asymptotic elasticity of utility functions and optimal investment in incomplete markets. *Annals of Applied Probability 9*(3), 904–950.

Kullback, S. and R. A. Leibler (1951). On information and sufficiency. *The annals of mathematical statistics 22*(1), 79–86.

Kulldorff, M. (1993). Optimal control of favorable games with a time limit. *SIAM Journal on Control and Optimization 31*(1), 52–69.

Leo, B. (1961). Optimal gambling systems for favorable games. In *Proceedings of the Fourth Berkeley Symposium on Mathematical Statistics and Probability*. University of California Press, Berkeley, CA.

Leung, T. and M. Lorig (2016). Optimal static quadratic hedging. *Quantitative Finance 16*(9), 1341–1355.

Malkiel, B. G. (1973). *A random walk down Wall Street: including a life-cycle guide to personal investing*. WW Norton & Company.

Malkiel, B. G. (1995). Returns from investing in equity mutual funds 1971 to 1991. *The Journal of finance 50*(2), 549–572.

Malkiel, B. G. (2003). The efficient market hypothesis and its critics. *Journal of economic perspectives 17*(1), 59–82.

Malkiel, B. G. (2005). Reflections on the efficient market hypothesis: 30 years later. *Financial review 40*(1), 1–9.

Mazur, M., M. Dang, and M. Vega (2021). Covid-19 and the march 2020 stock market crash. evidence from S&P1500. *Finance Research Letters 38*, 101690.

Merton, R. C. (1969). Lifetime portfolio selection under uncertainty: The continuous-time case. *The review of Economics and Statistics 51*, 247–257.

Merton, R. C. (1975). Optimum consumption and portfolio rules in a continuous-time model. In *Stochastic Optimization Models in Finance*, pp. 621–661. Elsevier.

Metcalf, G. E. and B. G. Malkiel (1994). The wall street journal contests: The experts, the darts, and the efficient market hypothesis. *Applied Financial Economics 4*(5), 371–374.

Mirza, N., B. Naqvi, B. Rahat, and S. Rizvi (2020). Price reaction, volatility timing funds' performance during covid-19. *Finance Research Letters 36*, 101657.

Nachman, D. C. (1988). Spanning and completeness with options. *The review of financial studies 1*(3), 311–328.

Navrátil, R., S. Taylor, and J. Večeř (2021). On equity market inefficiency during the COVID-19 pandemic. *International Review of Financial Analysis 77*, 101820.

Navrátil, R., S. Taylor, and J. Večeř (2022). On the Utility Maximization of the Discrepancy between a Perceived and Market Implied Risk Neutral Distribution. *European Journal of Operational Research*.

Neely, C. J., D. E. Rapach, J. Tu, and G. Zhou (2014). Forecasting the equity risk premium: the role of technical indicators. *Management science 60*(7), 1772–1791.

Nguyen, D. T., D. H. B. Phan, M. T. Chwee, and N. V. K. Long (2021). An assessment of how COVID-19 changed the global equity market. *Economic Analysis and Policy 69*, 480–491.

Pan, Z., D. Pettenuzzo, and Y. Wang (2020). Forecasting stock returns: A predictor-constrained approach. *Journal of Empirical Finance 55*, 200–217.

Ramelli, S. and A. F. Wagner (2020). Feverish stock price reactions to COVID-19. *The Review of Corporate Finance Studies 9*(3), 622–655.

Rapach, D. E., J. K. Strauss, and G. Zhou (2010). Out-of-sample equity premium prediction: Combination forecasts and links to the real economy. *The Review of Financial Studies 23*(2), 821–862.

Richard, M. and J. Večeř (2021). Efficiency testing of prediction markets: Martingale approach, likelihood ratio and bayes factor analysis. *Risks 9*(2).

Roberts, H. (1967). Statistical versus clinical prediction of the stock market. Unpublished manuscript.

Rogers, L. and M. Tehranchi (2010). Can the implied volatility surface move by parallel shifts? *Finance and Stochastics 14*(2), 235–248.

Rogers, L. C. (2013). *Optimal investment*, Volume 1007. Springer.

Roper, M. (2010). Arbitrage free implied volatility surfaces. preprint.

Rüschendorf, L. and S. Vanduffel (2019). On the construction of optimal payoffs. *Decisions in Economics and Finance 43*(1), 129–153.

Samuelson, P. A. (1965). Proof that properly anticipated prices fluctuate randomly. *Industrial Management Review 6*(2), 41–49.

Schwert, G. W. (2003). Anomalies and market efficiency. *Handbook of the Economics of Finance 1*, 939–974.

Sewell, M. (2011). History of the efficient market hypothesis. Research Note RN/11/04, University College London, London.

Shreve, S. E. and J. Večeř (2000). Options on a traded account: Vacation calls, vacation puts and passport options. *Finance and Stochastics 4*(3), 255–274.

Stoll, H. R. (1969). The relationship between put and call option prices. *The Journal of Finance 24*(5), 801–824.

Stroock, D. W. and S. R. Varadhan (1969). Diffusion processes with continuous coefficients, i. *Communications on Pure and Applied Mathematics 22*(3), 345–400.

Taylor, S. and J. Večeř (2021). The premium reduction of European, American, and perpetual log return options. *The Journal of Derivatives 28*(4), 7–23.

Topcu, M. and O. Gulal (2020). The impact of COVID-19 on emerging stock markets. *Finance Research Letters 36*, 101691.

Vavasis, S. A. (1990). Quadratic programming is in NP. *Information Processing Letters 36*(2), 73–77.

Večeř, J. (2001). A new PDE approach for pricing arithmetic average Asian options. *Journal of computational finance 4*(4), 105–113.

Večeř, J. (2011). *Stochastic finance: A numeraire approach*. CRC Press.

Večeř, J. (2020). Optimal distributional trading gain: Generalizations of merton's portfolio problem with implications to bayesian statistics. Unpublished manuscript.

Večeř, J., J. Kampen, and R. Navrátil (2020). Options on a traded account: symmetric treatment of the underlying assets. *Quantitative Finance 20*(1), 37–47.

Zhang, Y., F. Ma, B. Shi, and D. Huang (2018). Forecasting the prices of crude oil: An iterated combination approach. *Energy Economics 70*, 472–483.

Zhang, Y., Q. Zeng, F. Ma, and B. Shi (2019). Forecasting stock returns: Do less powerful predictors help? *Economic Modelling 78*, 32–39.

List of publications

1. Večeř, J., J. Kampen, and R. Navrátil (2020). Options on a traded account: symmetric treatment of the underlying assets. *Quantitative Finance 20* (1), 37–47.

2. Navrátil, R., S. Taylor, and J. Večeř (2021). On equity market inefficiency during the COVID-19 pandemic. *International Review of Financial Analysis 77*, 101820.

3. Navrátil, R., S. Taylor, and J. Večeř (2022). On the Utility Maximization of the Discrepancy between a Perceived and Market Implied Risk Neutral Distribution, *European Journal of Operational Research*.